Bioengineering the In Vitro Ovarian Follicle Microenvironment

by

Hong Zhou

A dissertation submitted in partial fulfillment
of the requirements for the degree of
Doctor of Philosophy
(Biomedical Engineering)
in The University of Michigan
2017

Doctoral Committee:

Assistant Professor Ariella Shikanov, Chair
Assistant Professor Rhima M. Coleman
Assistant Professor Lei Lei
Professor Rita Loch-Caruso
Professor Lonnie D. Shea

Hong Zhou

hongchou@umich.edu

ORCID iD: 0000-0002-6754-9087

DEDICATION

This dissertation is dedicated to my parents and my family, who have been encouraging and forgiving as always, and to the five wonderful and adventurous years of my PhD.

ACKNOWLEDGEMENTS

First, I would like to acknowledge my advisor, Dr. Ariella Shikanov, without whom none of the following work could have been achieved. Thank you, Ariella, for accepting me as a student of yours during the hard times and for holding my hands through all the ups and downs. I could never have become the researcher I am today without your guidance, your encouragement, and your support. I will forever be grateful for your nurturing during my PhD training.

Then, I would like to acknowledge my Dissertation Committee: Drs. Rhima M. Coleman, Lei Lei, Rita Loch-Caruso, Lonnie D. Shea, and Min Xu. Thank you very much for all your invaluable inputs and feedback that made this dissertation better and for helping me putting my PhD journey to a perfect ending. It has been a great honor and lots of fun working with all of you. Thank you for allowing me insights to different perspectives on same topics.

Next, I would like to acknowledge the late Dr. Alan J. Hunt, who first saw the potentials in me and generously took me in to start my journey for PhD. It was a pity to have only worked with you for such a short time but your optimist attitude, your bravery on cracking tough questions, and your perpetual curiosity will continue to guide me wherever I go. I hope that you would be pleased with my work while enjoying the beer on the planet where scientists are treated as rock stars.

I would also like to acknowledge all my lab mates, past and current, my colleagues, and all my collaborators. Without the help of you, I could have never graduated. And more importantly, it was you who made my journey to PhD so much more fun and enjoyable.

Lastly, I would like to thank all my friends and all the people I have encountered during these years, especially my violin teacher, Mr. David Ormai, the tennis buddies and pros I met at the Huron Valley tennis club, and the Wine and Sprit Education Trust (WSET), for all the fun memories that I will always treasure.

TABLE OF CONTENTS

LIST OF FIGURES

LIST OF APPENDICES

Appendix

ABSTRACT

Follicles are the functional units of the ovary and are composed of a germ cell (the oocyte) and layers of somatic cells (granulosa and theca cells). The ovaries contain a limited number of immature follicles. Serving as the ovarian reserve, follicles have the potential to develop and produce mature oocytes capable of fertilization in a highly regulated process called folliculogenesis. Chemo- and radiation therapies used as cancer treatments can have unintended effects on patients such as detrimental effects on the non-replenishable ovarian reserve, resulting primary ovarian insufficiency (POI) and/or infertility. Clinically established fertility preservation methods, such as egg and embryo cryopreservation, are not applicable to all patients. This gap has motivated the development of new strategies to produce mature oocytes to restore fertility at a later date. Among the emerging technologies, in vitro ovarian follicle growth (IVFG) systems represent great translational potentials to harvest fertilizable eggs regardless of patients' age or hormone stimulation. Isolated single follicles can be cultured in two-dimensional (2D) or three-dimensional (3D) systems. Specifically among 3D methods, encapsulated in vitro follicle growth (eIVFG) systems have been developed to mimic the native 3D physiological environment of the ovaries by maintaining a spherical morphology and the cell-cell and cell-matrix interactions between the oocyte and somatic cells of the follicle.

To better understand reflect various signals (growth factors, hormones, extracellular matrixes, mechanics, etc.) in the culture environment, we investigated multiple aspects of the eIVFG environment to provide guiding principles to facilitate the development of alternative fertility preservation options. We first started with secondary follicles that can autonomously grow in vitro and examined the effects of xenobiotics on developing follicles in vitro. This knowledge not only complemented our current understanding of the toxicity of chemotherapy drugs and environmental toxicants. More importantly, the application of such a high-throughput eIVFG

system together with its dynamic culture environment provides a faster and cheaper alternative toxicity evaluation method compared to traditional animal models. Next, we examined the interactions between small, early stage (late primary and early secondary) follicles and supporting stromal cells. By allowing such interactions in our novel biomimetic matrix, we were able to harvest mature, fertilizable oocytes from small follicles. Additionally, by using supporting cells derived in a patient-specific way, this synthetic and xeno-free matrix represents great translational potentials for clinical application. Lastly, we examined the paracrine cues present in various culture environments by monitoring the dynamic activities of specific transcription factors (TFs) in real time. For the first time ever lentiviral transduction of the follicles, we delivered specific TF reporters. By quantifying bioluminescence intensity from the reporters, we investigated the underlying mechanism that results in a number-dependent manner of folliculogenesis. Additionally, this technique can serve as a powerful tool to probe potential TFs on a large scale. By quantifying in real time the dynamic activities of specific TFs, this technique can provide insightful knowledge to the causation between TF activities and phenotypical changes.

In conclusion, by examining multiple aspects of the in vitro ovarian follicle environment, this dissertation provides new understanding of the bioengineering principles in numerous in vitro follicle culture applications and in the field of reproductive biology more broadly. By providing novel solutions to ongoing clinical issues, the research described in this dissertation reveals a translational opportunity for combining biomaterials technology and the field of reproductive biology.

CHAPTER

I. Introduction

As the central organ in the female reproductive system, the ovary is responsible for producing healthy fertilizable oocytes. By secreting sex hormones, the ovary also serves as an important endocrine gland that links reproductive and non-reproductive organs in females to the timing of ovarian cycles. Ovaries are the sites where pluripotent epiblasts-like primordial germ cells (PGCs) differentiate to form follicles, develop and mature. Early in fetal life, the PGCs undergo a period of proliferation (mitosis). Following the initial proliferative stage, PGCs enter meiosis to differentiate into primary oocytes. Primary oocytes that are arrested at meiosis prophase I interact with ovarian somatic cells to form the primordial follicles during gestation (Anderson and Hirshfield 1992; Baillet and Mandon-Pepin 2012).

Ovarian follicles are the functional and morphological units of the ovaries. They consist of a meiotically arrested germ cell (the oocyte) and multiple surrounding somatic cells (granulosa and theca cells) as well as a basement membrane (BM). In mammals, primordial follicles serve as a resting and finite pool of the most undeveloped oocytes available during the female reproductive life span (Edson et al. 2009). During postnatal development, groups of follicles are recruited as needed. Follicle recruitment is in general subdivided into 2 categories: the initial activation of primordial follicles throughout female reproductive life, and the cyclic recruitment after puberty of a limited number of small primary follicles from the growing cohorts, during which a subset of follicles are selected for dominance and ovulation (McGee and Hsueh 2000).

Upon puberty, ovarian follicle development (folliculogenesis) is a highly orchestrated event by the timely coordination of the hypothalamus-pituitary-gland-gonad (HPG) axis (Fig. 1). Released from the hypothalamus, the gonadotropin releasing hormone (GnRH) circulates to the

anterior pituitary gland to stimulate the release of follicle stimulating hormone (FSH) and luteinizing hormone (LH). FSH induces the early growth of the ovarian follicles, but the final maturation requires LH as well. Development of ovarian follicles is usually characterized by: 1) growth of the primary oocyte; 2) proliferation of the granulosa cells; and 3) development of the theca cells (Moore et al. 2015). With mitotic expansion of granulosa cells, single-layered primary follicles are transformed into multi-layered secondary follicles (Oktem and Urman 2010). As follicles continue to increase in size, a single large fluid-filled cavity, called the antrum, is formed, serving as a vital and dynamic microenvironment for the oocyte and the follicular cells. At this stage, along with increased vascularization of the theca layer and proliferation of somatic cells, growing oocytes in antral follicles migrate asymmetrically to one side of the follicle, where they are surrounded by the cumulus granulosa cells. In response to LH and FSH, growing follicles also produce indispensable hormones, estradiol and progesterone, that regulate development and functions of female reproductive organs (Fig. 1). Stimulated by LH, theca cells produce androgen, which is then converted to estradiol by granulosa cells under the stimulation of FSH. Hormones produced by the follicles negatively feed back to the hypothalamus and anterior pituitary gland to maintain physiologically balanced endocrine functions. The LH surge also seems to induce resumption of the first meiotic division of primary oocytes, prompting the progression to mature secondary oocytes ready for fertilization (Wigglesworth et al. 2013). Throughout the progression of follicle development and maturation, bidirectional signaling is required between oocytes and the surrounding somatic cells (Burns et al. 2002). The oocyte serves as the dominant factor orchestrating the onset of folliculogenesis and regulating somatic cell proliferation and differentiation during follicular development (Knight and Glister 2006). Maintenance of oocyte meiotic arrest by the granulosa cells in return, is also indispensable for normal female fertility (Burns et al. 2002; Peng et al. 2013).

To recapitulate the key events of folliculogenesis, various in vitro follicle culture systems have been established, such as on the traditional two-dimensional (2D) cell culture surfaces and encapsulated three-dimensional (3D) in vitro follicle growth (eIVFG) systems. It is beyond the scope of this dissertation to discuss in detail the 2D systems, which contributed to our knowledge of follicle biology, yet failed to successfully translate into larger species, including humans. On

the other hand, 3D culture systems more effectively simulate physiological conditions, providing essential support for the overall architecture of developing follicles in vitro.

The first 3D eIVFG was based on alginate, which is a natural biopolymer and served as a tissue engineering scaffold for various applications (Drury and Mooney 2003; Kuo and Ma 2001; Lee and Mooney 2001). With low cytotoxicity, alginate is readily available and gels under gentle conditions with bivalent cations such as Ca^{2+}. Because of its biocompatibility, alginate has been successfully used for follicle encapsulation and culture in vitro (J Xu et al. 2011; Xu et al. 2006). As follicle develops in vitro, alginate provides the necessary 3D structural support that mimics the environment of ovarian tissue while supporting somatic cells and their interactions with the oocyte to optimize oocyte development.

The best results for the in vitro culture of ovarian follicles were demonstrated in low alginate concentrations (0.25% to 0.5%) for both mice (West-Farrell et al. 2009; E. R. West et al. 2007; Xu et al. 2006) and non-human primates (Jin et al. 2010; Xu et al. 2010), because alginate does not degrade at the same rate as follicles grow (Boontheekul et al. 2005). Low concentrations of alginate promote greater follicle survival, antrum formation, follicular growth, steroid secretion and resumption of meiosis compared to high concentrations (E. R. West et al. 2007). Despite of the success in mice and several large mammalian species, the translation of alginate work to human remains challenging. Human ovarian follicles require extended culture period and reach a much greater terminal size compared to other species (Telfer and Zelinski 2013), indicating that human ovarian follicle in vitro culture requires a dynamic cell-responsive environment (Qu et al. 2015).

To better engineer the in vitro ovarian follicle environment for human translation, this dissertation first started with secondary follicles, examining an already established dynamic eIVFG system in fibrin alginate and its application in in vitro toxicological testing. Various toxicants, drugs and their metabolites carry potential ovarian toxicity. Ovarian follicles are

susceptible to this type of damage at all stages of their development. In this part of the dissertation, we first demonstrated the usefulness of a hydrogel based 3-dimensional (3D) mouse ovarian follicle culture as a tool to study ovarian toxicity in a different setup. The 3D *in vitro* culture, based on fibrin alginate interpenetrating network (FA-IPN), preserves the architecture of the ovarian follicle and physiological structure-function relationship. The fibrin component in the system is degraded by plasmin and appears as a clear circle around the encapsulated follicle. The degradation area of the follicle is strongly correlated with follicle survival and growth. We then applied the novel 3D high-throughput (HTP) *in vitro* ovarian follicle culture system to study the ovotoxic effects of an anti-cancer drug, Doxorobucin (DXR) and mixtures of environmental toxicants such as 7,12-dimethylbenz[a]anthracene (DMBA) and lindane. We established concentration-dependent responses of follicles when exposed to selected toxicants and identified lethal concentrations of the tested toxicants that kill 10% and 50% of the population of cultured follicles (LC10s and LC50s).

With the knowledge of secondary follicle development in vitro, the dissertation then moved on to investigate how to better support smaller follicles (late primary and early secondary) development in vitro with a translational approach for clinical application in fertility preservation. Contrary to alginate, poly-ethylene glycol (PEG) is a biocompatible synthetic polymer with tunable physical properties. Consequently, PEG hydrogels can be degraded by soly proteolysis, thus providing a xeno-free, cell-responsive scaffold for the co-encapsulation of mouse primary and early secondary ovarian follicles (80 – 120 μm) with mouse adipose derived stem cells (ADSCs). Similar to accepted approaches to utilize feeder cells to promote the undifferentiated growth of embryonic stem cells (ESCs), co-encapsulated ADSCs provide critical paracrine factors necessary for early-stage follicle survival and maturation. The dual-site crosslinker, YKNS/VPMS, significantly improved ADSCs survival compared to YKNS, which was previously used for multi-layer secondary follicle culture. More importantly, this enhanced PEG hydrogel culture significantly improved the survival and maturation of the early-stage follicles cultured in vitro. The use of the biocompatible and biodegradable PEG hydrogels offers a xeno-free culture system that could be used to culture large species and human follicles.

Moreover, ADSCs can be derived in a patient specific way in clinical settings, therefore making this approach highly translational.

Lastly, to better understand how follicles interact with the in vitro environment, the dissertation investigated several critical transcription factors and their dynamic activities during folliculogenesis, providing insights to the development of the next generation of eIVFG systems. Multiple aspects of IVFG environments profoundly affect follicle development and maturation. Paracrine cues in the environment trigger intracellular signaling cascades that result in up- or down-regulation of transcription factors (TFs) – powerful players in follicle development. Recent studies have shown that culturing small follicles in groups of 10 (10X) or with support cells improves follicle survival, growth and maturation rates. However, little is known about the paracrine signaling mechanism and the identity of key TFs. We employed TRACER (Transcriptional Activity CEll aRrays) for continuous, real-time dynamic quantification of TF activity in mouse ovarian follicle cultured in alginate hydrogels. We evaluated the expression of 4 TFs (p53, NF-κB, Gli, and HIF1) associated with follicle development at various stage in ovarian follicles cultured in groups of 5 (5X, controls) or 10 (10X). Our results demonstrated that distinct differential TF activities revealed potential mechanism underlying the different phenotypes in the 2 culture schemes. Combined with phenotype monitoring and hormone analysis, our approach captures the dynamics of TF activities in follicles cultured in different environments, identifying conserved paracrine signaling mechanisms under beneficial co-culture effects.

Collectively, by examining different aspects of eIVFG and various eIVFG systems designed specifically for certain stages of follicles, this dissertation aims to provide novel insights to ongoing clinical issues. The research described in this dissertation also reveals a translational opportunity for combining biomaterials technology and the field of reproductive biology.

CHAPTER

II. High-throughput (HTP) toxicology test system in 3-dimensional (3D) murine ovarian follicle culture

Previously published as: *PloS one* 10.10 (2015): e0140205.

1. Introduction

Ovaries are the central reproductive organs during the pre-pubescent and reproductive years. Ovarian follicle is the functional and morphological unit composed of the germ cell (the oocyte) and the surrounding somatic cells (theca and granulosa cells). The somatic cells produce hormones necessary for the regulation of the reproductive system, and communicate with the oocyte for its maintenance growth and development. During the process of follicular growth, i.e., folliculogenesis, the cross-talk between the germ and somatic compartments enables the enclosed immature oocyte to develop into a mature fertilizable ovum. Xenobiotic exposure disrupting oocyte-to-somatic cells interaction can lead to deleterious effects on folliculogenesis, resulting in oocyte incompetence, genetic and epigenetic changes, and dis-regulated hormone production. Thus it would affect the reproductive system at different levels. Considering the finite number of undeveloped (primordial) follicles in mammalian females, any damage to the primordial follicle pool is irreversible and results in premature ovarian failure (Combes et al. 2004; Hareng et al. 2005).

Evaluation and prediction of potential reproductive toxicity is a public health priority. However, based on the requirements of the US Environmental Protection Agency and the European REACH program, a complete set of in vivo tests for a single chemical requires use of thousands of animals, making costs and time spent prohibitive (Vandenberg et al. 2012).

This difficulty has motivated the development of *in vitro* high-throughput (HTP) screening assays to prioritize chemicals for in-depth investigation (Miller et al. 2006; Symonds et al. 2006; Tomic et al. 2006). With few exceptions, cell based *in vitro* screening assays employ tissue culture plastic (TCP) as the standard substratum, which is easy to use, relatively inexpensive and has a long shelf life. Similar methods are used for *in vitro* screening assays for reproductive toxicology studies, where, mouse ovarian follicles are cultured on such TCP surfaces in a 2-dimensional (2D) manner for an average of 72 hours with various toxicant exposure (Kreeger et al. 2005; Pangas et al. 2003). This approach is limited for short periods of toxicant exposure and non-physiological flattened deformed follicular phenotype (Hirshfield 1991; Miller et al. 2005) due to lack of 3D tissue support. Furthermore, 2D culture does not adequately replicate the physiologically relevant cellular microenvironment and therefore provides unreliable results (Kreeger et al. 2005; Pangas et al. 2003). Follicles are large 3-dimensional (3D) structures that significantly expand in volume during development. Under physiological conditions the oocyte is enclosed in a dense circle of somatic cells allowing them to communicate through transzonal projections (TZPs) that extend through the zona pellucida and connect with each other via gap junctions on the oocyte membrane (Melvin E Andersen and Daniel Krewski 2009).

Deprived of the spatial support in traditional 2D cultures, the oocyte is disadvantaged by lacking the necessary crosstalk to somatic cells due to gap junction disruption and a fully exposed antrum. The antrum, a closed fluid-filled cavity under physiological conditions, develops nearby the oocyte as the follicle expands. Residing in the center of the avascular follicles, the expansion of the antrum and the formation of the follicular fluid within is a key indicator of follicular growth, which heralds the development of a follicle to pre-ovulatory stage. Molecules in the follicular fluid includes hyaluronan, chondroitin sulfate proteoglycan versican and inter-α-trypsin inhibitor, suggesting that the antrum is osmotically active (Clarke et al. 2006; Matti et al. 2010). In addition, the presence of antrum may serve as a buffering system, protecting follicles from abrupt changes in hormone concentrations or toxic exposure. On the contrary, in the non-physiological setting of 2D cultures, the oocyte is not protected from sudden toxic exposures with little ability to adjust, which may result in irrelevant toxicity data.

In this study we aimed to design a 3D system that allows both culturing follicles in *in-vivo*-like conditions and continuous morphological, genetic and biochemical sampling, using the previously reported fibrin-alginate interpenetrating network (FA-IPN) (Shikanov et al. 2009, 2011b). FA-IPN is a dynamic culture system for *in vitro* follicle cultures. Naturally derived, alginate is slowly degrading and biologically inert to ovarian tissue. As such, it provides structural support for the follicles during the extended (10 to 12 days) culture period. Fibrin however, is a biologically active protein and degrades as follicles grow in response to follicle stimulating hormone (FSH). Fibrin degradation appears as a clear circle around the encapsulated follicle, increasing with the duration of culture. Importantly, if the follicle is damaged, fibrin degradation will significantly slow down or stop due to lack of the proteolytic activity normally carried out by proteases from functioning granulosa cells of a viable follicle (Shikanov et al. 2009, 2011b). As a result, follicle health and survival can be correlated with the proteolytic activity by quantifying fibrin degradation, which serves as the base for the proposed system.

Following initial design stage, we validated the system performance by exposing cultured follicles to doxorubicin (DXO), a moderately ovotoxic chemotherapeutic agent (Ben-Aharon et al. 2010). Follicles exposed to increasing doses of DXR demonstrated decreased survival rate, and decreased fibrin degradation. We utilized MATLAB®'s image processing toolbox to capture the changes in follicle dimensions and degradation of surrounding matrix. This approach allowed quantitative analysis of the effect of toxicants on folliculogenesis and to compare multiple conditions with variations in duration of exposure, toxicant types and/or concentration.

2. Material and Methods

All chemicals were purchased from Sigma-Aldrich (St. Louis, MO) unless otherwise specified. Media formulations were purchased from Invitrogen (Carlsbad, CA). Nalgin MV-120 sodium alginate (Carrageenan, Xanthan, Alginate, Ingredients Solution, Inc., Waldo, ME, USA) and the fibrinogen-thrombin kits (Baxter Healthcare, BioScience Division, Westlake Village, CA) were used for fibrin-alginate gel formation.

2.1 Animals

Mice were purchased (Harlan, Indianapolis, IN), and housed in ventilated cages in a temperature and light controlled environment (12L: 12D) and provided with food and water. Animals were treated in accordance with the guidelines and regulations set forth by the National Institutes of Health Guide for the Care and Use of Laboratory Animals and the established Institutional Animal Use and Care protocol at the University of Michigan. Experiments with animals were performed in strict accordance with the protocols approved by the Institutional Animal Care and Use Committee (IACUC) at the University of Michigan (PRO00004106). All experiments were performed under isofluorane anesthesia, and all efforts were made to minimize suffering.

2.2 Follicle isolation, encapsulation and culture

Two-layered secondary follicles ranging from 120 to 135 μm were mechanically isolated from ovaries of D12-D14 female F1 hybrids (C57BL/6JRccHsd inbred × CBA/J CrHsd) and were then encapsulated in 7.5 μL of fibrin alginate gel based on "the drop method" described by Shikanov et al. with modifications (Shikanov et al. 2011b). Briefly, the final fibrin alginate mixture consisted of 12.5 mg/mL fibrinogen and 0.2% (w/v) alginate while thrombin concentration was adjusted to 12.5 mg/mL. The cross-linking time for beads in thrombin/Ca^{2+} solution was 2 minutes. Encapsulated follicles were cultured in α-MEM based growth media (GM), supplemented with 1 mg/mL Fetuin, 3 mg/mL bovine serum albumin (BSA, MP Biomedicals, Irvine, CA), 0.1% insulin-transferrin-selenium (ITS), and 10 mIU/mL recombinant human follicle stimulating hormone (rhFSH, GONAL-f ® 75 IU, Merck Serono, S.A.). Every 2 days, the cultured follicles were imaged by a light microscope (DMI 3000, Leica, Germany) with follicle diameters measured with the Leica software LAS V4.3 (Leica, Germany) while half (50 μL) of the growth media was replaced by pre-equilibrated, fresh media.

A stock solution of aprotinin was dissolved in DPBS and then diluted in growth media before media changing. In this study, we used aprotinin to control fibrin degradation and its concentrations ranged from 0.025 to 0.05 TIU/mL.

2.3 Oocyte maturation

After 12 days of culture, healthy follicles with diameters between 300 and 350 μm were identified. The alginate was degraded by placing the alginate beads with the follicles in 100 μL αMEM medium containing 1% fetal bovine serum (FBS) and 10 mIU/mL alginate lyase (MP Biomedicals, Irvine, CA) for 2 minutes at 37 ˚C and 5% CO_2. After retrieving the follicles from the alginate beads, all the follicles were transferred to an IVF dish with maturation media composed of αMEM, 10% FBS, 5 ng/mL epithelial growth factor (EGF), 1.5 IU/mL human chorionic gonadotropin (hCG), and 10 mIU/ml rhFSH for 12-14 hours at 37 ˚C and 5% CO_2. Oocytes were then denuded from the surrounding cumulus granulosa cells by 0.1% hyaluronidase and gentle aspiration through a mouth pipette. The oocytes were considered at metaphase II (MII) if a polar body was present in the perivitelline space.

2.4 Quantitative Measurement

Quantitative measurements were performed both manually and by using MATLAB® (code available upon request) and ImageJ (Rasband, W.S., ImageJ, National Institutes of Health, Bethesda, MD, USA, http://imagej.nih.gov/ij/, 1997-2014). Areas of fibrin degradation were first measured manually using ImageJ by drawing two orthogonal lines across the degraded area. We then calculated the area (A) of fibrin degradation using the diameter results ($A = \pi(\frac{d}{2})^2$). In the meantime, images were converted to binary by our custom MATLAB® program (Fig. 3). To achieve this, a threshold value was first determined by the program automatically analyzing the images with evenly exposed background. Then, areas with values higher than the defined threshold were converted to black whereas areas with lower than threshold values were converted to white in the binary images. Before submitting images for program to analyze fibrin degradation area, the sizes of follicles were calculated to compensate the area loss in the fibrin degradation circle due to follicle expansion using ImageJ. Then, area of degraded fibrin was measured by using the “Analyze” menu. Fibrin degradation area from both methods (M for

manual calculation and A for program measured areas) were recorded and compared as a factor indicating follicle health.

To decrease variance, we took the following approaches: a) when capturing the images, we ensured a homogenous lighting in the background; b) we imaged beads that were floating in the center of the well and not close to the wall; c) we built a standard value of fibrin degradation area in control conditions, especially when switching to a different batch of aprotinin; d) adjusted features such as “threshold” and “fuzz factors” in the program; e) opted for manual definition of the boundary of fibrin degradation when necessary.

2.5 Exposure of secondary follicles to doxorubicin

For all doxorubicin treatments in this study, a stock solution of DXR was dissolved in dimethylsulfoxide (DMSO) and then diluted in growth media to achieve various DXR final concentrations. Doxorubicin actual concentrations in growth media were confirmed by measuring the auto-fluorescence of DXR using a fluorescence plate reader at room temperature (Fluoroskan Ascent, Labsystems, Finland, excitation 490 nm, emission 590nm). Since the plate reader cannot detect any fluorescence besides background readings for concentrations lower than 10 nM, the lower DXR concentrations used in this study (1 nM, 0.1 nM, 0.01 nM and 0.005 nM) were determined based on sequential dilution of the 10 nM solution.

For secondary follicles (120-130 μm in this study), 0.05% DMSO in GM was used as vehicle control. This lower concentration than what has previously been used for antral follicle culture (0.075%) (Peretz and Flaws 2013; Ziv-Gal et al. 2013) together with aprotinin showed no significant effects on *in vitro* folliculogenesis (data not shown).

2.6 Statistical analysis

Statistical analyses were performed using statistical software R (Lucent Technologies, USA). Two-sided t-test was performed to determine differences in follicle diameters between control and aprotinin treatment group at any given time point and fibrin degradation area data between

the two groups. Two-sided one-way ANOVA followed by t-tests was employed to test differences in follicle diameters for control and all doxorubicin treatment groups and following fibrin degradation. One-sided t-test was adapted by the MATLAB® to output follicle health evaluation based on fibrin degradation calculation. Values of $p < 0.05$ were considered statistically significant.

3. Results and Discussion

3.1 Optimal aprotinin concentration preserved intact fibrin degradation circle without affecting follicle health.

During follicle culture, the fibrin component in the IPN is gradually degraded and diffuses from the hydrogel via proteolysis, with the initial clearance occurring adjacent to the follicle then progressing outwards to the edge of the hydrogel bead (Shikanov et al. 2009). The fibrin removal mirrors the follicle growth and volumetric expansion whereas the much slower degrading alginate remains as a structural and mechanical support. Thus, it is important to have both fibrin and alginate in the IPN to support folliculogenesis *in vitro* and for the fibrin component to serve as an optical density indicator of the follicle growth. Healthy growing follicles demonstrate strong proteolytic activity, which results in fast and poorly controlled fibrin degradation. Addition of aprotinin, a small molecule that inhibits plasmin proteolytic degradation, resulted in a slower fibrin degradation and more controllable optical density change. Our goal was to optimize aprotinin concentration to delay the fibrin degradation up to 8 days after encapsulation (D8). We identified the ideal range of the aprotinin concentration by varying concentrations in the follicle culture media during the first 4 days of the culture. Suboptimal concentrations of aprotinin (0.001 TIU/mL) resulted in uncontrolled fast fibrin degradation, while an overdose of aprotinin (0.01 TIU/mL) lead to follicle death due to matrix stiffness (Shikanov et al. 2011b).

Our results showed that appropriate aprotinin concentration (0.025-0.05 TIU/mL) could sustain the required rate of degradation till D8, when antrum usually forms in growing follicles (Fig. 2a). We also measured follicle diameters to compare follicle growth in both conditions (Fig. 2b). To

confirm follicle health, we compared oocytes harvested from both conditions by *in vitro* maturation (IVM) (Fig. 2c). We confirmed that follicle health and oocyte maturation rate was not affected by this treatment as we did not see significant differences in survival rate (73.1% VS 70.2%, Table 1) or metaphase II (MII) rate (78.2% VS 81.0%, Table 1) between the two conditions.

Table 1. Summaries of follicle growth under different conditions.

	%survival	%antrum	Diameter (D6, μm)	Diameter (D12, μm)	%MII
GM	73.1	87.0	177.46±5.33	322.46±11.50	78.2
GM+Apr	70.2	86.4	223.91±11.70	288.45±23.10	81.0
DXR treatments					
200 nM	0	0	150.20±5.04	143.63±6.96	0
10 nM	0	0	128.91±2.49	129.13±3.36	0
1 nM	0	0	102.59±1.97	100.59±2.33	0
0.1 nM	0	0	106.70±4.05	100.80±3.83	0
0.01 nM	35.4	28.6	175.12±3.01	179.51±7.18	0
0.005 nM	47.6	64.3	178.06±9.48	217.61±14.03*	0

%survive = (the number of survived follicles) ÷ (total number of follicles culture); %antrum = (the number of follicles with antrum) ÷ (the number of survived follicles); %MII = (the number of MII oocytes) ÷ (total number of oocytes matured). Follicle diameter data was presented as mean ± SEM. *: $p<0.05$.

3.2 *In vitro* fibrin degradation positively correlated with *in vitro* folliculogenesis, serving as the foundation of the proposed system

We established a correlation between fibrin degradation and follicle health, demonstrating that healthy follicles can actively degrade fibrin in the FA-IPN during culture, while the unhealthy ones cannot. Examples of original and MATLAB® processed images are shown in Fig. 3a. The left column showed images of a live and a dead follicle after 6 days of culture in FA-IPN. We specifically chose D6 images for this quantification because of the correlation between antrum formation and follicle atresia (Clarke et al. 2006; Matti et al. 2010). The right column showed MATLAB® processed binary images in which the fibrin degradation circles were intensified by this conversion. We used both manual and automated MATLAB®/ImageJ (Schneider et al.

2012) to measure changes in optical clarity due to fibrin removal and the results from both manual calculation and program measurements were recorded and compared in Fig. 3b. We did not see any significant difference between the two methods, confirming that the program is suitable to measure fibrin degradation in attempt to evaluate follicle health. However, a slightly greater variation was observed in program measurements, which could be due to the more forgiving aspect of manual calculation.

The proposed measuring process for the high-throughput approach is demonstrated in the flow chart of the image analysis in Fig. 4. Stacks of original images of FA-IPNs are first converted to binary images, in which original optical clarity due to fibrin removal would appear as white whereas follicles and areas with fibrin presence would appear as black. Since the "black" follicles reside in the white area of fibrin degradation, we then correct for area loss due to follicle expansion for further MATLAB® program analyses. The program output is then based on the comparison of fibrin degradation area to control images. Since the system was designed to test for positive toxic effects on follicle health, therefore if the fibrin degradation area is significantly smaller (< mean – 1.5×SD), the output will be "X", indicating positive toxic effects, i.e., dead follicles; if equal, output "?", indicating further analysis may be necessary; and lastly if the degradation area is same as the control if the output is "√", indicating absence of toxic effects, i.e., healthy follicles.

3.3 Doxorubicin treatments confirmed system functionality and identified the IC50 for secondary follicles.

To test our system, we treated cultured follicles with doxorubicin (DXR), a chemotherapeutic agent used to treat multiple cancers, including breast and ovarian cancer. DXR is an anthracycline that works by intercalating DNA, thus preventing replication and transcription. Depending on cell type and drug dose, DXR can cause topoisomerase II-dependent double-strand DNA breaks or induce oxidative stress (Rebbaa et al. 2003). Recent evidence suggests that doxorubicin is moderately ovotoxic via direct apoptotic effects on follicles/oocytes and/or an impact on the entire ovary, which may potentially leads to infertility and premature ovarian

failure (POF) (Ataya and Moghissi 1989; Ben-Aharon et al. 2010; Jurisicova et al. 2006; Kim et al. 2006; Lee et al. 2006; Morgan et al. 2013; Perez et al. 1997; Rebbaa et al. 2003).

We exposed cultured follicles to multiple concentrations of doxorubicin, ranging from 0 to 200nM (Fig. 5). This range was determined based on what have been previously established as therapeutic plasma levels in patients undergoing DXR chemotherapy (Barpe et al. 2010; Rebbaa et al. 2001; Rebbaa et al. 2003; Wilkinson and Mawer 1974). None of the follicles survived in conditions with doxorubicin concentrations greater than 0.01nM (Table 1). We observed partial follicle survival of 35.4% (n=80) in 0.01nM treatment and 47.6% (n=92) in 0.005nM, compared to controls (73.1% and 70.2%, Table 1), which is in agreement with other reports (Ben-Aharon et al. 2010; Lee et al. 2006; Perez et al. 1997), Interestingly, follicles that survived 0.01 and 0.005 nM doxorubicin exposures could not complete the maturation process. Some of the follicles did not contain oocytes, especially in 0.01 nM group (data not shown), and all oocytes were meiotically arrested compared to progression to meiosis II in controls (Table 1).

Importantly, the diameter of survived follicles after 12 days of culture was significantly smaller than control conditions, which contributed to the meiotic arrest of the follicles. This delay in meiosis progression could be due to the mechanism of doxorubicin. DXR acts by intercalating DNA, and therefore prevents replication and transcription. As granulosa cells actively proliferate during folliculogenesis, DXR would interfere with this process, leading to impaired granulosa cell functions. The impacted granulosa cellular functions in turn, lead to impediment in the crosstalk to oocytes and therefore their arrest in meiosis. Details of underlying mechanism for this phenomenon are still under investigation in our lab. We are also interested in factors that may rescue the arrest oocytes, thus re-activate meiosis progression.

Similarly, we performed both manual calculation and MATLAB® program measurement to quantify fibrin degradation with different DXR concentrations (Fig. 6). In consistency with the smaller follicle sizes on D12 of culture, our results also showed significantly smaller area of

degraded fibrin on D6 for live follicles in the 0.005 nM DXR treatment group. For DXR concentrations higher than 0.01 nM, there was no detectable fibrin degradation by the program in most of the images, even though some images showed little if any degradation by eye.

4. Conclusion

The described approach uses a novel tool to screen multiple ovotoxicants and perform mechanistic studies in a physiologically relevant environment. Our results expand the armamentarium of *in vitro* screening assays for reproductive toxicology. We designed a 3D HTP *in vitro* ovarian follicle culture system using FA-IPN, which was successfully tested to evaluate the ovotoxic effects of Doxorubicin. The control of the fibrin degradation rate allowed toxicity screening for extended periods of culture, without disruption of follicle development. The customized automated MATLAB® image processing software supported the hands-off approach to screen multiple conditions in a high throughput manner. To summarize, we established a 3D *in vitro* ovarian follicle culture HTP system that could be used to screen toxicants for female reproductive system.

5. Disclosures

The authors declare that there are no conflicts of interest. This work has been published in PLoS One in 2015.

6. Funding

This work was supported by the start-up funding from the University of Michigan to AS.

7. Acknowledgement

The authors would like to acknowledge Ingredients Solution, Inc. and Baxter International Inc., who kindly provided the alginate and fibrinogen-thrombin kits (through a Material Transfer Agreement to AS) respectively for the use in the FA-IPNs. The authors would also like to thank all the members of the Shikanov lab for their support and input throughout the project.

CHAPTER

III. Detection of lindane and 7,12-dimethylbenz[a]anthrance toxicity at low concentrations in a three-dimensional ovarian follicle culture system

In conjunction with: Cara J. Young, Rita Loch-Caruso, Ariella Shikanov

1. Introduction

Contamination of the environment with organic pollutants has emerged as a significant public health concern due to the pervasive nature of these xenobiotics. Such contaminants could target the ovaries, thus exerting long-lasting adverse effects on women's reproductive health. Females are born with finite numbers of follicles, which sustain the ovarian endocrine function and fertility (Hirshfield 1991). Ovotoxic xenobiotic exposure can deplete the non-renewable follicular reserve, resulting in premature ovarian insufficiency (POI) (Bhattacharya and Keating 2012; Hoyer and Keating 2014; Martin et al. 2009). Noticeably, follicles at all stages of development can be impacted by xenobiotic exposure, leading to deleterious effects on follicle development, oocyte competence, ovulation and hormone production (Mattison 1993).

A large number of chemicals affect ovarian functions. Lindane (gamma-hexachlorocyclohexane), a persistent organic pollutant used as a pesticide/insecticide, causes impairments of female fertility by altering ovarian follicle development and function in women, laboratory and farm animals (Tiemann 2008). Lindane inhibits intercellular communication through gap junctions (Loch-Caruso et al. 2004; Loch-Caruso et al. 2005), and suppresses follicle-stimulating hormone (FSH) and transforming growth factor beta 1 (TGF β1)-stimulated steroidogenesis in rats (Ke et al. 2005). Additionally, lindane can also abolish oocyte-directed follicle organizing activity in vitro (Li and Mather 1997). The use of lindane was banned in

agriculture by the Stockholm Convention on Persistent Organic Pollutants (Vanden Bilcke 2002). However, it continues to be available as a pharmacological treatment of scabies and lice. Because of its widespread use, lipophilic nature, and resistance to biodegradation, low concentrations of lindane can persist in lipid-rich human tissues (Kutz et al. 1991). However, lindane toxicity to ovarian follicles at low concentrations is yet to be established, especially in a 3D culture environment.

7,12-dimethylbenz[a]anthracene (DMBA) is an immunosuppressor and a powerful organ-specific laboratory carcinogen (Miyata et al. 2001). As a polycyclic aromatic hydrocarbon (PAH), DMBA is found in car exhaust fume and cigarette smoke (Gelboin 1980). It is evidenced that female smokers experience ovarian senescence at an earlier age compared to their non-smoking counterparts (Jick et al. 1977). It has been shown that DMBA exposure induces DNA double strand breaks and subsequent DNA repair response in cultured neonatal rat ovaries (Ganesan et al. 2013). DMBA depletes ovarian follicles at all developmental stages as suggested by in vitro neonatal ovary cultures (Bhattacharya and Keating 2012; Ganesan et al. 2013; Ganesan et al. 2015; Igawa et al. 2009; Nteeba et al. 2014). DMBA toxicity to single follicles, however, has not been established in vitro. Such knowledge can provide insights to low concentration effects of environment pollutants and compensate current regulations.

Follicles are the functional units of ovaries, and because of their non-renewable nature are most sensitive to chemical or physical damage (Lebbe et al. 2017). During follicular development, primordial follicles undergo a series of critical changes in character, both histologically and hormonally. Primordial follicles activate and develop into primary follicles and later secondary. A secondary follicle is a growing follicle consisting of an oocyte and two or more layers of supporting granulosa cells. It has been well established that secondary follicles can be cultured and matured individually and independent of ovarian tissue or feeder cells (Xu et al. 2006). Encapsulated in vitro follicle growth (eIVFG) systems, such as fibrin-alginate interpenetrating networks (FA-IPNs), recapitulate key events of mammalian follicle development in physiological, in-vivo-like conditions and serve as a tool to screen for toxic effects of

compounds (Zhou et al. 2015). In the FA-IPN eIVFG system, follicles are individually cultured in a 96-well plate, which allows study of low-concentration effects of toxicants with high sensitivity in each individual follicle and oocyte. Therefore, the proposed system serves as a robust proxy to study toxicity of xenobiotics on the growing pool of follicles (Braw-Tal 2002; Xiao et al. 2017a; Xu et al. 2015).

Noticeably, people are exposed to a cocktail of xenobiotics and yet, limited scientific information is available on potential toxic effects of mixtures of environmental pollutants on human reproductive health. Therefore, here we investigated ovarian follicle survival, growth, and maturation after exposure to lindane and DMBA individually and as lindane-DMBA mixtures.

In this study, we exposed mouse secondary ovarian follicles to lindane and DMBA on days 0, 2, and 4 of eIVFG. First, we identified the lethal concentrations of lindane and DMBA that kill 10% and 50% of the population of cultured follicles (LC10s and LC50s). Then, we exposed follicles to various combinations of mixtures of lindane and DMBA at concentrations with matching potency to evaluate the combinational effects of the two toxicants. Our results showed concentration-dependent adverse effects on follicles upon exposure to lindane and DMBA, either individually or in a mixture, at much lower concentrations than traditional toxicological methods.

2. Methods

All chemicals were purchased from Sigma-Aldrich (St. Louis, MO) unless otherwise specified. Media formulations were purchased from Thermo Fisher Scientific (Carlsbad, CA). Nalgin MV-120 sodium alginate (Carrageenan, Xanthan, Alginate, Ingredients Solution, Inc., Waldo, ME, USA) and the fibrinogen-thrombin kits (Baxter Healthcare, BioScience Division, Westlake Village, CA) were used for fibrin-alginate gel formation.

2.1 Animals

Mice were purchased (Harlan, Indianapolis, IN), and housed in ventilated cages in a temperature and light controlled environment (12L:12D), and provided with food and water. Animals were treated in accordance with the guidelines and regulations set forth by the National Institutes of Health Guide for the Care and Use of Laboratory Animals and the established Institutional Animal Use and Care (IACUC) protocol at the University of Michigan. Experiments with animals were performed in strict accordance with the protocols approved by the University of Michigan IACUC. All animals used in this study were euthanized by overdose of isoflurane via inhalation followed by decapitation.

2.2 Ovarian follicle isolation, encapsulation and culture

Secondary follicles (120 – 135 μm) were mechanically isolated from 12 – 14 day-old F1 hybrids (C57BL/6NHsd inbred × CBA/JCrHsd) as previously described (Shikanov et al. 2009; Zhou et al. 2015). Only follicles with intact morphology were selected for encapsulation and culture. Selected follicles were encapsulated individually in FA-IPN as previously described (Zhou et al. 2015). Encapsulated follicles were placed in 96-well plates, with each well containing 100 μL growth medium (50% αMEM Glutamax and 50% F-12 Glutamax supplemented with 1 mg/mL bovine fetuin, 3 mg/mL bovine serum albumin [BSA], 0.1% insulin-transferrin-selenium [ITS], and 10 mIU/mL urofollictropin (Bravelle® 75 IU urofollitropin for injection, Ferring Pharmaceuticals, Saint-Prex, Switzerland). For all experiments, follicles were cultured at 37 ˚C with 5% CO_2. Follicles were imaged every 2 days using an inverted Leica DMI 3000 microscope with 20X objectives (Leica Microsystems, Bufflo Grove, IL). After imaging, half of the growth medium (50 μL) was replaced with pre-equilibrated, fresh medium.

Follicles were considered dead if they showed dark granulosa cell layers, and/or if the oocyte was visibly fragmented. Survival curves were created using Graphpad Prism 7 software by recording the numbers of dead follicles on specific days of cultures. Dead follicles were excluded retrospectively in growth curves. Diameters of live follicle were obtained by averaging 2 perpendicular measurements form basement membrane to basement membrane of individual

follicles in ImageJ software (National Institute of Health, Bethesda, MD). Growth curves of survived follicles were then obtained by plotting the average follicle diameters over time.

2.3 In vitro exposure of toxicants to follicles

Cultured follicles were exposed in vitro to either lindane or DMBA or both toxicants on Days 0, 2, and 4 of eIVFG. Lindane and DMBA were first dissolved in dimethyl sulfoxide (DMSO) and then diluted with growth media to reach desired concentrations. The final concentrations of DMSO were kept at 0.05% for all toxicant treatment conditions, which was consistent with previous publications (Zhou et al. 2015; Ziv-Gal et al. 2013). If treated, toxicants of the same concentration were also added to the fresh media on Days 2 and 4 to keep the toxicant concentration constant. Starting on Day 6, fresh media without toxicant was used when changing media.

2.4 In vitro follicle maturation (IVFM)

In vitro follicle maturation was performed on day 12 of eIVFG as previously described (Zhou et al. 2015). Oocytes were denuded from surrounding cumulus cells using 0.3% hyaluronidase. Oocytes were considered as metaphase II (MII), if a polar body was present in the perivitelline space. If the nucleus was clearly visible, oocytes were considered arrested at prophase I in the germinal vesicle stage (GV). If the nucleus was not visible, oocytes were considered to have undergone germinal vesicle breakdown (GVBD). Fragmented and/or shrunken oocytes were considered as degenerated (DG).

2.5 Statistical analysis

All statistical analyses were performed in GraphPad Prism 7 software. Follicle survival and growth were analyzed from 3 to 5 independent cultures in which 15 – 30 follicles were included for each experimental group. Follicle growth in different treatment groups was analyzed using

two-way ANOVA. *Post hoc* Dunnett's multiple comparisons test was performed to determine treatment effects compared to control. The significance level was set at $p < 0.05$.

3. Results

3.1 Concentration-dependent response to lindane

Our results demonstrate the concentration-dependent toxicity of lindane on cultured secondary ovarian follicles. In the control group, the FA-IPN encapsulation maintained the 3D architecture of follicles and supported follicle growth from secondary to antral stage (Fig. 7A), with follicle diameters increased from 133.2 ± 2.7 μm on day 0 to 323.4 ± 11.8 μm (Fig. 7C) on day 12. Follicle survival and growth were comparable between untreated controls and 0.25 μM lindane (Fig. 7), but significantly decreased when follicles were treated with higher concentrations of lindane. When treated with 0.5 μM lindane, follicle survival significantly decreased from 95.5% on day 2 to 37.3% on day 12 of culture (Fig. 7B), and the diameters of surviving follicles were significantly smaller (Fig. 7C). Moreover, oocytes in the surviving follicles exposed to 0.5 μM lindane that reached the diameter of 265.8 ± 13.1 μm on day 12 of eIVFG (Fig. 1C) presented with an elongated, oval-shape (Fig. 7A). When treated with 5 μM lindane, more than 80% of the follicles died within the first 8 days of culture (Fig. 7B), often showing extruded and/or degenerated oocytes (Fig. 7A): only 3.7% of follicles survived after 12 days of eIVFG. Normalizing to control, we determined that 0.5 μM lindane is the LC50 for in vitro cultured single secondary follicles and 0.25 μM lindane as the LC10.

3.2 **Concentration-dependent response to DMBA**

Similar to lindane, DMBA showed a concentration-dependent pattern of toxicity to cultured ovarian follicles (Fig. 8A). The survival and growth of follicles exposed to 6.25 nM DMBA slightly decreased compared to untreated controls, with 61.2% of follicles still alive on day 12 of eIVFG, compared to 71.3% in controls (Fig. 8B and 8C). When treated with 12.5 nM DMBA, follicle survival significantly decreased to 32.4% on day 12 of culture ($p < 0.0001$, Fig. 8B and 8C). After 4 days of exposure, follicles treated with 12.5 nM of DMBA grew from 168.7 ± 14.5

μm on day 6 to 201.2 ± 15.8 μm on day 12 (Fig. 8C), compared to 323.4 ± 11.8 μm on day 12 in controls. Additionally, when treated with 25 nM of DMBA, only 17.6% of follicles survived after 6 days of culture. Normalizing survival data to controls, we determined the LC10 and LC50 of DMBA for secondary follicles to be 6.25 nM and 12.5 nM, respectively. The significantly lower LC50 of DMBA indicated that DMBA is a more potent toxicant than lindane.

3.3 Concentration-dependent response to mixtures of lindane and DMBA

To examine the combinational effects, we exposed in vitro secondary ovarian follicles to mixtures of lindane and DMBA based on their potencies as individual toxicants. Two mixtures were tested to investigate the interactions between the two toxicants: one mixture was at the toxicant LC10s (0.25 μM lindane + 6.25 nM DMBA) and the second mixture at the LC50s (0.5 μM lindane + 12.5 nM DMBA).

Similar to individual toxicant exposures, we observed concentration-dependent responses of cultured follicles when exposed to the LC10 and LC50 mixtures of lindane and DMBA (Fig. 9A). When compared to untreated controls, follicle survival rate on day 12 in the LC10 mixture was only slightly lower than the controls, compared to a more significant decrease in the LC50 mixture (Fig. 9B). Interestingly, the growth of the follicles exposed to the mixtures of DMBA and lindane exhibited a pattern that resembled follicles exposed to lindane alone and not DMBA. The mean diameter of the follicles exposed to the mixture on day 12 (296.4 ± 13.0 μm in LC10 mixture, 258.5 ± 19.2 μm in LC50 mixture) closely matched diameters of follicles exposed to lindane alone (295.9 ± 10.9 μm in 0.25 μM, 265.8 ± 13.1 μm in 0.5 μM), and were slightly larger than those exposed to DMBA alone (285.4 ± 21.3 μm in 6.25 nM, 201.2 ± 15.8 μm in 12.5 nM) (Fig. 9C). This finding suggests a dominant role of lindane in the toxicity on follicle growth in the mixtures.

3.4 Effects of lindane and DMBA on oocyte quality

In vivo, immature oocytes must undergo a process of maturation from prophase I to metaphase II as follicles mature. Similarly, oocytes cultured in vitro must mature and progress to metaphase II in response to exogenous gonadotropins upon in vitro maturation. By examining the stages of the oocytes harvested from surviving follicles after toxicant exposure, we investigated how low concentrations of toxicant affected oocytes quality in surviving follicles.

Exposure to lindane and DMBA singularly and as mixtures demonstrated concentration-dependent effects on oocyte quality, resulting in greater rates of immature and degenerated oocytes and lower rates of oocytes that resumed meiosis, as indicated by oocytes arrested in GV stage (Fig. 10). When treated with 0.25 µM of lindane, only a slight increase (10%) was observed in oocytes arrested in GV stage compared to untreated controls, and a slight decrease (10%) in degenerated oocytes after IVFM. Exposure of the follicles to 0.5 µM lindane caused a significant (2.6-fold) increase in GV and a less pronounced 10% decrease in DG (Fig. 10). These results further demonstrate how oocyte quality decreases as a function of increasing toxicant concentration. A similar decrease in oocyte quality was observed in DMBA-treated follicles. The majority of oocytes from 6.25 nM DMBA treatment were arrested in GV, which was a 3-fold increase, compared to the controls (Fig. 10). Noticeably, the 12.5 nM DMBA treatment resulted in mostly degenerated oocytes, which was a 4.3-fold increase compared to controls (Fig. 10). Clearly, exposure to toxicants in early days (days 0, 2, and 4) of eIVFG shifted oocyte quality towards meiosis-incompetent stages after 12 days in culture. The shift was more apparent in DMBA treatments than in lindane, further implying the higher toxicity of DMBA than that of lindane.

Interestingly, follicle exposure to mixtures of lindane and DMBA on days 0, 2, and 4 of eIVFG, resulted in attenuated effects on the oocytes, compared to exposure to single toxicants (Fig. 10). An increase in immature oocytes was only 0.1-fold in the LC10 mixture, and 0.4-fold in the LC50 mixture, compared to controls (Fig. 10). The observed attenuated effect of the mixture on oocytes is consistent with the less affected follicle survival and growth in the mixture conditions (Fig. 9).

4. Discussion

Organic xenobiotics, such as lindane and DMBA, act at extremely low serum concentrations because of their lipophilic and pervasive nature. This study investigated for the first time the direct toxic effects of lindane and DMBA on individual in vitro cultured mouse secondary follicles. We used a 3D hydrogel-based in vitro culture system that allows for toxicant assessment in follicles cultured in in-vivo-like, physiological conditions. Our results demonstrated that lindane and DMBA adversely affect individually cultured mouse secondary ovarian follicles at micromolar and/or nanomolar levels. The concentrations of lindane and DMBA used in this study are in the same range as concentrations of other xenobiotics, such as doxorubicin, that have been previously established for individually cultured mouse secondary ovarian follicles by our and other groups (Xiao et al. 2017b; Zhou et al. 2015).

The data about outcomes of human exposure to environmental toxicants are limited. Current toxicity research on human degenerative diseases relies strongly on animal models, mainly rodents. Whole-animal studies allow for the examination of complex phenotypes that often involve multiple mechanisms, and they may better represent human exposure situations. Lindane has been shown to be toxic to the reproductive systems in both males and females in various species (Basavarajappa et al. 2016; Cyr et al. 2016; Sharma et al. 2017; Yuksel et al. 2016), even at low doses (0.25 mg/kg/day, 1/1000th of the LD50 of lindane) (Sharma et al. 2017). Similarly, DMBA, a common PAH, is also known to have adverse effects on fertility and ovarian functions, such as litter loss ((Basavarajappa et al. 2016) and ovarian follicle depletion (Shiverick 2017). While they offer certain advantages over cell-based testing assays, animal models can be labor intensive, time consuming and costly, and therefore are used to test relatively small numbers of chemicals (Collins et al. 2008). In contrast, in vitro assays allow greater flexibility and can rapidly provide information on large numbers of chemicals at low cost. Compared to animal studies, in vitro assays allow grouping chemicals according to their effects on key biological pathways and/or testing chemicals over a broad range of concentrations to capture varied exposure scenarios in a rapid and relatively inexpensive manner (M. E. Andersen and D.

Krewski 2009). Consistent with animal studies, various in vitro assays confirmed the toxicity of lindane and DMBA to the female reproductive system (Bhattacharya and Keating 2012; Ganesan et al. 2013; Igawa et al. 2009; Li and Mather 1997), using organ culture and ovarian follicle and oocyte cultures. Yet, a significant challenge remains as to how to maintain the physiological 3D structure of a multicellular and multicomponent nature of ovarian follicles and tissues of the reproductive tract.

The 3D hydrogel-based culture system addresses the challenges of maintaining the multilayered structure of ovarian follicles and allows focusing on a specific follicle population. With the 3D support from the hydrogel, the follicles develop in a more physiological environment, maintaining a fluid-filled antrum and expanding to their in vivo preovulatory sizes. The enclosed antrum, together with the antral fluid, mimic the diffusion patterns in vivo, and could serve as a buffer or as a reservoir in follicles exposure to toxicants. Because of the unique properties of the enclosed antrum and presence of the antral fluid, the low concentrations used in our study could better elucidate the mechanisms of the toxicity of lindane and DMBA to developing follicles in an in-vivo-like environment. Our results demonstrated the toxicity of lindane and DMBA to the growing pool of ovarian follicles at low concentrations and their adverse effects on oocytes from surviving follicles. These findings complemented what has already been established for the moderate and high concentrations. Considering the complexity of potentially non-monotonic dose-response curves, studying the toxic effects at micro doses are of considerable importance for scientific and regulatory communities (Vandenberg et al. 2012). Importantly, recent epidemiological data suggested links between environmentally relevant low concentrations and disease prevalence via industrial accidents or occupational applications (Vandenberg et al. 2012).

Lindane and DMBA affect follicle development via different mechanisms. Lindane alters folliculogenesis by inhibiting gap junction formation between the granulosa cells (Li and Mather 1997; Tiemann 2008) and suppresses FSH and TGF-β1-stimulated progesterone production (Ke et al. 2005; Nejaty et al. 2001). The effects of lindane on gap junctions can be detected at 24 hours post incubation with 40 μM of lindane (Ke et al. 2005). Upon bioactivation, lindane

undergoes further complex metabolism via CYP450s, which leads to lindane conjugation and deactivation (Fig. 11B). However, in the case of DMBA, in addition to toxicity caused by the parent toxicant, metabolites formed via bioactivation also have detrimental effects on ovaries. DMBA requires bioactivation via cytochrome p450 (CYP 450) isoforms 1A1 (CYP 1A1) and 1B1 (CYP 1B1) and microsomal epoxide hydrolase (mEH) (Igawa et al. 2009; Shimada et al. 2003). It has been previously shown that the ovaries are capable of bioactivating DMBA via CYP 450s that are present in granulosa cells (Ganesan et al. 2015; Nteeba et al. 2014). The metabolite, DMBA-3, 4-diol, was shown to have a greater toxicity to cultured neonatal mice and rat ovaries than the parent agent (Igawa et al. 2009). Consequently, we observed that DMBA is more toxic than lindane to in vitro cultured ovarian follicles, given that LC10 of lindane is 40 times greater than that of DMBA.

We hypothesized that lindane and DMBA will produce a synergistic or additive effect, resulting in augmented toxic effects when combined. Interestingly, we did not observe such interactions between the two toxicants in our culture system. Instead, our results suggest that follicles exposed to the mixture of lindane and DMBA resembled the response of the follicles exposed to lindane alone. The oocyte quality from mixture treatments was inferior to the oocyte quality in control follicles. However, when compared to the oocytes exposed to individual toxicants, the decrease in oocyte quality was ameliorated, suggesting potential competitive interactions between lindane and DMBA. This phenomenon could be explained by the competition of the CYP450s in granulosa cells upon exposure to the mixtures. Given the 40-fold difference between lindane and DMBA concentrations, the abundance of lindane molecules would have a greater chance of interacting with the limited number of CYP450s present in the granulosa cells of a single follicle. As lindane molecules outcompete DMBA molecules, follicle survival and growth shifted towards lindane only exposure. Additionally, the detoxification of lindane may help ameliorate the decrease in oocyte quality as seen in individual toxicant exposure.

Taken together, our results in 3D in vitro system complemented the existing data regarding toxicity of lindane and DMBA to mouse ovarian follicles at higher concentrations. The in-vivo-

like 3D matrix provides a biomimetic, physiological environment for the cultured follicles, similar to animal studies. Yet, the 3D culture assay is less time consuming, allowing for decoupling various components and significantly less expensive compared to animals. The data collected from these experiments could be used for in silico modeling for forecasting potential complex toxicity and create useful models for preventing, treating and limiting environmental disasters.

5. Conclusions

We applied a 3D in vitro ovarian follicle culture system to study the toxic effects of lindane and DMBA separately and as mixtures. As follicles were individually cultured in in-vivo-like environment, we were able to detect lindane and DMBA toxicity at ultra-low concentrations, complementing data established in moderate and/or high concentrations. Follicle survival and growth were affected by toxicant exposure in a concentration-dependent manner. Oocyte quality from the surviving follicles showed a shift towards meiotically incompetent stages compared to control, consistent with decreased follicle survival and inhibited follicle growth. Interestingly, when exposed to mixtures of lindane and DMBA at LC10s and LC50s, lindane was dictating the toxic effects, possibly due to the greater number of lindane molecules. Additionally, the inferiority of oocyte quality was ameliorated compared to individual toxicant exposure, indicating competitive interactions between lindane and DMBA. Taken together, the proposed system could serve as a new tool to study mixtures of environment toxicants in a physiological setting, providing much needed information on how simultaneous exposure to multiple toxicants.

CHAPTER

IV. A novel biomimetic matrix supports early stage follicle development for translational fertility preservation applications

In conjunction with: Claire E. Tomaszewski, AnneMarie E. Opipari, Lisa J. Green, Ariella Shikanov

1. Introduction

With improved survival rates among young patients with cancer, recent bench-to-bedside translation of new techniques to preserve fertility, and increased awareness of reduced fertility, options for family planning are now being offered to patients who have received a diagnosis of cancer (Jeruss and Woodruff 2009). It remains challenging for the biomedical community to develop safe fertility preservation methods for patients with cancer, especially the improvement of personalized, patient-specific approaches and the identification and reduction of the risks of cancer relapses (Woodruff 2007). Current methods of fertility preservation include hormone stimulation in women followed by either embryo or oocyte cryopreservation. As an established component of assisted reproductive technologies (ARTs), the success rate of oocyte cryopreservation has risen, and the increasing use of vitrification offers has improved outcome. Consequently, increasing numbers of women undergo oocyte cryopreservation for both medical and social reasons (Argyle et al. 2016; Noyes et al. 2009). Both techniques, however, require a delay in cancer treatment for up to 1 month, which may not be an option for some patients (Jeruss and Woodruff 2009). Additionally, neither can be used for pre-pubertal patients. New methods, such as autologous tissue transplantation, are also on the horizon (Agarwal and Chang 2007; Donnez et al. 2004; Donnez et al. 2013; Erin R West et al. 2007). However, there are potential risks of reseeding malignant cells back, especially for patients with hematological cancers.

In vitro culture of ovarian follicles that results in fertilizable oocytes has great potential in providing fertility preservation options for both pre-pubertal and post-pubertal patients. Since patients do not need to go through hormone stimulation, there is no need or risks of delaying the cancer treatment. Additionally, immature follicles are cultured in vitro, thus greatly reducing the risks of reintroducing cancerous cells back to patients. A number of encapsulated in vitro follicle growth (eIVFG) systems for single follicles have been established for a number of species, including human (Shikanov et al. 2009; Shikanov et al. 2011a; Xiao et al. 2015; J Xu et al. 2011; Xu et al. 2013b; Xu et al. 2006; Xu et al. 2009a; Xu et al. 2009b; M Xu et al. 2011). However, most of the above eIVFG are designed for secondary follicles with at least two layers of granulosa cells (type 4), starting from ~130 μm in diameters. However, smaller immature follicles less than 120 μm in diameter, including primordial, primary and early secondary follicles, are more abundant in the ovary and developing successful culture systems for these classes of follicles will maximize the potential of eIVFG systems. To obtain mature, fertilizable oocytes, new culture systems need to be established for smaller follicles as they need additional soluble and insoluble factors in the beginning of in vitro folliculogenesis, before acquiring autonomy after reaching 130 – 150 μm in diameters.

Indeed, efforts have been put to developing eIVFG systems for primary and early secondary follicles. Follicles in the early stages of development are gonadotropin-independent, responding mostly to the various local paracrine and autocrine factors from surrounding somatic cells, such as stromal cells, macrophages, and other neighboring follicles (Hornick et al. 2013; Laronda et al. 2014; Tagler et al. 2012). These additional cells/follicles have been shown to improve follicular growth and development, through production of essential factors, in addition to the removal of toxic wastes from the culture medium (Hajializadeh et al. 2008). However, the gap still remains between translating eIVFG systems established for smaller follicles to clinical application. On one hand, co-culturing multiple human follicles in a single environment could be of low efficiency and potentially wasteful. As humans are mono-ovulatory species, co-culturing multiple follicles together results in a potential dominant follicle selection, an obstacle that cannot be overcome with physiological levels of hormones. Co-culturing individual follicles with stromal cells that serve as feeder cells and provide the smaller follicles with the additional

support presents as a translational alternative. However, currently established co-culture eIVFG systems such as those with macrophages or theca–interstitial cells (TICS) (Tingen et al. 2011), lack translational sources of cells to provide for the smaller follicles. Therefore, it is a must to find a feeder cells source that can be used in clinical settings in a patient-specific way.

Adipose derived stem cells (ADSCs) are a clinically translational option to support in vitro culture of ovarian follicles. Adipose tissue is an abundant, accessible, and replenishable source of adult stem cells that can be isolated in patient-specific ways from liposuction waste tissue by collagenase digestion and differential centrifugation (Gimble and Guilak 2003). These ADSCs are multipotent and have been used in various applications for regenerative medicine (Gimble et al. 2007). Factors secreted by ADSCs in vitro, including vascular endothelial growth factor (VEGF) and basic fibroblast growth factor (bFGF), can help with the initial survival of smaller follicles in vitro (Markstrom et al. 2002). With their translational potentials, ADSCs pose a novel alternative source for co-culture of ovarian follicles.

In addition to tailoring the source of feeder cells to patients, another essential aspect of developing new eIVFG for clinical applications is the in vitro culture microenvironment, such as rigidity and degradability during the follicle culture period. Smaller follicles, such as primordial and primary, reside in the cortex, which is the more rigid part of the ovaries, compared to the softer medulla parts where growing follicles usually are (Shikanov et al. 2011a). This characteristic architectural design of the ovaries and follicles distribution in vivo also indicates the need for a dynamic and degradable in vitro microenvironment to accommodate the volumetric expansion, especially for larger species than mouse (Telfer and Zelinski 2013). As the initial survival of the smaller follicles may require the additional support from ADSCs, it is also necessary to consider the survival and proliferation of ADSCs.

With its tunable physical properties, poly (ethylene glycol) (PEG) is a biocompatible synthetic polymer that can be modified to meet the requirements of both ovarian follicles and ADSCs.

PEG hydrogels crosslinked with proteolytic sequences, can be degraded in response to cell-secreted proteases, thus creating space for follicular expansion without exerting excessive compressive force. It has been shown that PEG hydrogels enabled in vitro encapsulation and maturation of individual mouse secondary ovarian follicles (140 – 150 μm) (Shikanov et al. 2011a). In this chapter, we investigated a novel beneficial co-encapsulation system for mouse primary and early secondary ovarian follicles (90 – 110 μm) co-encapsulated ADSCs derived from female mice. Specifically, we pioneered a PEG hydrogel that incorporates degradable crosslinkers that are both plasmin and matrix metalloproteases (MMP) sensitive to simultaneously meet the requirement of expanding follicles and proliferating cells.

2. Materials and Methods

2.1 Hydrogel materials and preparation

8-arm PEG-Vinyl sulfone (PEG-VS, hexaglycerol, 40,000 g mol^{-1}, >99% purity, Jenkem Technology) was used without further modification. Two different tri-functional crosslinking peptide were compared for the co-encapsulation of follicles and ADSCs: plasmin-sensitive Ac-G**C**YK↓NSG**C**YK↓NS**C**G (YKNS) (1739.0 g/mol, >90%, GenScript, cleavage site indicated by ↓, cysteines with reactive thiols in bold) and MMP-sensitive Ac-G**C**RDVP↓MSMRGGDR**C**GYK↓NS**C**G-COOH (YKNS/VPMS) (2397.1 g/mol, >90%, CelTech). The hydrogels were formed via Michael-type addition (MTA) chemistry in 50 mM HEPES buffer at 37 ˚C under physiological pH (7.4). The stoichiometric ratio of -VS to thiol (-SH) groups was kept at 1:1 ratio for all experiments. Gelation was allowed for 5 mins for YKNS gels and 10 mins for YKNS/VPMS gels before terminating by transferring gels to pre-equilibrated media and/or phosphate buffered saline (PBS).

To investigate the swelling properties and rigidity of hydrogels under similar conditions that maintain ovarian follicle and ADSCs viability, crosslinked gels were subsequently submerged in PBS prior to measuring either swelling ratio or storage moduli. The storage moduli (G') were studied after overnight swelling in PBS using AR-G2 rheometer (TA Instruments, New Castle,

DE) equipped with 20mm parallel plates. To calculate swelling ratios, individual gels were weight after 24 hours of swelling in PBS. The mass swelling ratio (Q_m) was calculated by dividing the mass of the swollen hydrogels (m_s) by the theoretical mass of the dry gel components (m_d) as follow:

$$Q_m = \frac{m_s}{m_d}$$

2.2 Cell viability assay

Encapsulated ADSCs were stained with a LIVE/DEAD (488/570) kit (ThermoFisher) on Day 7 to evaluate cell viability with some modification to the manufacturer's protocol. Upon aspirating the medium from the wells, the gels were quickly rinsed with 100 µL of PBS. Then, 100 µL of the LIVE/DEAD dye was subsequently added to each well. The gels were incubated with the dye for 15 minutes at room temperature before imaging.

2.3 Follicle isolation and co-encapsulation with ADSCs

Details of the isolation and encapsulation process can be found in the appendix to this dissertation. Briefly, primary and early secondary mouse ovarian follicles (≤120 µm) were mechanically isolated from prepubertal female mice (F1 hybrids of C57B6 × CBA/J) that were 10 – 12 days of age. Healthy looking follicles were then individually encapsulated in 5% PEG-VS crosslinked with either YKNS or YKNS/VPMS. The PEG-VS and crosslinking peptides were dissolved in the isotonic HEPES buffer (pH=7.4 at 37°C) then mixed at a 1:1 volumetric ratio. Gels were mixed at a reactive group stoichiometric ratio of 1:1 (VS:SH) to reduce the impact of disulfide bond formation in the peptide solution on the cross-linking efficiency during cell culture. The ADSCs were then resuspended in this mixture of precursors to 5×10^5 cells/mL. This cell suspension was subsequently cast between parafilm-coated glass slides before individual follicle addition to each 10 µL gel. The gels were allowed to cross-link at 37 ˚C for 5 minutes for YKNS and for 10 minutes for YKNS/VPMS before terminating the chemical reaction by transferring to pre-equilibrated maintenance media (MM).

2.4 Follicle culture and maturation in vitro

Individually encapsulated follicles with ADSCs were allowed to rest in MM for at least 30 minutes before being transferred to wells of 96-well plates for culture. Same culturing schemes were followed as described in the appendix with slight modification. Individual gels containing follicles and ADSCs were cultured with 150 µL of growth media (GM). Every 2 days, half of the media (75 µL) was replaced with fresh, pre-equilibrated GM after imaging.

To evaluate the translational potential of our culture for fertility preservation, the quality of the oocytes harvested from cultures was examined by in vitro follicle maturation (IVFM) as previously described (Zhou et al. 2015) with some modification. Instead of digesting the gel, after 12 days of culture, gels containing follicles reaching at least 300 µm were selected and transferred to a 35 mm dish with pre-equilibrated MM. Working under a dissection scope, the mature follicles and/or the cumulus oocyte complexes (COCs) were carefully dissected out of the gels using 26G ½ needles. Mature follicles and COCs were subsequently transferred to pre-equilibrated maturation media (MatM) and incubated for 20 hours. After cumulus expansion, 0.1% hyaluronidase was added with a gentle aspiration with a pipette to separate oocytes and the cumulus granulosa cells. The oocytes were considered at metaphase II (MII) if a polar body was present in the perivitelline space. If the germinal vesicle was still visible, the oocyte was classified as GV. If appeared segmented, the oocyte was considered degenerated (DG).

2.5 Statistical analyses

All statistical analyses were performed using ANOVA with a Bonferroni post-test. $P < 0.05$ was considered significant (Prism, GraphPad).

3. Results

3.1 Hydrogel properties under physiological conditions

We modified the previously established PEG-VS based hydrogel for the co-encapsulation of early stage mouse ovarian follicles and ADSCs. PEG-VS based hydrogels were used because of its solely proteolytic degradation. To make the hydrogel degradable by both follicles and ADSCs, we combined the reported plasmin-sensitive YKNS sequence with a MMP-sensitive sequence VPMS (Fig. 12).

To study how the addition of VPMS affected hydrogel properties, we first compared the storage moduli (G') of gels crosslinked with either YKNS or YKNS/VPMS (Fig. 13). For gels crosslinked with YKNS, the storage modulus reached 3200 Pa after 5 minutes of gelation and overnight swelling under physiological conditions. However, with the addition of VPMS, the storage modulus significantly dropped to 2200 Pa after 10 minutes of gelation and overnight swelling. This significant decrease in the rigidity of the scaffold was also confirmed with swelling ratio studies. After subjecting gels to swelling for 24 hours under physiological conditions, we calculated the swelling ratios of YKNS and YKNS/VPMS gels based on the theoretical dry weight (5 mg). Consistent with the storage moduli data, upon the addition of VPMS, $Q_m$significantly increased from 28.5 to 32.0 after 24 hours of swelling under physiological conditions.

3.2 ADSCs survival was improved in hydrogels prepared with YKNS/VPMS

PEG-VS hydrogels with the same solid concentrations, but crosslinked with different peptide sequences, exhibit significantly different mechanical properties. Before co-encapsulating follicles with ADSCs, we first tested the survival of ADSCs only to assure that early stage follicles can receive potential support from the surviving ADSCs. We hypothesized that follicles need external support during early days of development in vitro, before reaching autonomy at late secondary stage. Therefore, the survival of ADSCs in the first 7 days is more critical than later.

To examine the survival of ADSCs in YKNS and YKNS/VPMS gels, we performed cell viability test on Day 7 (Fig. 14). ADSCs appeared to survive better in YKNS/VPMS gels. After counting the number of live and dead cells, we did not see any difference in the number of dead cells between the two conditions. However, a slight higher number of live cells were observed in YKNS/VPMS gels, indicating that the lower storage modulus of YKNS/VPMS gels may be beneficial to ADSCs initial survival.

3.3 Follicle survival, growth and maturation

Likely due to the improved survival of ADSCs, we observed a higher survival rate, a better growth, and a more successful maturation of follicles co-encapsulated with ADSCs in YKNS/VPMS. To focus on the effect of ADSCs on survival of the follicles at different developmental stages, we divided follicles into 3 groups as follows: <90 μm, 90 – 110 μm, and >110 μm.

Of all follicles starting below 90 μm, none survived in the YKNS gels compared to a 33.3% survival in YKNS/VPMS gels after 12 days of culture (Fig. 15). For late primary and early secondary follicles starting between 90 – 110 μm in diameters, 81.8% of these follicles survived in YKNS/VPMS gels (Fig. 16) compared to a significantly lower 14.3% in YKNS gels. A similar trend was also observed for follicles starting larger than 110 μm in diameters. In YKNS/VPMS gels, 62.5% of the follicles survived in YKNS/VPMS gels (Fig. 16) compared to a 42.1% survival rate in YKNS gels (Fig. 15).

In addition to the greater survival rates of follicles cultured in YKNS/VPMS gels, we also observed an increase in the terminal sizes of surviving follicles. This increase in terminal size could explain the more successful maturation results as shown in Fig. 16. We were able to harvest mature oocytes that reached MII, indicating possibility of fertilization compared to only GVBD oocytes harvested from follicles cultured in YKNS.

4. Discussion

In this chapter, we investigated the effects of peptides sensitive to MMP-driven degradation (VPMS) in an established PEG-VS based hydrogel system to promote in vitro development of early stage follicles. Considering the necessity of additional support for the initial survival of small follicles, we also examined a novel source of feeder cells, ADSCs, to improve the survival, growth and maturation of early stage follicles (≤120 μm). Our results demonstrated that ADSCs can serve as feeder cells to promote small follicles development cultured in eIVFG systems. With the addition of VPMS, the mechanical properties, such as the stiffness of the matrix and the consequent swelling ratios, were significantly modified. Cultured in a softer matrix, ADSCs showed a slightly higher survival rate over the first 7 days of culture, when the additional ADSC-secreted factors are more important compared to the later stages of folliculogenesis. Consequently, we observed improved rates of survival, growth, and maturation of follicles cultured in YKNS/VPMS gels.

Herein, we demonstrated for the first time the improved rates of survival, growth, and maturation of early stage follicles using dynamic, xeno-free PEG-VS based hydrogel systems. PEG-VS hydrogels remain an excellent option for applications in regenerative medicines because they are solely proteolytic degradable, compared to some of its counterparts such as PEG acrylate which can be hydrolytically labile (Shikanov et al. 2011a). Apart from degradability, PEG-VS polymers can form hydrogels through end-linked crosslinking via MTA under physiological conditions. The gelation and consequently the cell encapsulating condition should be non-toxic to cells in order to maintain cell viability. The need to maintain cell viability during the encapsulation process can be contradictory to maintaining the desired physical properties. As witnessed in this chapter, the addition of VPMS to YKNS significantly decreased the stiffness of the encapsulating matrix and consequently increased the swelling ratio. However, the decreased mechanical properties did not adversely affect the survival and proliferation of the encapsulated cells. In fact, the decreased mechanical properties in return may have contributed in the improved survival of ADSCs, thus the improved development of the co-encapsulated follicles.

The addition of VPMS also ensured a better survival rate of ADSCs after encapsulation. With the addition of VPMS, we have, for the first time, demonstrated the possibility of combining different mechanisms of degradation in a single matrix. The combination of plasmin-sensitive sequence YKNS and MMP-sensitive sequence VPMS resulted in a beneficial environment for both the follicles and the ADSCs. Compared to the size of a follicle and the amount of proteases it can secrete, the size of a single cell is an order of magnitude smaller, thus the much fewer and more diluted proteases. Therefore, to ensure the survival of the ADSCs, especially when the co-encapsulated follicle is not autonomous yet before reaching ~125 μm, the addition of VPMS was necessary as demonstrated by our data (Fig. 14).

Additionally, we tested an alternative source of feeder cells, which hold a strong potential for translating eIVFG to human ovarian follicle in a clinical setting. As an established source of mesenchymal stem cells, ADSCs are easy to derive and are less controversial compared to many other stem cells. Derived mainly from adipose tissues, ADSCs can be derived in a patient-specific way, thus minimizing immune rejections. Together with the synthetic, xeno-free PEG-VS scaffold, our reported system shows great potential for human application. Compared to species such as rodents, human ovarian follicles require extended culture time periods to mature at a much larger terminal size. Currently available eIVFG approaches such as the alginate-based system (Xiao et al. 2015) represent significant breakthroughs of culturing human secondary follicles (165.8 ± 32.3 μm) in vitro for 30 – 40 days to harvest MII oocytes. The terminal sizes of follicles, however, reached to 600 μm compared to ~2 mm in vivo. As alginate is not degradable by follicles within the culture period, the compressive forces can restrict follicle development after reaching 400 – 500 μm, as manifested by the two-step system (Xiao et al. 2015). Compared to the two-step alginate-based systems, our PEG-VS based system is proteolytically degradable by the follicles and the co-encapsulated supporting ADSCs. Therefore, it can better accommodate follicle expansion during development without exerting excessive, restricting compressive forces. In addition, the supports provided by the co-encapsulated ADSCs could help small, early stage follicles survive and grow. As those follicles are more abundant in vivo, our system could provide a more efficient solution to harvest mature oocytes from eIVFG systems.

This alternative in vitro solution does not require stromal support from patient's native ovarian tissue, thus minimizing the exposure to potentially malignant cells. Aiming for the small, early stage follicles, this novel eIVFG system can also be applied for pre-pubertal patients who are not responsive to hormone stimulation.

In conclusion, we demonstrated a novel eIVFG system that representing great translational potential to be alternative fertility preservation option for women cancer survivors. Co-encapsulated in a xeno-free, solely proteolytic PEG-VS based scaffold, the patient-specific ADSCs provide necessary support for small, early stage follicle to mature in vitro. This system represents a more efficient alternative fertility preservation option that can be applied for all women cancer survivors, regardless of their ages.

CHAPTER

V. Dynamic transcription factor activity networks in response to ovarian follicle culture environments

In conjunction with: Joseph T. Decker, Claire E. Tomaszewski, Lonnie D. Shea, Ariella Shikanov

1. Introduction

Encapsulated in vitro follicle growth systems (eIVFGs) provide unique and versatile methods for studying ovarian follicle biology and translational potentials for alternative fertility preservation options. Current culture systems support the development of individual mouse follicles from the secondary stage onward. However, it has been a challenge to grow smaller follicles *in vitro* due to the dissociation of the oocyte from the surrounding somatic cells. The recent works on developing co-culturing systems for primary follicles (Hornick et al. 2013; Tagler et al. 2012; Tingen et al. 2011) demonstrated the importance of additional factors, such as soluble cytokines and extracellular matrix components, to support the survival and development of primary follicles. The underlying mechanism that explains the role of these factors, however, is yet to be understood. Such knowledge can significantly contribute to current and future literature on developing xeno-free, cell-free in vitro culture systems for early stage follicles.

Early stage follicle development is thought to be largely gonadotropin independent and instead under the control of paracrine and autocrine signals from several sources in the ovary, including stromal cells, macrophages, and other follicles (Peters et al. 1975). Considering the native mammalian ovarian environment, there is a distinct spatial and temporal dynamics that may influence follicle development. Primordial and primary follicles are found in vivo close to the rigid, collagen-dense ovarian cortex, whereas larger growing follicles are found in the interior

medulla, which is less rigid (Woodruff and Shea 2011). Therefore, a follicle is more likely to be growing itself if surrounded by other growing follicles. Indeed, as previously described, when co-cultured with in groups of either 5 (5X) or 10 follicles (10X), primary follicles can survive and grow better in vitro, compared to individually cultured ones (Hornick et al. 2013). This number-dependent manner of early stage follicle development is likely to be an outcome of multiple paracrine factors secreted in an orchestrated manner. As primordial follicle activation is also likely achieved with paracrine signaling, it is important to understand the identities of these essential paracrine signals and the mechanisms under which they regulate early stage follicle development in vitro.

As key regulators of in vitro follicle development and maturation, paracrine cues in the environment trigger intracellular signaling cascades that result in up- or down-regulation of transcription factors (TFs) – powerful players in follicle development. Despite of the multiple reports on several phenotypic improvements such as follicle survival, growth, and maturation, in response to various co-culturing eIVFG approaches, mechanistic understanding of the connections between the number-dependent manner of early follicle development and follicles' coordinated transcriptional response remain uncharacterized. Temporally coordinated activities of many TFs direct progressive changes in follicle development, necessitating the use of experimental methods that capture the dynamic, systems-level view of quantitative TF actions that lead to follicle survival or death under different environments, spanning relevant time scales. Herein, we described an integrated approach to quantitatively characterize the real-time dynamic quantification of TF activity in mouse ovarian follicles cultured in alginate hydrogels in groups of 5X or 10X.

After transduction of follicles with a lentiviral system, we examined both qualitative and quantitative luciferase expression from the normalization (control) vector in the follicles encapsulated and cultured in vitro. TF-specific constructs were delivered to follicles in parallel. By using bioluminescence imaging (BLI), we evaluated the expression of four TFs associated with follicle development at various stages of folliculogenesis: 1) p53: an important cell cycle

regulator; 2) NF-κB: an anti-apoptotic nuclear factor (Karin and Lin 2002); 3) Gli: an effector in the hedgehog signaling pathway; and 4) HIF1: a hypoxia-induced factor. BLI provided a rapid, non-invasive, and sensitive method to quantify luciferase levels, and was recorded repeatedly from each sample to monitor dynamic activity. TRACER results were subsequently correlated with in vitro follicle development data and hormone and cytokine profiles. Taken together, these results provide an overall picture of the evolving and complex interplay of transcriptional networks responsible for relaying biochemical and biophysical cues to the nucleus, which in turn directs gene expression and the number-dependent manner of primary follicle development.

2. Materials and methods

2.1 Lentivirus and transcription factor arrays

Lentivirus was produced by co-transfecting HEK-293T cells with previously described lentiviral packaging vectors (pMDL-GagPol, pRSV-Rev, PIVS-VSV-G) (Dull et al. 1998) and lentiviral vectors using JetPrime (Polyplus, Illkirch, France). After 48 hours, supernatants were collected and cell debris was spun down and removed. Viruses were concentrated using PEG-it (System Biosciences, Palo Alto, CA) and re-suspended in phosphate buffered saline (PBS).

TF reporters consist of a specific TF response element (TRE) cloned upstream of a minimal thymidine kinase promoter driving the gene for firefly luciferase (FLuc) or NanoLuciferase (NLuc) (Fig. 17A). TF reporter specificity and sensitivity studies are referenced on the TRANSFAC database. Each lentiviral reporter consists of three or four repeats of a TF-specific binding element driving expression of luciferase.

2.2 Follicle enzymatic isolation, transduction and encapsulation

To harvest large numbers of primary follicles and to facilitate the subsequent transduction by lentiviruses, we used enzymatic digestion of the ovaries to isolate individual follicles. For all experiments, ovaries were retrieved from female F1 mice (C57B6 × CBA/J) at the age of 10 – 12

days. After separating from surrounding connective tissues, ovaries were briefly washed with fresh, warm Leibovitz's L-15 medium (L15) (Thermo Fisher) before transferring to a 30 mm dish containing pre-equilibrated alpha modification of minimum essential medium (αMEM) (Thermo Fisher) and 0.5% (v/v) Pen/Strep (Thermo Fisher). After all the ovaries were transferred, 10% (v/v) Liberase DH at 13 Wünsch units/mL (Sigma-Aldrich) was added and gently mixed in the dish. The ovaries were incubated for a total of 35 – 45 minutes, followed by 5 minutes pipetting to break down the enzyme-digested tissues to individual follicles. The enzymatic digestion was then arrested by adding 10% (v/v) fetal bovine serum (FBS) (Thermo Fisher).

Immediately after the enzymatic isolation, the digest was treated as a follicle suspension and equally divided between transcription factors of interests. To transduce follicles, the divided digest was incubated with approximately 10 MOI of each TF activity-reporting lentivirus for 4 hours in maintenance medium (MM) prior to encapsulation in 0.3% (w/v) alginate (Ingredients Solution, Inc., Waldo, ME, USA).

Details of the encapsulation process can be found in the appendix of this dissertation. Briefly, healthy-looking primary follicles at 90 – 110 µm were selected from the digest and were encapsulated in 10 µL alginate in either groups of five (5X) or ten (10X) (Fig. 17B). Follicle-containing alginate was dropped in 50 mM $CaCl_2$ and 140 mM NaCl for 2 min to allow for complete cross-linking. The alginate beads were carefully transferred to pre-equilibrated MM to recover for up to 2 hours. Alginate beads were individually culture in 96-well plates, with each well containing 150 µL growth media (GM). Black walled 96-well plates with optical bottoms were used for bioluminescence measurements to minimize background and cross talk between wells.

2.4 Luciferase production measurements

NLuc reporters were used to measure luciferase production. Two days after follicle encapsulation and culture, luciferase production was measured by lysing the follicles. The 2-day

period is sufficient to ensure stable lentiviral gene expression. To harvest the encapsulated follicles, culture media was replaced by 100 µL aMEM containing 10 mIU/mL alginate lyase (Sigma Aldrich) for 2 minutes in the incubator. Follicles were removed from the degraded alginate and transferred to Nano-Glo® LCS dilution buffer (Promega) with Reporter Lysis Buffer (Promega). After pipetting to ensure a thorough breakdown of the follicular structures, Nano-Glo® Live Cell substrate was added to the lysate and luminescence was immediately measured using GloMax® 20/20 Single Tube Luminometer (Promega), followed by measuring the amount of dsDNA using NanoDrop™ Spectrophotometer (Thermo Fisher). To avoid potential fluctuation, alginate gels were sacrificed approximately 48 hours apart and before changing media. Triplicates of 10X follicles were used for each time point. Normalized relative luminescence unit (RLU) values were calculated accordingly for each replicate.

2.5 Bioluminescence imaging and measurements

Similarly, two days after follicle encapsulation and culture, live-follicle transcription factor activity measurement from 5 different TF reporters (TA control, p53, NF-κB, Gli, and HIF1) using a PerkinElmer's IVIS™ Spectrum imaging system at the Center of Molecular Imaging (CMI) of the University of Michigan. Xenolight luciferin substrate (Perkin Elmer) at 630 µM was added to each well 10 minutes prior to imaging. Bioluminescence measurements using the IVIS™ Spectrum was performed every 24 hours after day 2 of the culture. Every 2 days, half of the media (75 µL) was collected and replaced with fresh, pre-equilibrated GM containing luciferin after imaging.

For single-cell bioluminescence, NLuc reporters were used and individual 10X gels were imaged using an LV200 Bioluminescence Imaging System (Olympus). To minimize the floating, gels were transferred to a 30 mm dish with optical bottom. Sufficient GM containing NanoGlo® Live Cell Substrate was transferred from the original 96-well plate to cover the gel and PBS was added to the surroundings to prevent evaporation. All single-cell luminescence images were acquired with a 5-minute exposure time and a 200 EM gain. Brightfield and luminescence images were merged using ImageJ (Schneider et al. 2012). Individual gels were transferred back

to the original 96-well plates for continuous cultures. LV200 imaging was performed every 48 hours. Immediately after imaging, half of the media (75 µL) was collected and replaced with fresh, pre-equilibrated GM.

2.6 Hormone measurements

Collected media from both 10X and 5X gels were used for subsequent hormone and cytokine studies. Upon finishing a culture, we examined the survival of follicles in 10X and 5X conditions. Based on the terminal diameters, 2 wells per condition were pooled together to meet the minimum medium volume requirements. A sample size of 4 per time point per condition was analyzed for androstendione (A4), estradiol (E2) and progesterone (P4). The hormone assays were performed at the University of Virginia Center for Research in Reproduction Ligand Assay and Analysis Core and was supported by the NSF CAREER Award (#1552580) to AS.

2.7 Statistical analyses

Statistical analyses for the luciferase production and hormone data were performed in GraphPad Prism 7. For luciferase production, linear regression was performed. For hormone data, two-way ANOVA with repeated measure and Sidak's multiple comparisons tests were performed. Values of $p<0.05$ were considered significant. TF activity data was background subtracted, normalized to the median TA control value and log transformed as previously described (Decker et al. 2017). Differences in means between time points and conditions were evaluated by fitting an empirical hierarchical Bayesian linear model using the *limma* R package (Smyth et al. 2005). False discovery rate correction was used on the calculated p-values (Benjamini and Hochberg 1995). A p-value of <0.05 was considered to be statistically significant for the TF activity measurements.

3. Results

3.1 The number-dependent pattern of follicle survival and growth was preserved after transduction.

As has been previously observed, primary follicles starting between 85 – 100 μm cultured in groups show a number-dependent pattern of survival and growth when cultured in vitro (Hornick et al. 2013). After lentiviral transduction, the pattern was preserved, indicating that the transduction did not affect follicle development in vitro. Similar to what has been reported, in 10X groups, we observed a higher follicle survival rate (70%) after 12 days of in vitro culture in alginate, compared to a 42.9% survival rate in 5X groups (Fig. 18B). In addition to an increased survival rate, 10X groups also demonstrated improved follicle growth (Fig. 18 A and C). Morphologically, after 8 days of culture, follicles in 10X groups showed a greater overall increase in sizes and a greater number of follicles developed an antrum (Fig. 18A) compared to those cultured in groups of 5. Additionally, by Day 8 of eIVFG, average diameters of follicles in the 10X group reached 250.4 ± 66.4 μm (mean ± S.D.), compared to an average diameter of 215.1 ± 63.4 μm in the 5X groups (Fig. 18C). The differences in average follicle diameters became more significant as the culture progressed to Day 10 ($p=0.0017$) and Day 12 ($p<0.0001$) (Fig. 18C). The growth and development of the transduced follicles was consistent with what has been established (Hornick et al. 2013) and our controls, which demonstrated that lentiviral transduction did not affect normal folliculogenesis and can be applied to study the activities of TF activities during folliculogenesis.

3.2 Hormone profiles of 5X and 10X follicles evidenced the number-dependent manner of follicle development.

To understand the underlying mechanism of the number-dependent development pattern of follicles, we measured androstenedione (A4), estradiol (E2), and progesterone (P4) secreted by 5X and 10X follicles cultured in alginate at various time points (Fig. 19) to compare the follicle functional development between the groups. Overall, the concentrations of all hormones increased as the eIVFG progressed and follicles increased in sizes. The levels of E2 followed the general trend of increasing as follicle grew in the culture (Fig. 19B). We did not see any significant difference in E2 levels between 5X and 10X groups during the first 8 days of culture. However, the differences became significant on Day 10 ($p=0.0002$) and Day 12 ($p<0.0001$) of culture, indicating a more successful functional development of follicles cultured as groups of ten. The significantly higher E2 level was consistent with the much larger sizes of 10X follicles

on Day 10 and Day 12. The levels of P4 also followed the general trend that the concentration of P4 increased as average follicle diameter increased (Fig. 19C). We did not observe any significant difference between 5X and 10X follicles during the first 10 days of culture. On Day 12 of eIVFG, P4 reached 26.35 ± 12.53 ng/mL, which was significantly higher ($p<0.0001$) than that in the 5X follicles (5.40 ± 3.21 ng/mL). However, we did not observe any significant differences in A4 levels between 5X and 10X follicles at any time point (Fig. 19A). The similar levels of A4 could be due to similar starting diameters of follicles in either 5X or 10X groups: 98.7 ± 6.0 μm (10X) and 99.5 ± 6.0 μm (5X). Given the similar initial diameters, it was highly likely that follicles from both groups started with a similar number of theca cells that synthesize A4 during folliculogenesis. However, the ratio of E2/A4 was healthier in 10X follicles, which indicated that the granulosa cells in 10X follicles were healthier as evidenced by the significant increase of E2 converted from A4.

Taken together, culturing primary follicle in groups also supports the functional development in vitro, in addition to their overall survival and growth. As indicated by the number-dependent survival and growth pattern, 10X follicles secreted significantly more E2 towards later time points of the culture, consistent with their significantly larger sizes accordingly. The significantly higher P4 levels in 10X follicles on Day 12 of the culture and their larger terminal sizes are indicative of oocyte maturation potentials.

3.3 Luciferase expression from normalization vector was constant during the cultures.

In order to quantify TF-specific report activities, we first examined bioluminescence expression using normalization vectors. As a result of enzymatic digestion, isolated follicles were likely to have fragmented basement membranes, thus allowing lentiviruses to transduce granulosa cells. To ensure luciferase expression by the reporter, after 2 days of culture, we applied single-cell bioluminescence imaging technique to examine localized luciferase expression in transduced follicles (Fig. 20A). As shown by the merged image in Fig. 20A, granulosa cells towards the peripheral of the follicles had a greater rate of the lentiviral transduction. And the luciferase expression was localized in the confined areas of transduced granulosa cells. To monitor the

stability of luciferase expression from the normalization vector, we quantified the amount of total DNA and the intensity of bioluminescence by lysing 10X follicles every 2 days. As expected, the amount of total DNA significantly decreased on Day 6 of eIVFG ($p<0.0001$) compared to the baseline level on Day 2. This decrease coincided with the time of antrum formation, when granulosa cells undergo apoptosis to give rise to a fluid-filled cavity. Similarly to the amount of total DNA, the amount of luciferase measured from lysed follicles also significantly decreased on Day 6. Normalized to the amount of total DNA, the amount of luciferase produced by transduced follicles was constant (slope of linear regression formula was not significant than 0). This stable expression of luciferase indicated that transduced granulosa cells were proliferating at the same rate as the non-transduced one, which manifested as the preserved number-dependent manner of folliculogenesis (Fig. 18). More importantly, this stability demonstrated the rationale and feasibility of using normalization vectors as baseline measurements of TF activities.

3.4 Differential TF dynamic activities further reflected the number-dependent manner of primary follicle development in vitro.

To investigate specific TF activities as a result of different paracrine cues in the different culture environments, we delivered TF-specific reporter to follicles in parallel with the normalization vector. It has been shown that increased binding of TFs at the TRE results in increased luciferase production and a proportional increase in luminescence when an excess of substrate is added during imaging, thus providing a quantitative measure of relative transactivation (Decker et al. 2017). We investigated four TFs: p53, NF-κB, Gli and HIF1, to evaluate their effects on folliculogenesis. Background subtracted bioluminescence signals were normalized to baseline levels established by normalization vectors. Therefore, fluctuations observed as TF activities reflected the dynamic changes in the amount of specific TFs present at a given time point.

As a cell cycle regulator, in normal dividing cells, p53 transiently increases in temporal association with checkpoints of cell cycles (Kastan et al. 1992). As cells proceed through their cycles, p53 fluctuates. Indeed, we observed levels of p53 fluctuating during cultures in both 5X and 10X groups (Fig. 21A). Additionally, the levels of p53 in 10X follicles on Day 5 of culture

was significantly higher (p=0.013) than on Day 4 of culture, indicating a large number of cells proceeding through cell cycle. This trend was consistent with the slightly larger sizes of 10X follicles compared to 5X ones. We did not see any significant differences of p53 levels between 5X and 10X follicles, indicating that granulosa cells from 5X and 10X follicles were growing comparably on cellular levels, thus no significant differences in follicle diameters, especially during the first 8 days of culture.

The hedgehog pathway has recently been shown to be possible markers of pre-thecal cells and potentially involved in inducing theca cell differentiation (Young and McNeilly 2010). Hedgehog genes were shown to activate glioma-associated oncogene homolog (Gli) transcription factor in thecal cells and are perhaps related to ovulation (Young and McNeilly 2010). Interestingly, the levels of Gli peaked at different time points between 5X and 10X groups. In 10X follicles, Gli reached its peak level at Day 5 of the culture, compared to a much later Day 10 of culture in 5X follicles (Fig. 21C). Considering the time cells take to execute the changes in TFs, the earlier Gli peak in 10X follicles could lead to the significant increase of P4 on Day 12 of culture in 10X follicles. Due to the delay for TFs to take effects, even though Gli also peaked in 5X follicles, the much later peak did not result in a significant increase of P4 during the culture period.

Nuclear factor-kappa B (NF-κB) controls the expression of gene products that affect important cellular processes, such as cell survival, cell cycle, and apoptosis (Yeung et al. 2004). Transcriptionally active NF-κB has been identified as an inhibitor of apoptosis (Karin and Lin 2002). Interestingly, we observed an increase of NF-κB levels in 10X follicles on Day 5 of culture, compared to a much later peak of NF-κB in 5X follicles on Day 8 (Fig. 21B). Taken together with the antrum formation on/around Day 6 of eIVFG, we hypothesized that hypoxia as a result of cell proliferation in follicles could lead to the differential antrum formation rates between 5X and 10X follicles, thus the differences in survival and terminal sizes.

We subsequently examined the dynamic activities of hypoxia-inducible factor-1 (HIF1), together with NF-κB (Fig. 21D). Levels of HIF1 in 10X follicles significantly increased ($p=0.013$) on Day 6 of culture, when antrum formation is about to happen. Interestingly, HIF1 peak happened 1 day later than the peak of NF-κB in the same group of follicles, indicating the hypoxic stress on follicles as a consequence of cell proliferation. The hypoxic stress, in return, forced a portion of granulosa cells to undergo apoptosis to form antrum, thus the more significant differences in subsequent follicle survival and growth after the first 6 days of culture (Fig. 18 B and C). The consequences of apoptosis were also observed in the amount of total DNA and luciferase expression data (Fig. 20 B and C), as both values significantly decreased as cells undergoing apoptosis during antrum formation. Yet, the normalized luciferase production value remained constant even at this interesting time point, indicating that both transduced cells and non-transduced cells underwent apoptosis at the same portion. This implication further confirmed that lentiviral transduction did not affect normal cellular behaviors.

Interestingly in 5X follicles, the peak levels of NF-κB and HIF1 both happened on Day 8. The overlap of the counter-acting effects of TFs could offset each other, thus resulting in a much less successful attempt of follicles to form antrum during eIVFG. Indeed, we did not observe as prominent antrum formation in 5X follicles. Possibly due to this reason, 5X follicles demonstrated a lower survival rate and much smaller terminal sizes after 12 days of culture (Fig. 18).

4. Discussion

We have, for the first time, demonstrated the application of a lentiviral gene delivery system to mouse ovarian follicles to study the dynamic processes of folliculogenesis. The proposed approach investigated the dynamic activities of TFs during folliculogenesis and established their roles in the growth of early stage ovarian follicles in vitro. The study of the synchrony between the quantity and temporal distribution of TFs helped provide insights to the number-dependent manner of early stage follicles as a result of differential paracrine cues in the culture

environments. This knowledge may be used for developing xeno-free, cell-free culture systems as alternative fertility preservation options.

The lentiviral transduction of ovarian follicles did not affect any cellular behaviors, thus serving as a powerful tool to probe for underlying mechanisms of the number-dependent manner of primary follicle development in vitro. By delivering in parallel TF-specific reporters with normalization vectors, we were able to monitor the dynamic activities of selected TFs (p53, NF-κB, Gli, and HIF1) as a result of different paracrine cues in the culture environment. Our results supported that folliculogenesis is a carefully orchestrated event. Better coordinated TF quantity and temporal pattern in 10X follicles implied greater survival rate and better growth and functional development, compared to 5X follicles. These phenotypical differences between conditions were subsequently evidenced by monitoring follicle diameters and measuring hormones in the culture media. Taken together, the incorporation of TRACER provides a method for non-invasive and dynamic quantification of signaling pathways when investigating mechanisms.

Key factors and their roles during folliculogenesis have been identified and established using the latest developments in molecular biological technologies. The p53 family proteins have been shown to be involved in regulating granulosa cell function and oocyte quality and in protecting the fidelity of female germ cells during meiotic arrest and embryonic implantation (Hu et al. 2011; Liang et al. 2013; Makrigiannakis et al. 2000). The nuclear factor-κB (NF-κB) takes part in the regulation of the granulosa cell fate during ovarian follicular development (Chu et al. 2004; Wang et al. 2002). As a key player in the hedgehog signaling pathway, Gli has been described to be transcriptionally active in theca cells by stimulating theca cell proliferation and androgen biosynthesis (Spicer et al. 2009; Wijgerde et al. 2005). However, in order to capture the complexity of mechanistic pathways, we also need to understand the broad range of temporal activation profiles of TFs in response to the paracrine cues in the environments. Our approach provided large-scale, quantitative measurements of the dynamic activities of TFs in real time. And our results on p53, NF- κB, and Gli acquired from TRACER were consistent with what has

been previously established. More importantly, our results provided the real-time profiles of selected TFs during folliculogenesis, complementing current understanding of the dynamic activities of TFs.

Oxygen tension in the culture environment also has a key role in regulating cellular behaviors. It is well established that hypoxia-induced factor (HIF)-1 is a key mediator of hypoxic response (Ferrara et al. 2003; Semenza 2002). Specifically for follicles, it has been shown that hypoxic condition is an integral part for the survival and growth of early secondary stage follicles in vitro (Makanji et al. 2014) and is essential for initiation of the antrum formation, which is consistent with our results. Additionally, the levels of HIF1 increased before antrum formation and immediately decreased afterwards, indicating that follicles were cultured in low O_2 conditions until antrum formation and were subsequently exposed to higher O_2 during antral stage. Consequently, the 10X follicles showed higher survival and better growth. This phenomenon was supported by previous studies investigating follicles cultured in hypoxic conditions (Makanji et al. 2014). Interestingly, the upregulation of HIF1 in our system as a potential consequence of NF-κB upregulation was the opposite of what was previously observed in other cells (Walmsley et al. 2005). However, the difference could be due to the types of cells and the preservation of three-dimensional (3D) architecture of the ovarian follicles. The observed relationship in our study mirrored what happens in vivo when antrum forms during folliculogenesis, as hypoxic stress can be more prominent in a 3D setting.

Collectively, our results reflected the dynamic activities of TFs in real time. Comparing TF activities from 5X and 10X conditions, our data suggested a critical but sometimes overlooked dynamic synchrony between the quantity of specific TFs and their temporal distribution. Compared to traditional ways of probing for TFs, TRACER provides large-scale, quantitative measurements of TFs in real time. Via lentiviral transduction, TRACER is non-invasive and bioluminescence can be monitored continuously without lysis of cells and/or termination of cultures. More importantly, as the TF-specific reporters are integrated to the genome of transduced cells, quantitative measurements acquired from TRACER reflect the transcriptionally

active TFs, which may be hard to differentiate by other methods. The advantages of TRACER can enable new approaches to probe for essential TFs as cells organize into structures. The arrays may also find utility for investigating mechanisms regulating normal and abnormal tissue growth, biomaterial design, or as a platform for screening therapeutics.

In conclusion, we demonstrated a non-invasive approach to investigate the dynamic activities of selected TFs as a result of paracrine cues in different ovarian follicle in vitro culture environments. Our results agreed with what was previously established and provided additional important insights to the synchrony of the quantity of TFs and their temporal distribution. Considering the advantages of our approach, the arrays can be used for investigating numerous TFs as well as underlying signaling transduction and mechanisms in real time.

CHAPTER

VI. Conclusions

In adult females the number of ovarian follicles determines ovarian function and fertility. Healthy ovaries produce mature eggs and hormones that play important roles in maintaining fertility and female body functions. Follicles are extremely vulnerable to the environmental factors such as toxic drugs, pollution, radiation and aging, and cannot regenerate if damaged. Depletion of primordial follicles leads directly to premature ovarian failure, infertility and menopause.

Novel bioengineering solutions, such as in vitro culture and maturation of immature ovarian follicles to obtain fertilizable eggs present an important solution to a clinical problem. Theses novel solutions will emerge from research into biomaterials, drug delivery technologies, and engineering of the follicle microenvironment. By examining multiple aspects of the in vitro mouse ovarian follicle environment, this dissertation provides new understanding of the bioengineering principles in numerous in vitro follicle culture applications and in the field of reproductive biology more broadly. Folliculogenesis is a carefully orchestrated event that requires the precise coordination of various systems and/or tissues in vivo. A better understanding of this complicated biological process necessitates greater integration of molecular and cellular mechanism behind the processes (endocrine, paracrine, and autocrine regulation). With mechanistic considerations (i.e., bottom-up approach), our proposed investigation of dynamic activity of transcription factors, the TRACER approach, to decipher folliculogenesis in vitro provided experimental data (top-down approach) from a high-throughput approach to develop mechanistic models and underlies the field of systems biology.

Aiming to merge computational techniques and experimental data to uncover the mechanisms, TRACER provides a unique opportunity to quantitatively and dynamically probe for transcriptionally active transcription factors (TFs) networks. In the last two decades, there has been an explosion in the "omics" world, including transcriptomics, proteomics (Memili et al. 2007; Peddinti et al. 2010), metabolomics (Revelli et al. 2009), and epigenomics (Vanselow et al. 2010). Microarrays also have been extensively used to study folliculogenesis in isolated ovaries (Hasegawa et al. 2009), follicles (Yoon et al. 2006), oocytes (Pan et al. 2005), and granulosa or theca cells (Skinner et al. 2008) and in untreated (Sasson et al. 2003; Sriraman et al. 2006) or treated cell lines (Chin et al. 2002; Hernandez-Gonzalez et al. 2006; Wood et al. 2003). Unfortunately, most of the studies have limited themselves to identifying the most important gene(s) based on up- or down-regulations. These quantitative measurements acquired from static techniques were based on cell lysis and measurements of abundance, thus missing the dynamic changes over time and possibly consequent classification accuracy of the models. TRACER provides a distinct advantage over comparable techniques by serving as a platform to capture the dynamic changes of TFs. By measuring TF activities at multiple time points in a live cell assay, TRACER can be used to monitor continuous changes in cells and/or cultures, allowing for more accurate reflection of cellular and molecular processes. Together with a combination of analytical approaches, such as Principle Component Analysis (PCA) and Partial Least Squares Discriminant Analysis (PLSDA), key molecules involved in paracrine and autocrine signaling in the follicle can be identified in a systematic way to inform the development of universal media formulations to support in vitro follicle or organ culture. More importantly, construction of networks of interacting factors will reveal unknown relationships (or "signatures"), allowing for more accurate interpretation of the underlying mechanisms of complicated biological processes, such as folliculogenesis. With the mechanistic understanding of folliculogenesis and with the recent developments in the field of induced pluripotent cell that can convert adult skin cells back into an embryonic pluripotent stem cell, we can aim to recreate the process of de novo gametogenesis, restore gonadal function and fertility.

Additionally, proposed networks established from TRACER can be tailored to specific time points during in vitro follicle culture, thus having potentials to construct dynamic models to

predict the impacts of different environmental insults to follicle development in vitro. We pioneered in this dissertation to develop a novel biomaterial-based toxicology assay to study the effects of environmental toxicants on follicle health. With an in vitro follicle culture environment in FA-IPN that mimics the in vivo, we developed an image analysis based high-throughput system to detect toxicity of chemicals on cultured secondary follicles using either individual toxicants or mixtures. Moving forward, we can incorporate TRACER to better understand the underlying mechanisms of toxicity to follicles, which can also help us discover and predict synergistic and antagonistic effects and find potential therapies to mitigate the adverse effects on the female reproductive system.

Finally, the design of a biomimetic in vitro culture system and the application of TRACER could enable the translation of results from mouse models to humans to inform the development of fertility preservation techniques. In this dissertation, we demonstrated that adipose derived stem cells (ADSCs) promote early stage follicle development in vitro. With the autologous source of feeder cells and the xeno-free, biomimetic poly(ethylene glycol) (PEG) scaffold, our results showed great potential of translating to humans. Ultimately, we would like to culture human primordial follicles in a cell-free xeno-free environment to maturation. Looking ahead, applying TRACER could help us achieve this goal by serving as a powerful tool to better understand the bi-directional crosstalk between feeder cells and early stage follicles. By identifying key factors during different stages of folliculogenesis, we could supplement culture media in order to replace feeder cells. This advance in culture scheme will help accelerate translating knowledge we have learned in other animal models to human, thus providing additional fertility preservation options for patients regardless of their ages.

Taken together, using a mouse model, this dissertation provides a new tool to better understand the dynamic changes of key factors in in vitro folliculogenesis. This knowledge could enable the translation of results from mouse models to humans: to predict the impacts of different environmental insults to follicle development and to inform the development of fertility preservation techniques. Using a systematic approach, we provided a holographic view of new

understanding of the bioengineering principles in numerous in vitro follicle culture applications and in the field of reproductive biology more broadly.

APPENDICES

Appendix A.

Three-dimensional hydrogel-based culture to study the effects of toxicants on ovarian follicles

Previously accepted as a chapter in *Methods in Molecular Biology*

1. Introduction

Mammalian ovaries contain a finite number of follicles. As the functional units of the ovaries, ovarian follicles are responsible for a female's fertility and ovarian endocrine functions. *In vitro* follicle growth (IVFG) is an experimental tool that recapitulates key events of mammalian oogenesis and folliculogenesis *in vivo*. By monitoring follicle survival and growth, antral cavity formation, steroidogenesis and the ability of producing a mature egg, IVFG can serve as a accurate bioassay for studying essential biological processes related to female reproductive functions (Cortvrindt and Smitz 2002; Lenie and Smitz 2009; Peretz and Flaws 2013; Rotroff et al. 2013; Xu et al. 2015).

Various IVFG culture systems have been developed aiming to grow follicles from an immature stage to fully mature and fertilizable oocytes, which have been successful in mouse, rat, bovine, goat, non-human primates and human (Hirao et al. 1994; Jin et al. 2010; Laronda et al. 2014; McLaughlin and Telfer 2010; O'Brien et al. 2003; Silva et al. 2015; Spears et al. 1994; Xiao et al. 2015; Xu et al. 2013b). Three-dimensional IVFG systems in particular, provide physical support to preserve the architecture of developing follicles and maintain oocyte-somatic cell connections, thus promoting survival of early stage follicles (Shea et al. 2014). Encapsulated in either natural biomaterials such as alginate (Brito et al. 2014; Xu et al. 2006) and fibrin-alginate

(Shikanov et al. 2009, 2011b) or synthetic macromers such as polyethylene glycol (PEG) (Shikanov et al. 2011a), ovarian follicles are cultured in in-vivo-like conditions, allowing for continuous morphological, genetic and biochemical sampling.

An important application of IVFG is serving as a bioassay for reproductive toxicology screening. Safety information on new chemicals that are introduced into the US market each year is lacking due to the cost and time required for animal testing. Performing a complete set of regulatory tests for a single chemical requires thousands of animals and costs millions of dollars (Xu et al. 2015). IVFGs have been employed to determine how follicles are affected by drugs/their metabolites, and environmental factors, such as doxorubicin (DXR), organochloride pesticides (methoxychlor (MXC)) and environmental pollutants (7,12-dimethylbenz[a]anthracene (DMBA)). Compared to animal studies, IVFG represents a more simple and rapid tool that can be used to screen the effects of potential ovotoxic compounds on reproductive function and health (Cortvrindt and Smitz 2002; Stefansdottir et al. 2014; Xu et al. 2015), which can be useful to provide guidance to regulatory agencies as well as expectant mothers.

In this chapter, we describe a fibrin-alginate based hydrogel system (Shikanov et al. 2009) that has been developed for IVFG. In the fibrin alginate interpenetrating network (FA-IPN) system, the slowly degrading alginate is biologically inert to ovarian tissue, thus providing structural support for the follicle. Ovarian follicles encapsulated in FA-IPN secrete plasminogen activators (Beers 1975; El-Sadi et al. 2013), and can therefore degrade the fibrin component of the FA-IPN. The semi-degradable FA-IPNs provide a dynamic mechanical environment that facilitates follicle outward expansion while maintaining follicle architecture. Such systems have also been proven to enable IVFG in larger species such as baboon (M Xu et al. 2011) and rhesus macaque (Macaca mulatta) (Xu et al. 2013a). The degraded fibrin appears as an optically clear ring around the encapsulated follicle as the follicle culture progresses (Shikanov et al. 2009, 2011b; Zhou et al. 2015), correlating with the health and survival of the encapsulated follicles. Furthermore, a calibrated addition of aprotinin, which is a plasmin inhibitor, to the culture media results in controlled fibrin degradation and therefore broadens the applications for this system (Zhou et al.

2015) to screen for potential ovotoxicity induced by drugs and/or their metabolites and environmental toxicants.

2. **Materials**

2.1 General materials

1. One pair of straight fine scissors, 26 mm.

2. One pair of straight fine scissors, 24 mm.

3. One pair of straight forceps, #5.

4. One pair of curved forceps, #7.

5. Dissecting microscope with a heating stage.

6. Inverted imaging microscope with imaging software such as ImageJ.

2.2 *Ovarian follicle isolation*

1. First generation female hybrid offsprings of 2 inbred strains: C57BL/6JRccHsd (maternal) CBA/JCrHsd (paternal), 12 – 14 days of age.

2. 70% Ethanol and dissecting mats.

3. Dissection media (DM): Leibovitz's L-15 medium, heat inactivated fetal bovine serum (FBS), and Pen/Strep.

4. Maintenance media (MM): minimum essential media α (αMEM), FBS, and Pen/Strep.

5. Two 35 × 10 mm sterile petri dishes.

6. One 60 × 10 mm sterile petri dishes.

7. Center Well Dishes for IVF: use one (1) dish per each ovary.

8. Sterile 1.5 mL microcentrifuge tubes.

9. Two sterile insulin syringes with 27 ½ G needles.

2.3 Ovarian follicle encapsulation

1. Dulbecco's phosphate-buffered saline 1X (DPBS, no calcium, no magnesium).

2. Sterile alginate aliquots: Nalgin MV-120 alginate, activated charcoal.

3. Sterile fibrinogen and thrombin aliquots

4. Tris buffered saline (TBS) 25 mM with 0.15 M NaCl: Tris-HCl, Tris Base, and NaCl.

5. TBS 25 mM with 50 mM $CaCl_2$: Tris-HCl, Tris Base, $CaCl_2$•2 H_2O, and NaCl (crosslinking solution).

6. Baxter Tisseel Fibrin Sealant: Sealer Protein Solution (fibrinogen, total protein: 96 – 125 mg/mL, with synthetic aprotinin: 2250 – 3750 KIU/mL) and Thrombin Solution (human thrombin: 400 – 625 IU/mL with $CaCl_2$: 36 – 44 µmol/mL).

7. Sterile 1.5 mL microcentrifuge tubes.

8. Center Well Dishes for IVF dishes.

9. Steriflip conical tubes.

10. Sterile cellulose membrane syringe filters.

2.4 Ovarian follicle culture

1. DPBS

2. Growth media (GM): αMEM, 1mg/mL Fetuin, 3mg/mL bovine serum albumin (BSA), 5 µg/mL insulin, 5 µg/mL transferrin, and 5 ng/mL selenium, and 10 mIU/mL recombinant human follicle stimulating hormone (rhFSH).

3. Sterile aprotinin aliquot: aprotinin, 1X DPBS.

4. Sterile 1.5 mL microcentrifuge tubes.

3. Methods

All dissections should be performed in L15-based media (buffered for ambient air), on a 37 ˚C (temperature control) heated stage, and on a clean bench (laminar flow hood) to minimize potential contamination. Follicle isolation should take no longer than 30 minutes per ovary. For optimal results, keep the resected tissue outside the incubator for less than 1 hour. To minimize pH changes, limit exposure of αMEM-based media to ambient air. All animals are treated in accordance with the guidelines and regulations set forth by the national and institutional IACUC protocols.

3.1 Ovarian follicle isolation

1. Prior to the beginning of the experiment, sterilize all the equipment by spraying 70% ethanol and air drying on the clean bench or in the laminar hood.

2. Prepare DM by supplementing L-15 with 1% (v/v) FBS and 0.5% (v/v) Pen/Strep. Gently invert to mix well (see Note 1). Warm up the DM to 37 ˚C in a water bath (see Note 2).

3. Prepare MM by supplementing αMEM with 1% (v/v) FBS and 0.5% (v/v) Pen/Strep. Gently invert to mix well (see Note 3). Prepare IVF dishes with 1 mL of MM in the center ring and 3 mL of MM in the outer ring. Utilize one IVF dish for each isolated ovary. In addition, prepare another 35 mm dish with 1 mL of MM. Pre-equilibrate all the dishes for 20 minutes in the incubator prior to the beginning of the isolation.

4. Euthanize one female (12 – 14 days of age), according to the institutional IACUC-approved protocols. Remove both ovaries from the animal. In order to assure minimal damage to the ovaries, remove parts of the oviduct and uterus around the ovary as well. Place roughly dissected ovaries into a 35 mm dish with DM.

5. Use a dissecting scope and insulin syringes to separate the ovaries from uterus, fat pad and bursa (Fig. 22A) by placing one needle at the intersection of the bursa and the oviduct to anchor the reproductive tract in place, and dissecting with the other needle. Place the second needle directly next to the first but only grip the thin membrane of the bursa. Carefully nick the bursa to expose the entire ovary. Transfer clean ovaries using curved forceps or a pipette with a blunt tip (Fig. 22B) into the 35 mm dish with pre-equilibrated MM. If using forceps, try to not squish or damage the ovaries by applying excessive force. Repeat this process for both ovaries. Transfer one ovary to a 35 mm dish containing warm MM and place it in the incubator. Keep the other ovary in DM and start follicle isolation (Xu et al. 2006).

6. Set a timer for 30 minutes. Start isolating follicles by using two Insulin syringes with 27 ½ G needles. With one syringe in your non-dominant hand, anchor the ovary to the bottom of the dish. And with a syringe in your dominant hand, gently tease and "flick" individual follicles from the ovary (Fig. 23A). Try to remove most of surrounding ECM without puncturing the follicle. Dissect out as many follicles as possible within the 30 minutes. Transfer intact isolated secondary follicles (120 – 135 μm in diameters, 2 – 3 layers of granulosa cells) to the outer ring of an IVF dish (Fig. 23B and 23C) with MM. When transferring, use a P10 pipette to carefully pick up isolated follicles with minimum media. To avoid follicles sticking to the walls of the same pipette tip and/or to each other, aspirate a little media first to the very end of the tip and while aspirating the follicles, alternate between media and each follicle. When expelling the follicles into the outer ring of the IVF dish, use a sweeping motion such that the follicles in the tip will end up at different spots to avoid sticking to each other (see Note 4).

7. Repeat steps 3.1.1 – 3.1.6 for the remaining ovaries to complete the isolation.

3.2 Ovarian follicle encapsulation (see Note 5)

1. The alginate component of the FA-IPN is Nalgin MV-120 sodium alginate. To prepare sterile alginate aliquots (see Note 6), dissolve alginate in deionized water at a concentration of 0.1% (w/v) (see Note 7). Add activated charcoal [0.5 g charcoal/(g alginate)] to the alginate solution to remove organic impurities. Stir the mixture at room temperature for 15 minutes and let settle overnight. Following the charcoal treatment, sterile filter alginate solution through 0.20 μm fast

vacuum filtration units. Transfer the sterile alginate solution into Steriflip conical tubes to lyophilize. Aliquot the lyophilized sterile alginate into sterile 1.5 mL microcentrifuge tubes. One day before follicle isolation, reconstitute the sterile alginate aliquot with 1X DPBS to achieve 0.8% (w/v). Leave in the laminar hood overnight to completely dissolve (see Note 8). On the day of experiment, vortex the alginate solution for 30 seconds to thoroughly mix. Briefly centrifuge it afterwards to prevent microbubbles.

2. Prepare 25 mM TBS with 0.15 M NaCl by dissolving 3.5618 g of Tris-HCl, 0.2786 g of Tris Base, and 8.7750 g of NaCl in 1 L of deionized water. Titrate pH to 7.4 at room temperature. Sterile filter a proper amount of the solution before use.

3. Prepare the fibrinogen according to kit instructions (see Note 9). First, reconstitute fibrinogen to 100 mg/mL (total protein) with the provided Fibrinolysis Inhibitor Solution containing 3000 KIU/mL aprotinin. Then, dilute the reconstituted fibrinogen down to 50 mg/mL with additional 25 mM TBS with 0.15 M NaCl. Aliquot the diluted fibrinogen to sterile 1.5 mL microcentrifuge tubes as 100 µL/tube. Reconstitute thrombin to 500 IU/mL in the 40 µmol/mL $CaCl_2$ solution provided in the kit. Aliquot 50 µL/tube thrombin to sterile 1.5 mL microcentrifuge tubes (see Note 10).

4. Prepare 25 mM Tris buffered saline (TBS) with 50 mM $CaCl_2$ as the crosslinking solution. To make 1 L of this solution, dissolve in the deionized water the following: 3.5618 g of Tris-HCl, 0.2786 g of Tris Base, 7.3505 g of $CaCl_2$•2 H_2O (adjust this amount if using anhydrous $CaCl_2$), and 2.9220 g of NaCl (see Note 11). Titrate pH to 7.4 at room temperature. Sterile filter the solution prior to use.

5. After all the isolated follicles are transferred to MM (see Note 12), thaw fibrinogen and thrombin aliquot(s) based on the number of follicles isolated. To prepare fibrinogen/alginate solution (FA) for encapsulation, mix fibrinogen (50 mg/mL), 0.8% alginate MV (vortex prior to use), and 1X DPBS at 1:1:2 ratio (see Note 13). Pipette up and down to thoroughly mix (see Note 14). It is normal if the mixed solution appears milky. Dilute thrombin stock solution with sterile solution of 25 mM TBS with 50 mM $CaCl_2$ to reach a final concentration of thrombin at 25 mg/mL. Transfer this working thrombin solution to the inner ring of a new IVF dish. In the outer ring, put a droplet of ~10 – 20 µL of FA as the washing droplet. Prepare another 100 µL of

FA droplet at a different spot in the outer ring of the same IVF dish as the encapsulating droplet (Fig. 24) (see Note 15).

6. Inspect the follicles meant for encapsulation under 50X – 80X magnification. Use the following criteria to identify healthy follicles: 1) 2 – 3 layers of granulosa cells; 2) in the right size range; 3) with no separation between the oocyte and granulosa cells; 4) have round oocytes. Some theca cells or extra extracellular matrix are fine (see Note 16).

7. Using a dissecting scope, carefully pick up a good follicle using a P10 pipette with minimum media and transfer this follicle to the wash droplet (Fig. 24A). Gently pipette it up and down to remove excess media from the follicle before transferring it to the encapsulating droplet (see Notes 17 and 18). Work quickly because the FA solution is not viscous enough to prevent follicles settling to the bottom of the dish. If the follicle falls through the droplet of FA solution, it will be difficult to pick it back up and encapsulate because follicles tend to stick to the plastic.

8. After transferring the follicle to the encapsulating droplet, use a P10 pipette set to 7.5 µL. First, gently fill about half of the tip (~3.5 µL) with FA. Then, aspirate the follicle and complete the rest of the 7.5 µL with more FA.

9. Slowly expel the FA/follicle from the tip (at a ~45˚ angle over the thrombin/Ca^{2+} solution), so it hangs like a drop from the end of the tip (Fig. 24B). Very gently touch the very bottom of the drop to the thrombin/Ca^{2+} solution to form FA-IPN bead (see Note 19). Watch the position of the encapsulated follicles (Fig. 25B and 25C) before the beads are fully crosslinked and turn opaque (see Note 20). Sometimes the beads may be empty (Fig. 25A) as follicles may get stuck in the pipette tips. If the pipette tip touches the crosslinking solution while dropping the bead, the bead may end up with a hole (Fig. 25D).

10. Allow the bead to crosslink for 2 minutes (see Note 21). In the meantime, repeat steps 3-5 with the remaining follicles. Transfer fully crosslinked beads (Fig. 25C) to the 60 × 10 mm dish containing pre-equilibrated MM using a pair of curved forceps (Fig. 25D) (see Note 22).

11. Use a new 10 µL tip for each encapsulation – this prevents follicles sticking to the used tip and the possibility of calcium blocking the tip that accidentally comes in touch with the

crosslinking solution. Also, changing the tips will help prevent potential cross-contamination during encapsulation and will help maintain a healthy culture.

12. Alternate between the IVF dishes with isolated follicles. Keep only 1 IVF dish outside the incubator for no longer than 10 minutes (see Note 23). Even though not all of the follicles from a specific IVF dish will be encapsulated in one round, put the dish back to the incubator to let the MM re-equilibrate. In the meantime, move on to a different dish to continue encapsulation. Repeat steps 3.2.5 – 3.2.11 until all the isolated follicles have been encapsulated and all the beads are transferred to the 60 × 10 mm dish with pre-equilibrated MM (see Note 24). Count the number of beads and write the number on the lid.

3.3 Ovarian follicle culture

1. Mouse ovarian follicles are cultured in αMEM-based GM. To make GM, supplement αMEM (see Note 5.24) with 10 mg/mL Fetuin, 3 mg/mL BSA, 5 µg/mL insulin, 5 µg/mL transferrin, and 5 ng/mL selenium. Then, sterile filter the solution using 0.2 µm cellulose acetate syringe filter. Add 10 mIU/mL rhFSH and invert gently to mix (see Notes 25, 26, and 27).

2. To prepare aprotinin aliquots, calculate the amount of aprotinin using the information provided by the supplier (see Note 28). According to the total amount in the container, dissolve all the powder in sterile DPBS to obtain a concentration of 1 TIU/mL. Aliquot this stock solution as 50 or 100 µL aliquots and store at -20 ˚C (see Notes 29 and 30).

3. Count the number of beads by summing the numbers from step 12 in 3.2. Based on the total number of the follicles, calculate the desired volume of GM: V (GM) = the number of follicles × 100 µL × 105% (5% more for evaporation). Equilibrate the GM in a dish. Prepare 96-well plates as in Fig. 26. The center wells of the plate should be filled with GM (100 µL/well), 5 wells in each row, 3 rows in total. All the other wells should be filled with sterile DPBS (100 µL/well) to minimize evaporation. Transfer the plates into the incubator to equilibrate.

4. After all the plates are equilibrated, use curved forceps to carefully transfer one bead to each well of GM in the 96-well plates. Every 2 days, after completing the imaging of the cultured follicles (see 3.5), replace half (50 µL) of the GM in the well with fresh, pre-equilibrated GM.

3.4 Optimal aprotinin concentration determination

The degraded fibrin appears as an optically clear ring around the encapsulated follicle, which can be used as a surrogate for toxicant screening. To employ the optical clearance due to fibrin degradation, we have identified the range of aprotinin that maximized the control of fibrin degradation without affecting follicle growth. Suboptimal concentrations of aprotinin (less than 0.01 TIU/mL) resulted in uncontrolled fibrin degradation before ovotoxic effects could take place (Shikanov et al. 2011b; Zhou et al. 2015). Since fibrin gels contract *in vitro* (Huang et al. 2005), concentrations above 0.1 TIU/mL additionally lead to follicle death due to the inability to degrade fibrin and expand in condensed FA-IPN (Shikanov et al. 2011b). For the 12.5 mg/mL fibrin concentration in the FA-IPN, optimal aprotinin concentration is between 0.025 and 0.05 TIU/mL (Zhou et al. 2015). Aprotinin concentrations in this range slow down fibrin degradation and allow fibrin to be present at later time points to serve as the surrogate reporter for follicle health.

3.5 Follicle imaging and analyses

Image the cultured follicles every 2 days before changing the media. Turn on the imaging microscope and set up the imaging software. Position the first 96-well plate with follicles onto the microscope. First, use a lower magnification (e.g. 5X) to find the first bead in the first row. Then, record and measure the fibrin degradation ring around the follicle at 5X. Once you locate the bead in the well, switch to a higher magnification (e.g. 20X) to acquire an image of the follicle. Proceed to image all the follicles in the plate. Make sure the imaging does not take longer than 10 minutes; otherwise, place the plate back to the incubator and return to it 30 minutes later to let the GM re-equilibrate (see Note 31).

Follicle growth in FA-IPN can be monitored via imaging every other day (Fig. 27). Follicle morphology can be examined with a 20X objective (Fig. 27 A-D). To quantitatively measure follicle growth in FA-IPN, draw 2 orthogonal lines using ImageJ from basement membrane to

basement membrane across the oocyte (Fig. 27A insert), calculate the average of the two measurements for each follicle and generate a growth curve (Fig. 27E). Once the follicles reach 300 μm in diameter (Qu et al. 2015), *in vitro* follicle maturation (IVFM) can be performed to evaluate oocyte quality (Xu et al. 2006). The oocytes were considered to be in metaphase I (Fig. 27F-1), if neither the germinal vesicle (Fig. 27F-2) nor the first polar body was visible. If a polar body was present in the perivitelline space, the oocytes were classified as metaphase II (Fig. 27F). Fragmented or shrunken oocytes were classified as degenerated and were discarded (Fig. 27F-3). Healthy, competent oocytes from follicles cultured in FA-IPN should resume meiosis to metaphase II (MII) stage with 1 polar body present in the perivitelline space.

3.6 Follicles in FA-IPN for toxicology tests

We have demonstrated how the FA-IPN could be applied to test the ovotoxic effects of an anticancer drug doxorubicin (DXR) (Zhou et al. 2015). Follicles cultured in FA-IPN with aprotinin-controlled fibrin degradation can serve for *in vitro* screening of environmental toxicants such as 7,12-dimethylbenz[a]anthracene (DMBA) that has been previously shown to be ovotoxic (Igawa et al. 2009). To evaluate the effects of DMBA in our system, DMBA was dissolved in DMSO as a stock solution and was then further diluted with GM to reach a final concentration of 75 nM and 12.5 nM based on previous report (Igawa et al. 2009). The final concentration of DMSO in GM was kept at 0.5% (v/v) (Zhou et al. 2015). Follicles were treated with DMBA in GM on days 0, 2, and 4. When treating follicles encapsulated in FA-IPN with 12.5 nM DMBA, follicles affected by DMBA exposure showed little fibrin degradation (Fig. 28B) compared to untreated healthy follicles in the control condition (Fig. 28A). Quantification of fibrin degradation could also be applied as previously reported (Zhou et al. 2015). To confirm our findings using the fibrin degradation as the surrogate reporter, we also examined the follicle morphology at a higher magnification. Indeed, follicles reached smaller sizes, presented darker colors and had no antrum formations (Fig. 28B insert). Therefore, fibrin degradation area can serve as a surrogate reporter for follicle health.

4. Notes

1. DM is buffered with HEPES for the atmospheric CO_2 level and is therefore the media used for all the procedures and manipulations performed outside the incubator. DM can be stored at 4 ˚C for up to 4 weeks.

2. Do not warm up DM in the incubator because the HEPES cannot buffer for CO_2 and the media becomes acidic.

3. MM is the media used to keep the isolated follicles in the incubator for all the procedures after isolation and before the transfer into GM. MM can be stored at 4 ˚C for up to 4 weeks.

4. Try to keep follicles separated from each other in the media at all times to avoid them sticking to each other. If indeed, follicles aggregate, you can use the same approach with the needles to pull them apart for individual follicle encapsulation.

5. To minimize evaporation of FA droplets, follicle encapsulation should be done at room temperature. If you are performing follicle isolation on a heated stage, make sure you turn off the heating prior to follicle encapsulation.

6. Sterile alginate aliquots should be prepared ahead of time. The aliquots should be stored in -20 °C until use.

7. Aqueous solution of alginate at concentrations greater than 0.2% (w/v) results in a viscous, difficult to filter solution.

8. It is important to prepare the alginate solution the day before encapsulation experiments, because the dissolution of alginate is slow and this step can be time consuming.

9. If Tisseel sterile kit is unavailable, this is an alternative method to purify fibrinogen from other commercial sources such as Sigma.

a) Dissolve fibrinogen powder in MilliQ H_2O to reach an approximate concentration of 50 mg/mL. The supernatant contains the desired fibrinogen solution while the pellet is denatured protein or other particles, thus transfer the supernatant into new tubes.
b) While fibrinogen is dissolving, prepare the appropriate amount of TBS for dialysis. Each dialysis tube should comfortably hold up to 25mL of fibrinogen solution and needs to be dialyzed versus 4L of TBS. For example, with a flat width of 40 mm, cut the tubes to be

~30 cm long. Once the number of dialysis bags is determined, make a 4L solution of TBS for each dialysis bag by following the recipe below and titrate the pH to 7.4:

---- 17.44g Tris HCL

---- 2.56 g Tris Base

---- 32.00g NaCl

---- 0.80g KCl

c) Prepare dialysis tubing (M.W. = 6,000 – 8,000 Da), making sure to wet in TBS to separate. Wash each bag briefly with TBS in order to make sure there are no holes. Each dialysis tube can comfortably hold up to 25 mL of fibrinogen solution and needs to be dialyzed in 4 L of TBS. Clip one end of the dialysis tubing on each bag and hold bag half inside large TBS beaker.

d) Carefully transfer fibrinogen solution into bags and clip top of bags so that no solution is allowed to escape. Allow this closed dialysis bag to float in the TBS solution. Cover the beaker to prevent evaporation.

e) Place all TBS beakers with dialysis bags on top of stirring plates (stir at slow to medium speeds) and allow the dialysis to occur overnight (at least 6 hours).

f) Carefully remove fibrinogen solution from dialysis bags and filter through 5.0 µm PVDF filter (EMD Millipore, Billerica, MA) to remove crude impurities.

g) Measure the concentration of the fibrinogen solution after combining all the solutions using the NanoDrop 1000 spectrophotometer. Dilute the fibrinogen to desired concentration with sterile 25 mM TBS + 140 mM NaCl buffer if necessary.

h) Sterile filter the diluted fibrinogen solution through 0.22 µm PES membrane filter (EMD Millipore, Billerica, MA).

i) Aliquot fibrinogen solution into sterile 1.5 mL microcentrifuge tubes and store at -20 ˚C for short term storage (up to 1 year) and -80 ˚C for long term storage.

10. Sterile fibrinogen and thrombin aliquots should be prepared ahead of time. Both solutions are stored at -20 ˚C until use.

11. The osmolality of this solution should be 0.3624 Osm based on calculation.

12. Avoid leaving isolated follicles in MM for longer than 2 hours: follicles tend to stick to the plastic. If follicles stuck to the plastic, try to lift the follicle from the bottom of the dish by pipetting up and down. Avoid excessive shear forces which may lead to basement membrane damage.

13. Concentrations of the encapsulating matrix can be adjusted to fit a specific application by changing the concentrations of alginate in the range between 0.125% – 0.8%, fibrinogen 1 – 75 mg/mL, and thrombin 1 – 500 mg/mL. For example, if a hydrogel of interests is with final concentrations of 0.5% alginate and 12.5 mg/mL fibrinogen, mix 50 mg/mL fibrinogen with 1X DPBS and 1% alginate at 1:1:2 ratios.

14. Avoid vortexing this mixture: fibrinogen can get foamy. Pipetting up and down should be used to mix.

15. Practice making empty beads without follicles to optimize the angle and speed of extrusion

16. This step is very critical to obtaining follicles for a successful study. Only healthy appearing and undamaged follicles should be encapsulated. Keep multiple IVF dishes so you can alternate them in and out of the incubator to avoid lengthy exposure to ambient conditions.

17. Excessive remaining media can affect the crosslinking of FA-IPN, because of the dilution effect. Minimize the media uptake when transferring follicles.

18. Keep an eye on the wash droplet: change as needed if it gets pink due to the remaining media when transferring follicles.

19. When touching the calcium solution with the FA droplet, avoid the tip of the pipette touching the solution to prevent leaving a “hole” in the final FA-IPN bead (Fig. 26D).

20. To help better keep the follicles towards the center of the beads (Fig. 26), practice with some less-than-ideal follicles first to adjust how much of the 7.5 µL to take before taking up the target follicles.

21. The 50 mM concentration of $CaCl_2$ causes very fast gelation of the alginate. For a 7.5 µL bead, exposure to crosslinking solution for 2 minutes is sufficient for complete gelation.

22. When multiple FA-IPNs are present in the thrombin/Ca^{2+} crosslinking solution, highly crosslinked beads appear more opaque than those that are less crosslinked (Fig. 24C). This optical difference may help in identifying FA-IPNs for transferring to MM (Fig. 24D) to avoid extended exposure of follicles to Ca^{2+} ions.

23. To avoid drastic pH changes, limit the exposure of αMEM-based media such as MM and GM to ambient air for no longer than 10 minutes.

24. It is necessary to leave FA-IPNs in the MM for at least 30 minutes before plating the beads into GM: this process allows equilibration of the alginate matrix with the media.

25. The αMEM used for making GM should be opened in less than a month.

26. GM can be stored at 4 °C for up to 2 weeks.

27. If follicle isolation process is performed on a laboratory bench and/or the tissue used is obtained in an unsterile way, directly from an abattoir for example, add 0.5% (v/v) Pen/Strep to GM to prevent potential contamination during the culture.

28. For example, for 3-7 TIU/(mg solid), apply an average of 5.5 TIU/(mg solid) to calculate the total amount of aprotinin.

29. Aprotinin aliquots can be store at -20 °C for short term or -80 °C for long term storage.

30. Do not refreeze aprotinin solution. Use a fresh aliquot every time.

31. Plates with GM should not stay out of the incubator for more than 10 minutes at a time. Preferably, finish imaging all the follicles at one time to minimize the pH changes that are damaging to the cultured follicles. Adjust the number of wells with GM based on how long it takes to complete the imaging of one plate.

5. Acknowledgements

This work is supported by Reproductive Science Program (RSP) institutional funding (NIH U046944) from the University of Michigan to AS.

Appendix B.

Synthetic PEG hydrogel for engineering the environment of ovarian follicles

Previously accepted as a chapter in *Methods in Molecular Biology*

1. Introduction

In vitro culture of mouse ovarian follicles is a powerful technique to study folliculogenesis, the process of follicle development, and is a means to obtain fertilizable oocytes as a potential fertility preservation option. Ovarian follicles are the functional units of the ovary and consist of an oocyte surrounded by at least one layer of granulosa cells. The somatic compartment synthesizes and secretes hormones necessary for the orchestration of the inter-relationship between other parts of the reproductive system and the central nervous system. Mammalian females are born with a finite pool of primordial follicles and their loss is irreversible. Folliculogenesis involves recruitment of primordial follicles from the resting into the growing pool, progressing through several developmental stages: primordial, primary, secondary, preantral multilayered secondary and antral. The importance of cell-cell and oocyte-cells interactions in a growing follicle presents various challenges for *in vitro* culture in traditionally flat (two-dimensional) cultures (Shea et al. 2014). Since the first culture of ovarian follicles was reported, the overall survival rate of the cultured follicles and maturation rates of the oocytes has steadily improved due to optimized culture media and the introduction of 3-dimensional (3D) culture techniques (Tagler et al. 2013). Follicle encapsulation in a 3D environment preserves the spherical shape of the growing follicle, from the initial stages when the follicle is only 100 μm in diameter to the final stages when it reaches 350 μm in diameter (Shikanov et al. 2011a). Maintaining 3D architecture of a growing follicle is essential to allow for antrum formation, a fluid filled cavity inside the growing follicle that promotes diffusion of nutrients and oxygen to the oocyte and the growing cells. Lastly, the preservation of the spherical shape maintains juxtacrine signaling between the oocyte and the surrounding granulosa through tight junctions.

Previously developed 3D culture systems have used alginate and most recently a combined fibrin-alginate system (Dolmans et al. 2007; Shikanov et al. 2009). These systems allowed for mouse follicle growth and maintained follicle structure but have a limited range for controlling mechanical and biological properties, such as stiffness and degradation, via chemical modification. The non-degradable nature of alginate limits growth of follicles from large animals. For example, mouse follicles have to reach only 350 μm in diameter to be considered ready for maturation, while human follicles have to reach at least 5 mm. The growth prohibitive properties of alginate were demonstrated recently with a human follicle that was first cultured in a 3D alginate matrix, but after it reached 500 μm in diameter the alginate was removed to allow further expansion of the follicle in a free floating media (Xiao et al. 2015). The ex-capsulated human follicles showed improved maturation rate when first grown in alginate and then removed from the alginate and cultured in a 2D environment to allow increasing follicle expansion (Xiao et al. 2015). Therefore, a biocompatible dynamic system is needed that can be modified for properties such as cell-driven degradation and material stiffness, while also accommodating the volumetric expansion of the encapsulated follicle.

We developed a 3D PEG-based system for follicle encapsulation and culture *in vitro*. PEG hydrogels have shown to support folliculogenesis and produce fertilizable oocytes (Shikanov et al. 2011a**).** The major advantage of PEG over natural hydrogel materials is the versatility of mechanical and biological modifications to match physiological requirements. Crosslinking PEG with peptides susceptible to degradation by different proteases, such as plasmin and MMPs, forms tunable PEG hydrogels with cell-controlled remodeling. Furthermore PEG hydrogels can be modified with bioactive peptides such as RGD to support cell adhesion and migration (Zhu 2010). Follicle co-encapsulation with support cells, such as feeder mouse embryonic fibroblasts (MEF), allows for improved survival rate of mice follicles (Tingen et al. 2011). Most importantly, modifications of mechanical and biological properties are performed *in situ* in physiological conditions that are not harmful to follicles. Here, we outline a method for co-encapsulating small (100 – 120 μm in diameter) ovarian follicles with mouse embryonic fibroblasts within PEG hydrogels for *in vitro* culture. The described approach improves the

survival and maturation rate of the smaller follicles that do not survive *in vitro* when cultured individually or without the feeder cells.

2. Materials

2.1 General Materials

1. One pair of straight fine scissors, 26 mm.

2. One pair of straight fine scissors, 24 mm.

3. One pair of straight forceps, #5.

4. One pair of curved forceps, #7.

5. Cell counter (automated or hemocytometer)

6. Dissecting microscope with a heating stage.

7. Inverted imaging microscope with imaging software.

2.2 Hydrogel Precursors

1. 8-arm polyethylene glycol vinyl sulfone (PEG-VS) (molecular weight M.W. = 40,000 g/mol).

2. 3-arm Peptide Crosslinker: YKNS (GCYKNSGCYKNSCG, M.W. = 1663.9 g/mol).

3. Cell adhesive peptide: RGD (GCGYGRGDSGP, M.W. = 1067.1 g/mol).

4. Sterile 50 mM HEPES buffer: HEPES free acid, NaCl.

5. Sterile 1.5 mL microcentrifuge tubes.

2.3 Ovarian follicle isolation

1. First generation female hybrid offsprings of 2 inbred strains: C57BL/6JRccHsd (maternal) CBA/JCrHsd (paternal), 12 – 14 days of age.

2. 70% Ethanol and dissecting mats.

3. Dissection media (DM): Leibovitz's L-15 medium, 10% heat inactivated fetal bovine serum (FBS), and 0.5% Pen/Strep.

4. Maintenance media (MM): minimum essential media α (αMEM), 10% FBS, and 0.5% Pen/Strep.

5. Two 35 × 10 mm sterile petri dishes.

6. One 60 × 10 mm sterile petri dishes.

7. Center Well Dishes for IVF: use one (1) dish per each ovary.

8. Sterile 1.5 mL microcentrifuge tubes.

9. Two sterile insulin syringes with 27 ½ G needles.

2.4 Cell culture

1. Mouse Embryonic Fibroblasts (MEFs).

2. DMEM culture media: DMEM, 10% FBS, 1% Pen/Strep.

3. T-75 culture flask.

2.5 Follicle and MEFs co-encapsulation and culture

1. Microscopes slides: with and without 2 mm spacers.

2. Parafilm®.

2. Sterile 96-well plates.

3. 60 × 10 mm sterile petri dishes.

4. MM.

5. Dulbecco's phosphate-buffered saline 1X (DPBS, no calcium, no magnesium).

6. Growth media (GM): αMEM, 1mg/mL Fetuin, 3mg/mL bovine serum albumin (BSA), 5 µg/mL insulin, 5 µg/mL transferrin, and 5 ng/mL selenium, and 10 mIU/mL recombinant human follicle stimulating hormone (rhFSH).

7. 0.25% Trypsin/EDTA.

8. Sterile 1.5 mL Centrifuge tubes.

9. Sterile 15 mL conical tubes.

3. Methods (see Fig. 29 as an overview)

3.1 PEG precursor calculation – to be completed the day before the experiment

For follicles co-encapsulated with MEFs cells, the PEG condition we use is 5% 8-arm PEG-VS modified with 0.5 mM RGD crosslinked with YKNS. Each follicle is encapsulated in 10 µL gels and based on the number of isolated follicles the total volume of the gel (V_{tot}) can be calculated. Usually, we first estimate the amounts of PEG precursors (m_{100}) in 100 µL of gel and then calculate the minimal amounts needed to reach the total final volume. Based on how much is weighed exactly ($m_{weighed}$), we adjust the volume of HEPES buffer needed to dissolve all the precursors. For all calculation, the stoichiometric ratio should be 1:1 between the VS groups available to crosslink on PEG and the functional groups (SH) on the crosslinker (YKNS).

For the specific encapsulation condition in this chapter: 5% 8-arm PEG-VS modified with 0.5 mM RGD crosslinked with YKNS, in 100 µL gel, follow the steps below:

1. To make, 100 µL of a 5% PEG gel, first calculate the mass of PEG powder needed to make that volume: $m_{100}\ (PEG) = \frac{5}{100} \times 100\ \mu L\ \times 1 \frac{mg}{\mu L} = 5\ mg$, where $\frac{5}{100}$ is 5% and 1 $\frac{mg}{mL}$ is the assumption that the density of powder is 1.

Based on the calculated mass of PEG, then calculate the mole number of PEG (n): n (PEG) = $\frac{m\ (PEG)}{M.W.(PEG)} = \frac{5\ mg}{40000\ g/mol} = \frac{5}{40000} mmol = 0.125\ \mu mol$

2. Calculate the mass of RGD to modify PEG with by calculating the moles of RGD: n (RGD) = $0.5\ \times 10^{-3} \frac{mol}{L} \times 100 \times 10^{-6} L = 0.05\ \mu mol$, where $0.5\ \times 10^{-3} \frac{mol}{L}$ is 0.5 mM of RGD in the gel and $100 \times 10^{-6} L$ is the 100 µL of the gel to prepare.

Calculate the mass of RGD powder needed to add to the gel mixture to obstain 0.5 mM RGD:

m_{100} (RGD) = n (RGD) × M.W. (RGD) = 0.05 µmol × 1067.1 = 53.4 µg ≈ 0.053 mg.

3. From here, we need to calculate the number of arms on PEG that are used to react with RGD [n (blocked)]. Since there is only 1 L-cysteine in RGD, therefore, arms of PEG blocked by RGD is equal to the mole of RGD: n (blocked) = n (RGD) = $0.05\ \mu mol$.

4. Next, we calculate the number of arms of PEG still available for crosslinking [n (available)], which is the total number of PEG arms minus the ones being used for RGD modification:

n (available) = 8 × n (PEG) – n (blocked) = $8 \times 0.125\ \mu mol - 1 \times 0.05\ \mu mol = 0.95\ \mu mol$.

5. Because all the available arms are used for crosslinking and there are 3 functional groups (SH from L-cysteine) on each YKNS molecule, therefore, the mole of crosslinker needed is: n (YKNS) = $\frac{1}{3}$ × n (available) = $\frac{0.95}{3} \mu mol$.

Thus, the mass of crosslinker needed in 100 µL gel: m_{100} (YKNS) = n (YKNS) × M.W. (YKNS) = $\frac{0.95}{3} \times 1663.9\ \mu g = 526.9\ \mu g \approx 0.53 mg$.

Based on how many follicles obtained from each ovary and how many mice used, estimate the total volume of gel (V_{tot}) required for the experiment: $V_{tot} = 10\mu L \times the\ number\ of\ follicles$. It is recommended to have 10% extra volume of precursors as wash and to compensate for the volume loss during mixing.

Based on the calculation for 100 µL of gel and the total volume of gel, estimate the **minimal** amounts (m_{min}) of precursors you need to weigh: $m_{min} = \frac{V_{tot}}{100\ \mu L} \times m_{100}$.

In the 100 µL gel, PEG, RGD, and YKNS are mixed at a final volume ratio of V(PEG) : V(RGD) : V(YKNS) = 5 : 1 : 4. To adjust for the actual weighed amounts ($m_{weighed}$) of precursors, use the following calculation to adjust for the amount of HEPES buffer to be added to precursors (see Note 1):

PEG: $\frac{m_{100}(PEG)}{50\ \mu L} = \frac{m_{weighed}(PEG)}{m_{weighed}(PEG)+V_0(PEG)}$

RGD: $\frac{m_{100}(RGD)}{10\ \mu L} = \frac{m_{weighed}(RGD)}{m_{weighed}(RGD)+V_0(RGD)}$

YKNS: $\frac{m_{100}(YKNS)}{40\ \mu L} = \frac{m_{weighed}(YKNS)}{m_{weighed}(YKNS)+V_0(YKNS)}$

Solve for V_0 in the above equations: V_0 is the amount of sterile HEPES buffer you need to dissolve each tube of powder **prior to** mixing.

To form the gel, dissolve PEG and RGD individually first in sterile HEPES buffer and mix PEG and RGD solutions at a ratio of 5:1 and incubate at room temperature in ambient air for 15 mins. Then, add YKNS to the PEG/RGD mixture to reach the final volume ratio of V(PEG) : V(RGD)

: V(YKNS) = 5 : 1 : 4. Incubate this precursor mixture at 37 ºC in ambient air and gelation should happen in 10 minutes.

Note that RGD and YKNS gradually lose their reactivity once dissolved in HEPES buffer. As a result, use them within **15 mins** after dissolving individual components to ensure reactivity; otherwise, the gel may not form.

3.2 Ovarian follicle isolation

It is essential that the female mice are 12 – 14 days of age because at this age ovaries contain a large proportion of small follicles (100 – 120 μm diameter), which benefit the most from a co-culture with feeder cells (Tagler et al. 2012) (Fig. 30A – C). All dissections should be performed in L15-based media (buffered for ambient air), on a 37 ˚C (temperature control) heated stage, and on a clean bench (laminar flow hood) to minimize potential contamination. Follicle isolation should take no longer than 30 minutes per ovary. For optimal results, keep the resected tissue outside the incubator for less than 1 hour. To minimize pH changes, limit exposure of αMEM-based media to ambient air. All animals are treated in accordance with the guidelines and regulations set forth by the national and institutional IACUC protocols.

1. Prior to the beginning of the experiment, sterilize all the equipment by spraying 70% ethanol and air drying on the clean bench or in the laminar hood.

2. Prepare DM by supplementing L-15 with 1% (v/v) FBS and 0.5% (v/v) Pen/Strep. Gently invert to mix well (see Note 2). Warm up the DM to 37 ˚C in a water bath (see Note 3).

3. Prepare MM by supplementing αMEM with 1% (v/v) FBS and 0.5% (v/v) Pen/Strep. Gently invert to mix well (see Note 4). Prepare IVF dishes with 1 mL of MM in the center ring and 3 mL of MM in the outer ring. Utilize one IVF dish for each isolated ovary. In addition, prepare another 35 mm dish with 1 mL of MM. Pre-equilibrate all the dishes for 20 minutes in the incubator prior to the beginning of the isolation.

4. Euthanize one female (12 – 14 days of age), according to the institutional IACUC-approved protocols. Remove both ovaries from the animal. In order to assure minimal damage to the ovaries, remove parts of the oviduct and uterus around the ovary as well. Place roughly dissected ovaries into a 35 mm dish with DM.

5. Use a dissecting scope and insulin syringes to separate the ovaries from uterus, fat pad and bursa by placing one needle at the intersection of the bursa and the oviduct to anchor the reproductive tract in place, and dissecting with the other needle. Place the second needle directly next to the first but only grip the thin membrane of the bursa. Carefully nick the bursa to expose the entire ovary. Transfer clean ovaries using curved forceps or a pipette with a blunt tip into the 35 mm dish with pre-equilibrated MM. If using forceps, try not to squish or damage the ovaries by applying excessive force. Repeat this process for both ovaries. Transfer one ovary to a 35 mm dish containing warm MM and place it in the incubator. Keep the other ovary in DM and start follicle isolation (Xu et al. 2006).

6. Set a timer for 30 minutes. Start isolating follicles by using two Insulin syringes with 27 ½ G needles. With one syringe in your non-dominant hand, anchor the ovary to the bottom of the dish. And with a syringe in your dominant hand, gently tease and "flick" individual follicles from the ovary. Try to remove most surrounding ECM without puncturing the follicle. Dissect out as many follicles as possible within the 30 minutes. Transfer intact isolated secondary follicles (100 – 120 μm in diameters, 1 – 2 layers of granulosa cells) to the outer ring of an IVF dish with MM. When transferring, use a P10 pipette to carefully pick up isolated follicles with minimum media. To avoid follicles sticking to the walls of the same pipette tip and/or to each other, aspirate a little media first to the very end of the tip and while aspirating the follicles, alternate between media and each follicle. When expelling the follicles into the outer ring of the IVF dish, use a sweeping motion such that the follicles in the tip will end up at different spots to avoid sticking to each other (see Note 5).

7. Repeat steps 3.2.1 – 3.2.6 for the remaining ovaries to finish the isolation.

8. Select follicles for subsequent encapsulation and culture. Figure 2A shows a healthy follicle at a correct size range with a centrally located oocyte (white arrow head) surrounded with granulosa cells. As the culture progresses the follicle grows and expands (Fig. 30B) and forms a

fluid filled cavity, antrum, (Fig. 30C, black arrow head) on day 8. Follicles that are below 100 µm in diameter and appear darker with a punctured oocyte (Fig. 30D) do not progress during culture and eventually die by extruding the oocyte (black arrow, Fig. 30F).

9. Count the number of ideal follicles for encapsulation. Ultimately, you should be able to collect between 20 – 30 good follicles from 1 ovary.

3.3 Follicle and MEFs co-encapsulation in PEG

1. Five days before the day of experiment, seed mouse embryonic fibroblast (MEFs) cells at 8000 cells/cm^2 in a T-75 flask or according to established lab specific protocols.

2. Add 10 mL of DMEM (DMEM, 10% (v/v) FBS, 1% (v/v) Pen/Strep) and change media every other day. Ensure cells reach 80% – 90% confluency on the day of experiment.

3. Prepare 50 mM HEPES buffer by dissolving 1.911 g of HEPES free acid and 0.776 g of NaCl in 90 mL of MilliQ water. If necessary, use 1N NaOH to titrate pH to 7.62 at room temperature such that it reaches 7.4 once warmed to 37 ºC. Add water to 100 mL and measure the pH again. Sterile filter prior to use.

4. Mouse ovarian follicles are cultured in αMEM-based GM. To make GM, supplement αMEM with 10 mg/mL Fetuin, 3 mg/mL BSA, 5 µg/mL insulin, 5 µg/mL transferrin, and 5 ng/mL selenium. Then, sterile filter the solution using 0.2 µm cellulose acetate syringe filter. Add 10 mIU/mL rhFSH and invert gently to mix.

5. Sterilize microscope slides and accompanying strips of Parafilm® using 70% ethanol.

6. Once dry, cover the surfaces of microscope slides with Parafilm® in a sterile environment and keep within reach for encapsulation (see Figure 3A). For each workload of encapsulation (see Note 6), you need 1 slide with 2 mm spacers (slide #1), 1 slide without (slide #2), and 2 accompanying Parafilm® strips to cover the working surfaces on both slides.

7. Weigh out the proper amounts of PEG, RGD, and YKNS (see Note 7). Dissolve the PEG in appropriate HEPES volume as well as RGD in its appropriate volume allowing both to become fully dissolved in the buffer.

8. In a 1.5 mL centrifuge tube, mix PEG solution with RGD solution at a 5:1 ratio and mix by pipetting up and down for 15 seconds. Incubate at room temperature in ambient air for 15 mins.

9. In the meantime, trypsinize the cells according to established lab specific protocols or the following. In a sterile environment, remove all the media from the flask. Briefly rinse with 2 ml of DPBS and aspirate it out. Add 3 mL of 0.25% Trypsin/EDTA and incubate the cells for 3 – 5 mins in the incubator. Check after 3 mins and gently tap the flask if necessary to help MEFs detaching from the bottom of the flask.

10. After the majority (>90%) of the cells have detached from the flask, neutralize the trypsin by adding 3 mL of pre-warmed DMED culture media. Wash the surface twice by pipetting the liquid. Transfer all the liquid (~6 mL) to a 15 mL conical tube and perform cell counting.

11. Calculate the amount of cell suspension needed to encapsulate all the follicles at a concentration of 2×10^5 cells/mL (see Note 8) and aliquot into 1.5 mL microcentrifuge tubes based on how you prepare PEG, RGD, and YKNS aliquots.

12. Centrifuge at 200X g for 5 mins and keep warm at 37°C until use. Be sure to use cells within 1 hour.

13. Select 4 good follicles for encapsulation and transfer them to the center well of an IVF dish.

14. Add the calculated amount of HEPES to dissolve YKNS and gently pipette to mix.

15. Work quickly to remove the supernatant from a 1.5 mL tube containing cells. Add YKNS to the PEG/RGD mixture to reach a final ratio of V(PEG) : V(RGD) : V(YKNS) = 5 : 1 : 4. Resuspend the cell pellet in appropriate amount of this precursor mixture. Start a timer for 10 mins.

16. Work quickly to pipette 5 droplets of cell suspension in PEG precursors onto the the Parafilm® on slide #1: 4 encapsulating droplets of 10-μL and 1 “wash” droplet with 20 μL of PEG solution (see Fig. 31A).

17. Under the dissecting scope, use a P10 pipette to transfer 1 of the selected follicles to the "wash" droplet first. Pipette it up and down 5 times in the "wash" droplet to get rid of excess media (Fig. 31B, see Note 9).

18. Change pipette tips and repeat step 3.3.17 until all the 4 follicles are individually encapsulated in each encapsulation droplet.

19. Cover slide #1 with a Parafilm® covered slide #2. Flip the slides such that slide #1 is on top. Place the slides on a heating stage at 37 °C until gelation completes.

20. Once gelation completes, gently peel apart the slides. Use a pair of curved forceps, carefully transfer all the gels into a 60 × 10 mm sterile petri dishes containing pre-equilibrated MM.

21. Repeat steps 3.3.13 – 3.3.20 until all the follicles are co-encapsulated with MEFs. Use new Parafilm® strips every time to ensure hydrophobicity.

22. After completing the encapsulation process, transfer the gels to 96-well plates: 1 gel per well containing 150 μL of GM.

23. Incubate at 5% CO_2 and 37°C for 8-12 days, replacing half of the media and imaging every two days. On the day of the imaging, turn on the imaging microscope and set up the imaging software. Position the first 96-well plate with follicles onto the microscope. First, use a lower magnification (e.g. 5X) to find the first well with the follicle in a gel in the first row. Once you locate the hydrogel and the follicle in it in the well, switch to a higher magnification (e.g. 20X) to acquire an image of the follicle. Proceed to image all the follicles in the plate. Make sure the imaging does not take longer than 10 minutes; otherwise, return the plate back to the incubator and resume imaging of the same plate after at least 30 minutes when GM re-equilibrates.

24. Examine the follicle morphology with a 20X objective (Fig. 30A – F). To quantitatively measure follicle growth in PEG, draw 2 orthogonal lines using ImageJ from basement membrane to basement membrane across the oocyte, calculate the average of the two measurements for each follicle and generate a growth curve (Dolmans et al. 2007; Shikanov et al. 2011a; Tagler et al. 2013)**.** Once the follicles reach 300 μm in diameter, *in vitro* follicle maturation (IVFM) can be performed to evaluate oocyte quality following published procedures (Dolmans et al. 2007; Shikanov et al. 2011a; Tagler et al. 2013)**.**

4. Notes

1. In this specific condition, the precursors are mixed at a ratio of V(PEG) : V(RGD) : V(YKNS) = 5 : 1 : 4. That is, for example, in a 100 µL gel, 50 µL of HEPES is used to dissolve PEG, 10 µL of HEPES is used to dissolve RGD, and the remaining 40 µL of HEPES is used to dissolve YKNS.

2. DM is buffered with HEPES for the atmospheric CO_2 level and is therefore the media used for all the procedures and manipulations performed outside the incubator. DM can be stored at 4 ˚C for up to 4 weeks.

3. Do not warm up DM in the incubator because the HEPES cannot buffer for CO_2 and the media becomes acidic.

4. MM is the media used to keep the isolated follicles in the incubator for all the procedures after isolation and before the transfer into GM. MM can be stored at 4 ˚C for up to 4 weeks.

5. Try to keep follicles separated from each other in the media at all times to avoid them sticking to each other. If follicles do aggregate, apply the same approach with the needles to pull them apart for individual follicle encapsulation.

6. Given the 10 mins gelation time, after mixing all the precursors, encapsulate **no more than** 4 follicles. Once the user is more familiar with the process, the number of follicles in each encapsulation round can be adjusted.

7. Depending on how fast the user can encapsulate follicles and how many follicles the user encapsulates every experiment, it may be beneficial to make aliquots of PEG, RGD, and YKNS in advance, especially if less than 1 mg of the peptides is used every time to ensure accuracy. To make aliquots of PEG, RGD and YKNS, dissolve appropriate amounts of PEG, RGD, and YKNS in sterile filtered MilliQ water with 10% glacial acetic acid to a proper concentration, 1 mg/mL for RGD and YKNS for example. Aliquot desired amounts of each solution into tubes and freeze them at -20 °C. Snap freeze the tubes in liquid nitrogen before loading to a lyophilizer. Lyophilize until completely dry. Wrap the tubes with Parafilm® and store at -20 °C.

8. We use 2×10^5 cells/mL for MEFs and follicle co-encapsulation. The concentration of the cells is determined by the proliferation speed and nutrients consumption. MEFs are fast proliferating cells that, if seeded at greater concentrations, can overwhelm the culture and deprive the follicle from nutrients. For slower proliferating cells, greater concentrations may be used. Careful titration is needed when co-culturing different cells.

9. It is essential to wash away the excessive media in the wash droplet to ensure successful gelation because the serum in the media interferes with and can stop the gelation from happening. If necessary, set your 10 μL pipette to 0.5 μL to avoid taking too much media when transferring.

Acknowledgements

This work is supported by Reproductive Science Program (RSP) institutional funding (NIH U046944) from the University of Michigan to AS and the National Science Foundation (NSF) Graduate Research Fellowship Program (GRFP) to UM.

Appendix C.

Figures

Fig. 1 Simplified description of the hypothalamus-pituitary-gland-gonad (HPG) axis.

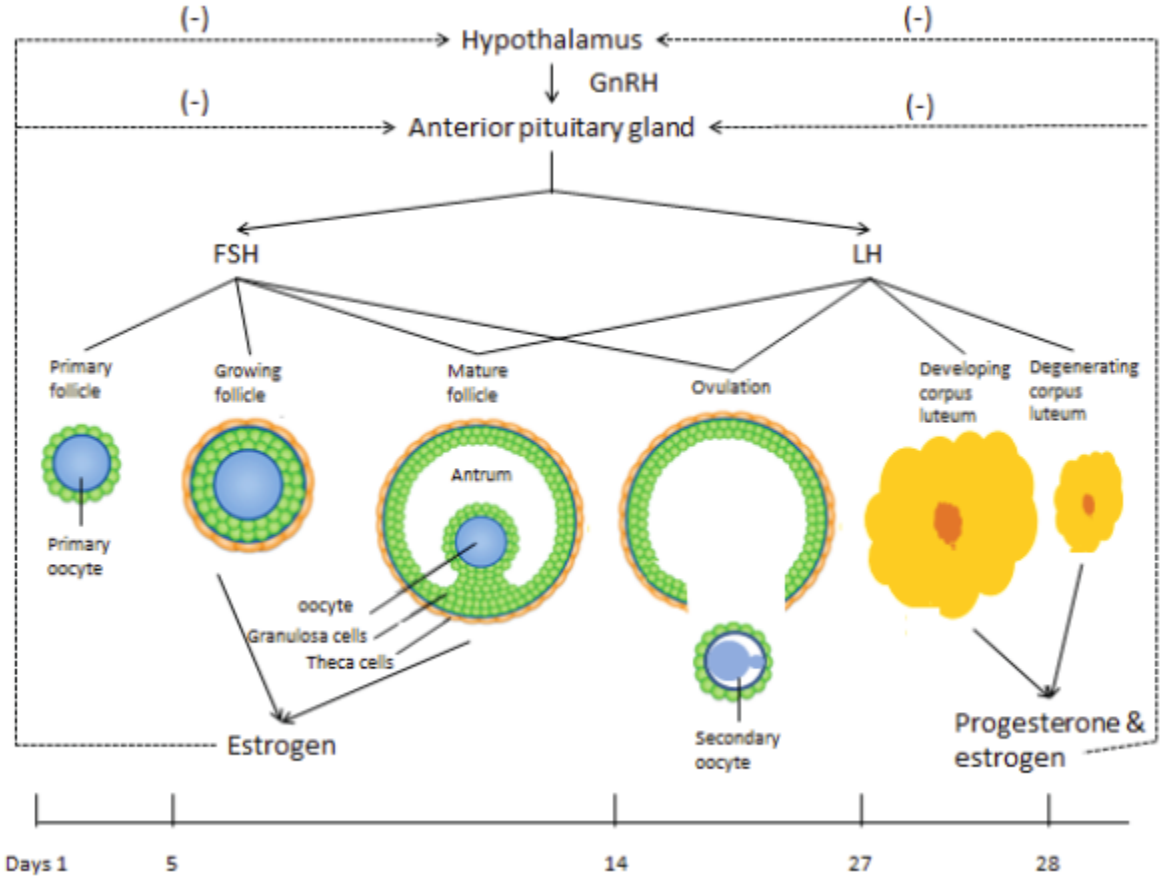

Fig. 2 Aprotinin-controlled fibrin degradation.

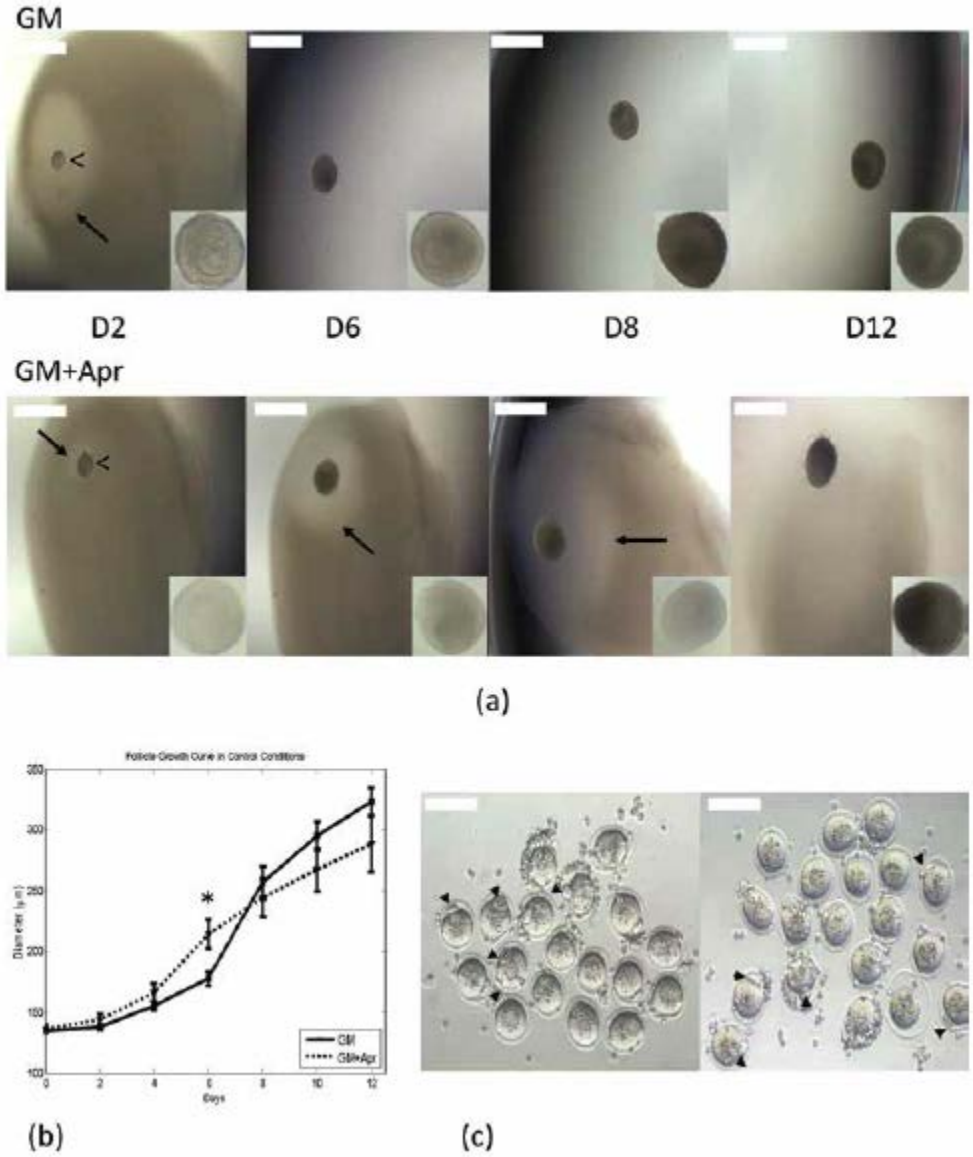

(a) Representative images of follicles encapsulated in FA-IPNs on different days of culture with higher magnification images of follicles in the lower right inserts. Comparison showed that optimized aprotinin concentration (0.025 to 0.05 TIU/mL) effectively delayed fibrin degradation till D8, a critical time for antrum formation. Arrow points to the fibrin degradation area surrounding the growing follicle. Arrow head ("<") points to the encapsulated follicle in the FA-IPN. Scale bar=500 μm. (b) Growth curves of follicles cultured in growth media with and without aprotinin. Data are shown as mean ± SEM, $p < 0.05$. n (total follicles, GM) = 286, n (total follicles, GM+Apr) = 258, n (total animals used) = 30, n (experiments) = 10 for each condition. (c) Representative images of *in vitro* follicle maturation (IVFM) results confirming oocyte quality from both GM (left) and GM+Apr (right) conditions. Data are shown as mean ± SEM, $p < 0.05$. MII rate (GM) = 78% ± 3%, MII rate (GM+Apr) = 81% ± 3%. Scale bar=100 μm.

Fig. 3 Correlation of fibrin degradation and follicle health, evaluated by both manual calculation (M) and automated MATLAB ® program (A).

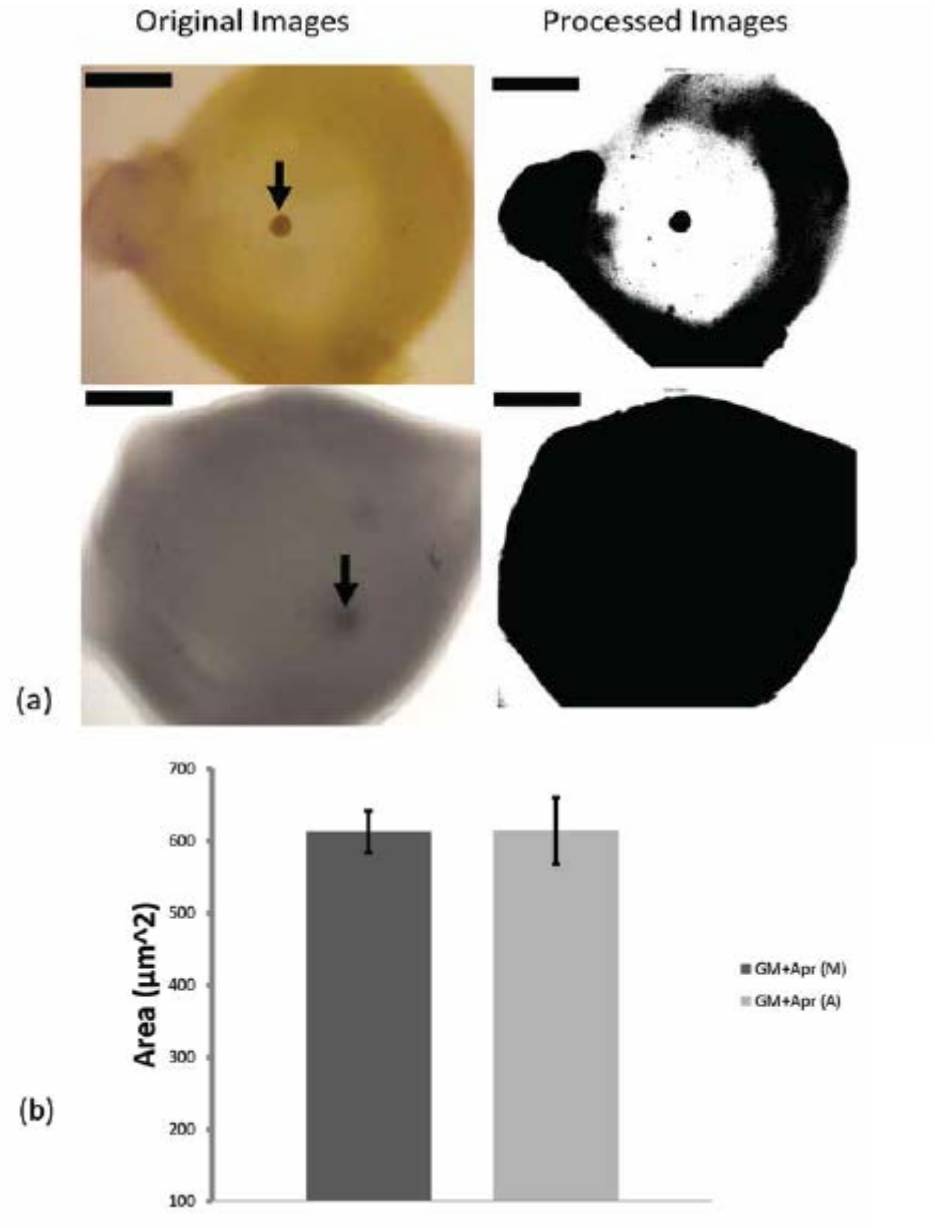

(a) Representative images of a live follicle (top) and a dead follicle (bottom) in brightfield images and processed binary images. Scale bar = 800 µm. (b) Results from manual calculation (M) and automated program measurement (A) of fibrin degradation in GM+Apr condition for live follicles on D6. Data presented as mean ± SEM, with n = 9 in each case.

Fig. 4 Illustration of the HTP system.

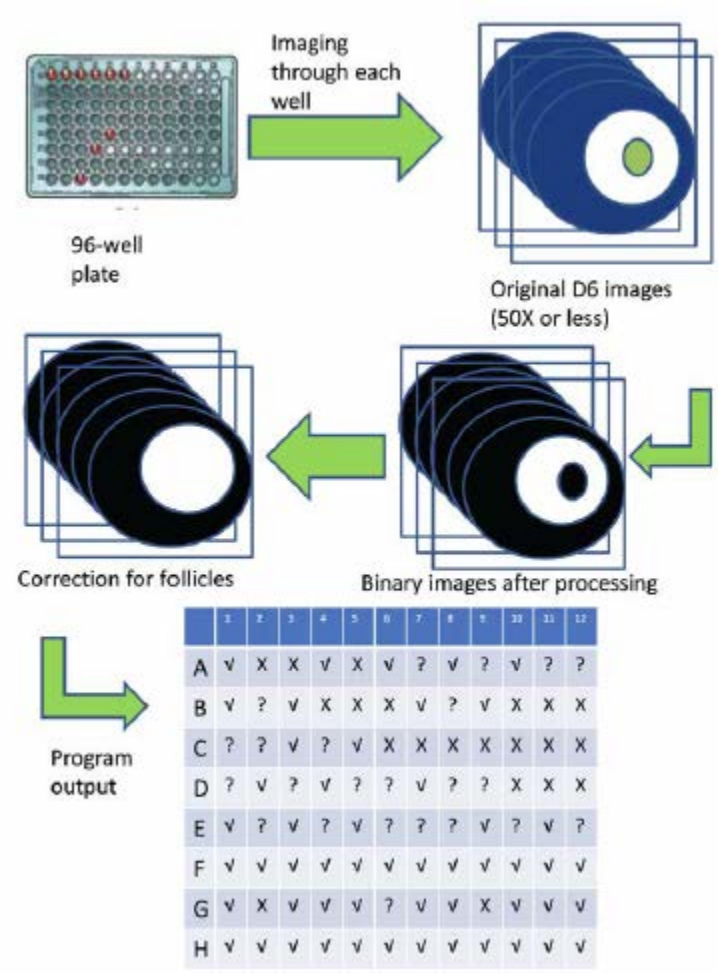

	1	2	3	4	5	6	7	8	9	10	11	12
A	√	X	X	√	X	√	?	√	?	√	?	?
B	√	?	√	X	X	X	√	?	√	X	X	X
C	?	?	√	?	√	X	X	X	X	X	X	X
D	?	√	?	√	?	?	√	?	?	X	X	X
E	√	?	√	?	√	?	?	?	√	?	√	?
F	√	√	√	√	√	√	√	√	√	√	√	√
G	√	X	√	√	√	?	√	√	X	√	√	√
H	√	√	√	√	√	√	√	√	√	√	√	√

Images captured from 96-well plates are converted using MATLAB ® program to binary images. After comparing the area of fibrin degradation (shown as white circles) to control conditions, the program will then output results of follicle health evaluated by fibrin degradation: "√" indicates healthy follicles, "X" dead ones, and "?" requiring further evaluation.

Fig. 5 System validation with Doxorubicin (DXR).

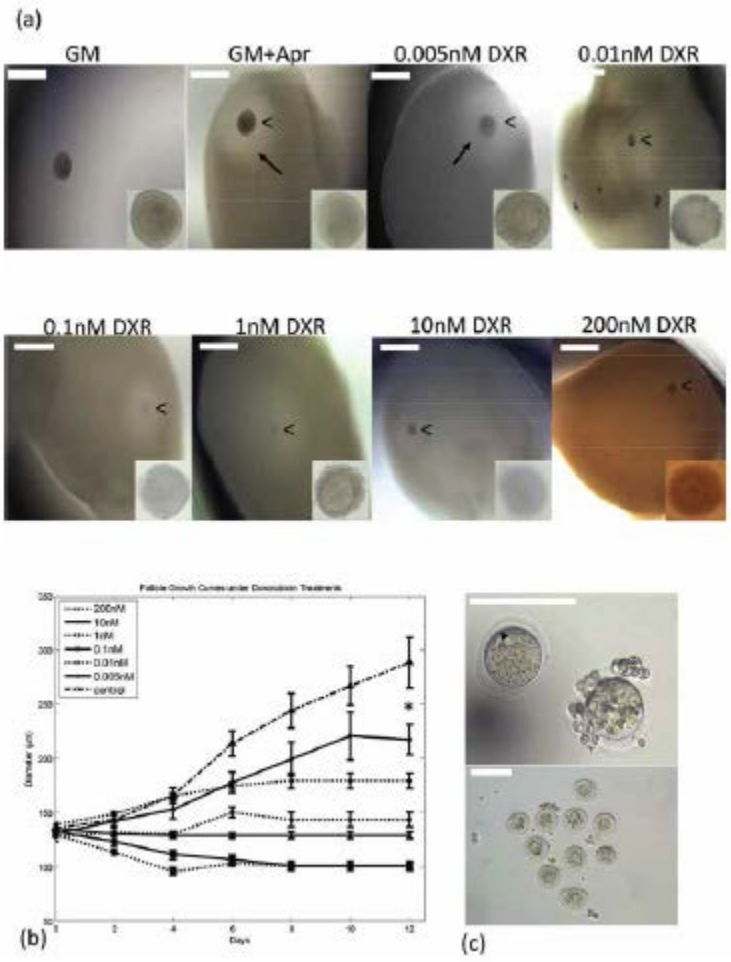

(a) Representative images of dose response of cultured follicles to DXR. Arrow points to the fibrin degradation area surrounding the growing follicle. Arrow head ("<") points to the encapsulated follicle in the FA-IPN. Scale bar = 500 µm. (b) Kaplan-Meier cumulative survival curves for DXR treatments and control. Sample sizes for each condition [n (condition) = total follicles, animal used, experiments]: n (200 nM) = 69, 4, 3; n (10 nM) = 52, 3, 3; n (1 nM) = 75, 3, 3; n (0.1 nM) = 75, 3, 3; n (0.01 nM) = 80, 3, 3; n (0.005 nM) = 92, 4, 3. (c) Representative images of *in vitro* follicle maturation (IVFM) results from survived follicles in the 0.01 nM (left) and 0.005 nM (right) DXR treatment group. Scale bar = 100 µm. (d) The diameters of surviving follicles in control conditions (GM and GM+Apr) and 0.005 nM and 0.01 nM DXR treatment groups. Data presented as mean ± SEM.

Fig. 6 Quantitative measurements of fibrin degradation with different DXR treatments.

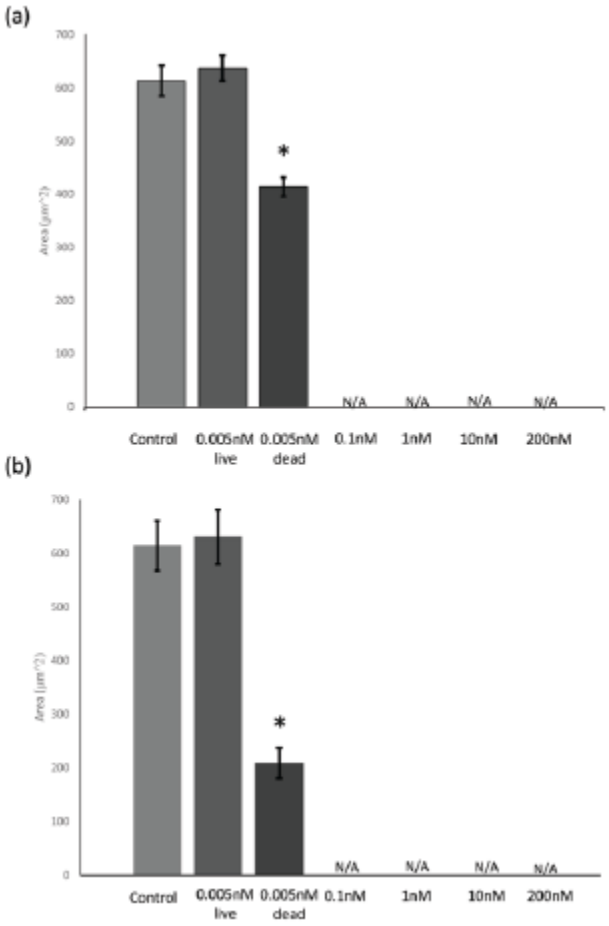

(a) Manual calculation of fibrin degradation area; (b) Automated MATLAB® measurement of fibrin degradation. Data presented as mean ± SEM, n = 9, † n (GM+Apr+0.005nM DXR, dead, automated) = 3, *: $p<0.05$.

Fig. 7 Lindane concentration-dependent effects on cultured ovarian follicles.

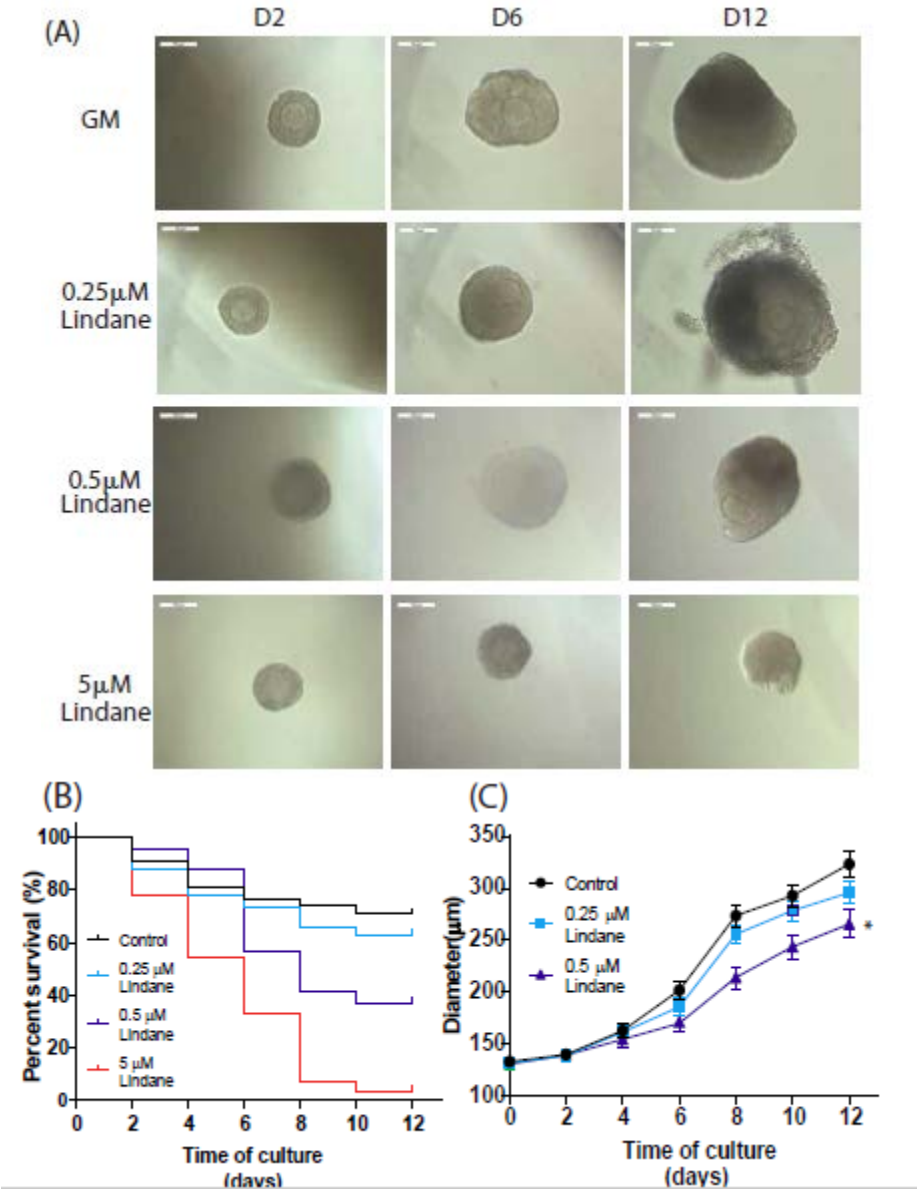

A. Representative images of lindane concentration-dependent effects on secondary follicles. Scale bar = 100 μm. B. Follicle survival after lindane treatments. N = 75 (control: GM), 128 (0.25 μM), 128 (0.5 μM), 104 (5 μM). C. Follicle growth curves with lindane treatments: data presented as mean ± SEM. N = 52 (control), 62 (0.25 μM), 45 (0.5 μM).

Fig. 8 DMBA concentration-dependent effects on cultured ovarian follicles.

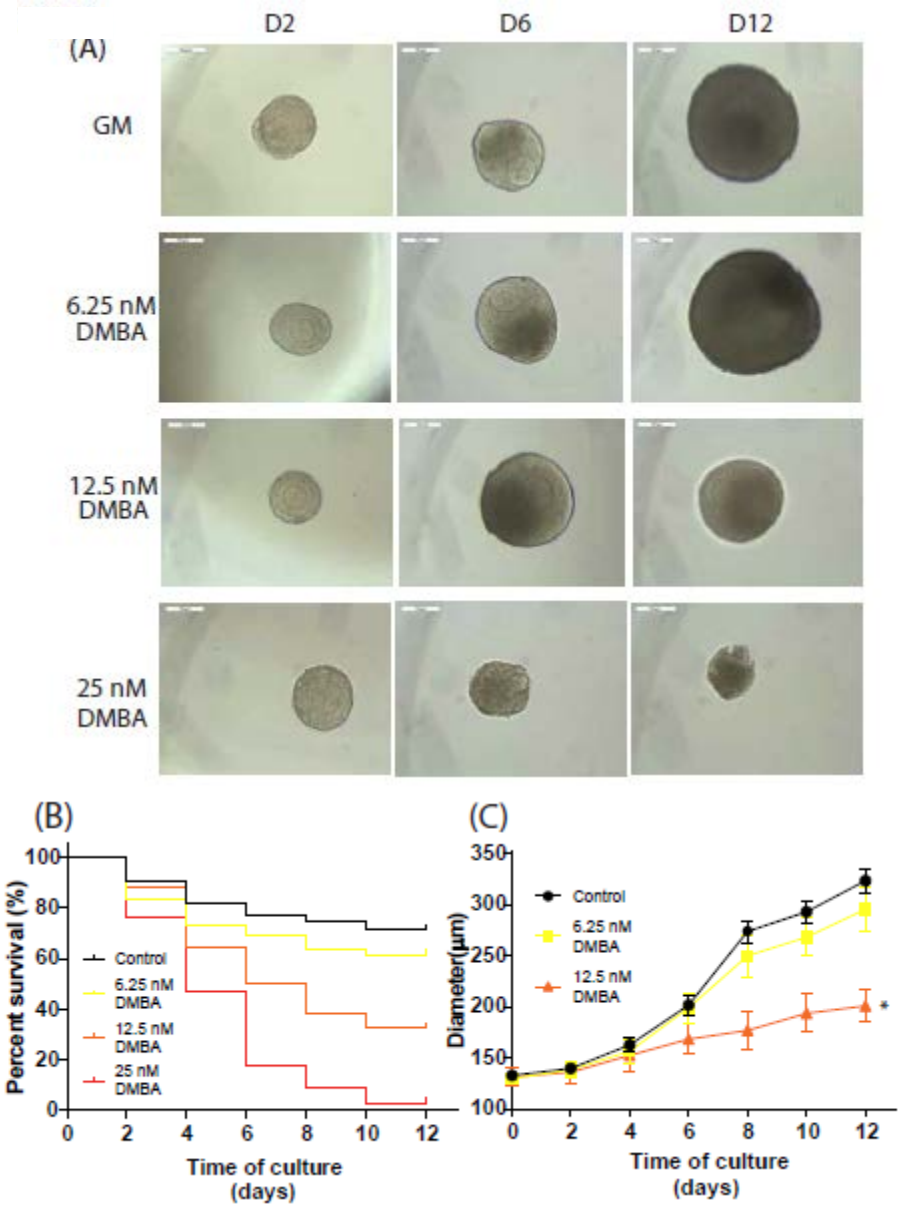

A. Representative images of DMBA does-dependent effects on secondary follicles. Scale bar = 100 μm. B. Follicle survival after DMBA treatments. N =75 (control: GM), 124 (6.25 nM), 128 (12.5 nM), 54 (25 nM). C. Follicle growth curves under DMBA treatments: data presented as mean ± SEM. N = 52 (control: GM), 62 (6.25 nM), 50 (12.5 nM).

Fig. 9 Combinational effects of Lindane and DMBA on cultured secondary ovarian follicles.

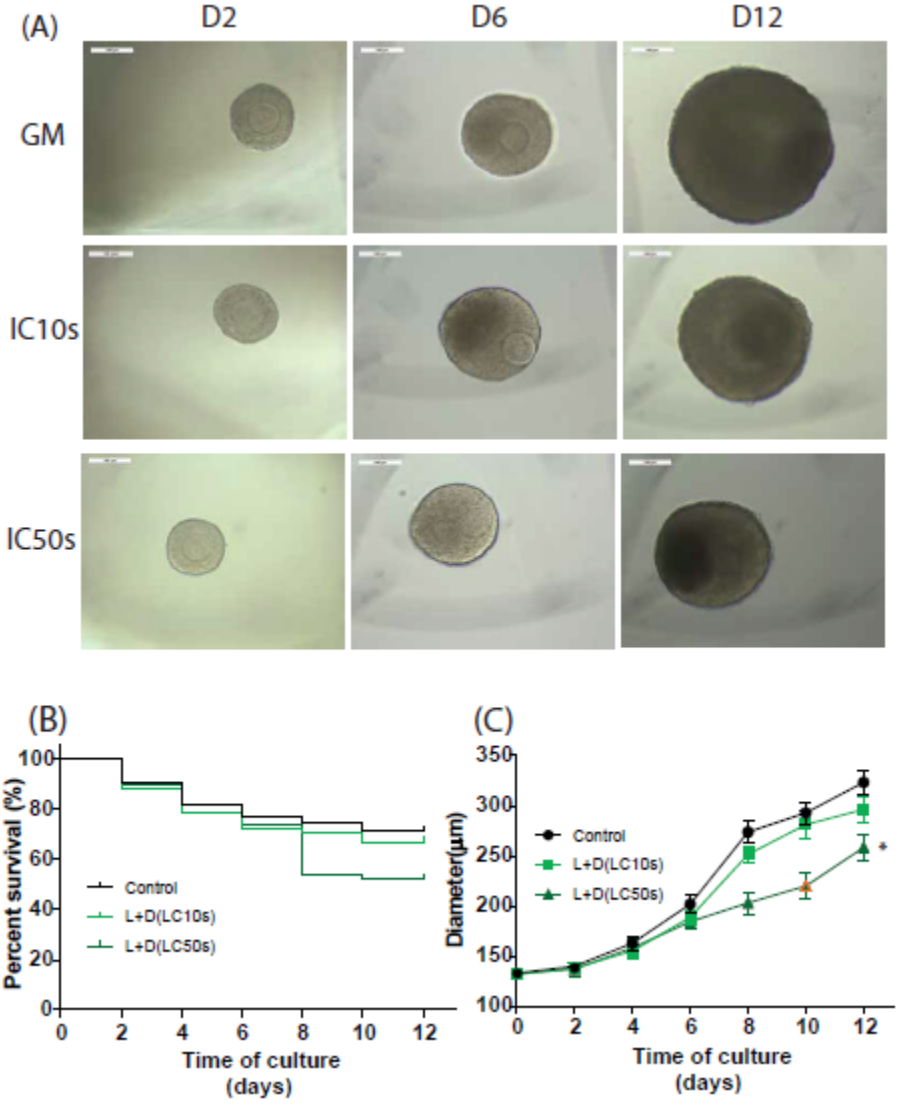

A. Representative images of Lindane and DMBA combinational effects on secondary follicles. Scale bar = 100 μm. B. Follicle survival under combination of Lindane and DMBA. n(control) = 75, n(LC10s) = 102, (LC50s) = 100. C. Follicle growth under combination of Lindane and DMBA: data presented as mean ± SEM; n(control) = 52, n(IC10s) = 34, n(IC50s) = 36.

Fig. 10 Lindane and DMBA effects on oocyte of survived follicles.

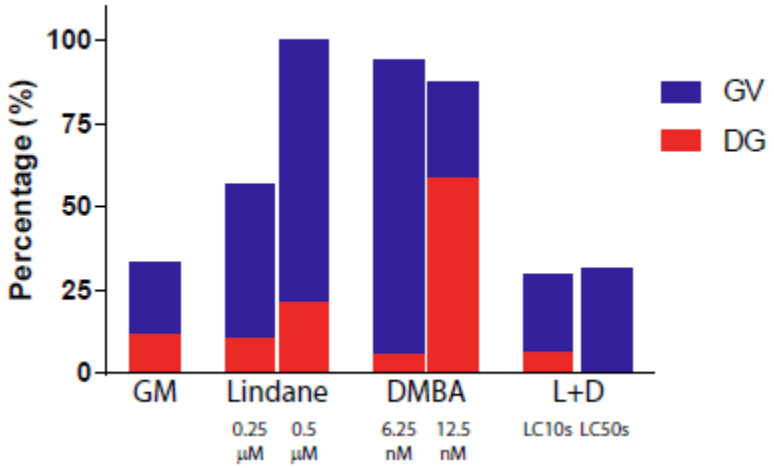

A percentage change was calculated as: $percentage\ change = \frac{treatment - control}{control}$. Data were pooled from at least 3 independent experiments in any conditions. Sample sizes were as follow: n = 45 (control), 38 (0.25 µM lindane), 20 (0.5 µM lindane); n = 28 (6.25 nM DMBA), 24 (12.5 nM DMBA); n = 34 (LC10s), 32 (LC50s).

Fig. 11 Lindane and DMBA effects on secondary ovarian follicles.

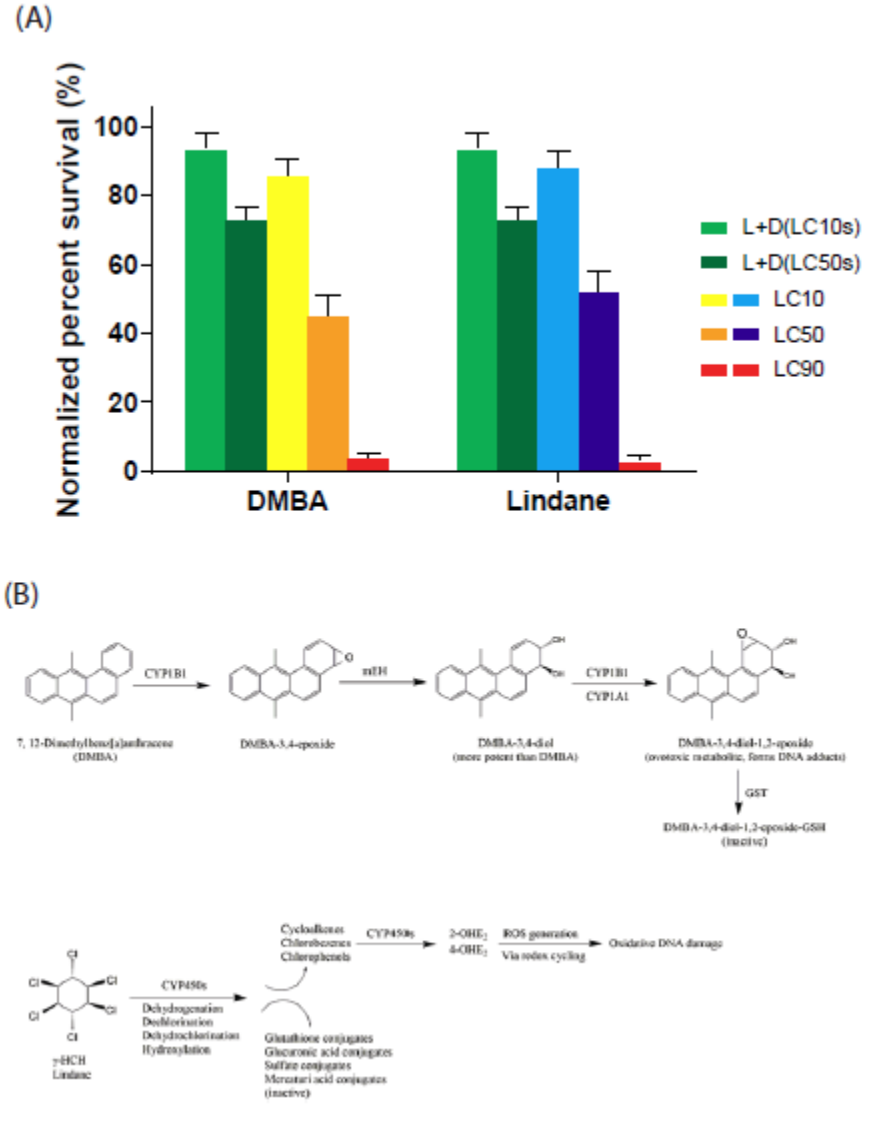

A. Concentration-dependent responses of lindane and DMBA on cultured ovarian follicles: data presented as mean ± SEM; n(0.25 µM lindane) = n(6.25 nM DBMA) = 5 cultures, n(0.5 µM lindane) = n(5 µM lindane) = n(12.5 nM DMBA) = n(25 nM DMBA) = 3 cultures, n(LC10s) = n(LC50s) = 6 cultures. B. Proposed follicle metabolisms of lindane and DMBA: summarized from literature (Bhattacharya and Keating 2011; Organization 1991).

Fig. 12 Hydrogel design of the novel scaffold containing dual degradation sites.

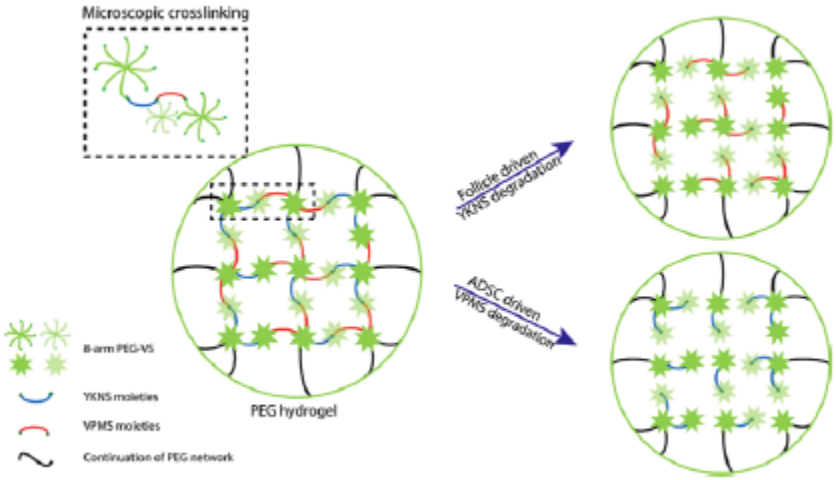

Fig. 13 Mechanical properties of YKNS and YKNS/VPMS gels.

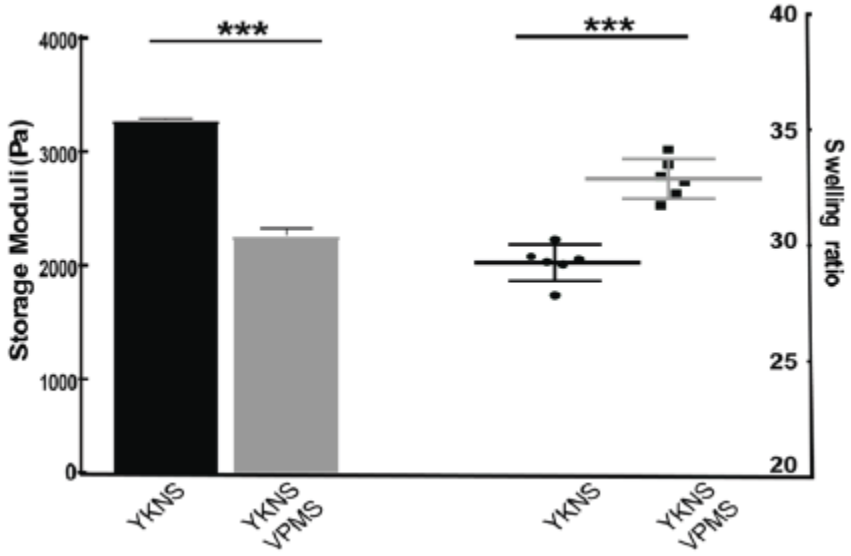

Sample sizes: n = 3 gels per condition (rheology), and n = 6 gels per condition (swelling ratios).

Fig. 14 Improved ADSC survival in YKNS/VPMS gels.

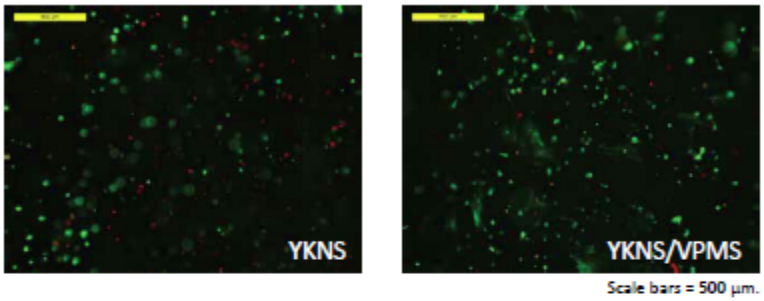

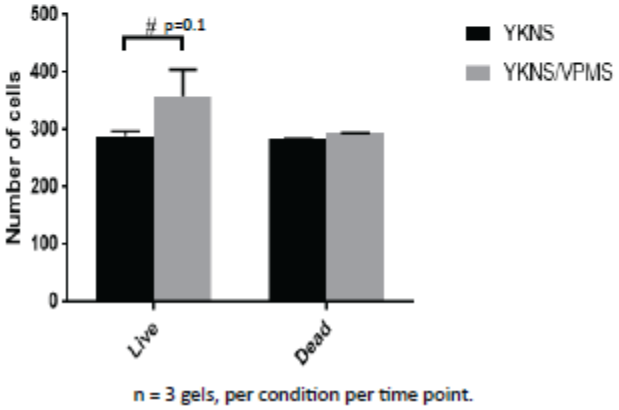

Sample size (n) = 3 gels per condition.

Fig. 15 Follicle survival, growth and maturation in YKNS gels.

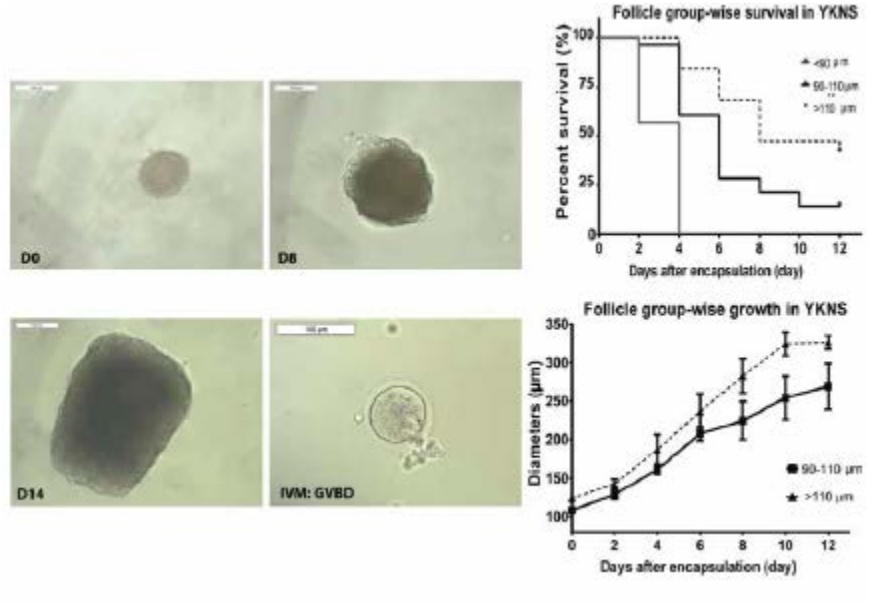

Sample sizes: for survival curves: n = 7 (<90 µm), 28 (90 – 110 µm), and 19 (> 110 µm); for growth curves: n = 0 (<90 µm), 4 (90 – 110 µm), and 6 (> 110 µm). Scale bar: 100 µm.

Fig. 16 Follicle survival, growth and maturation in YKNS/VPMS gels.

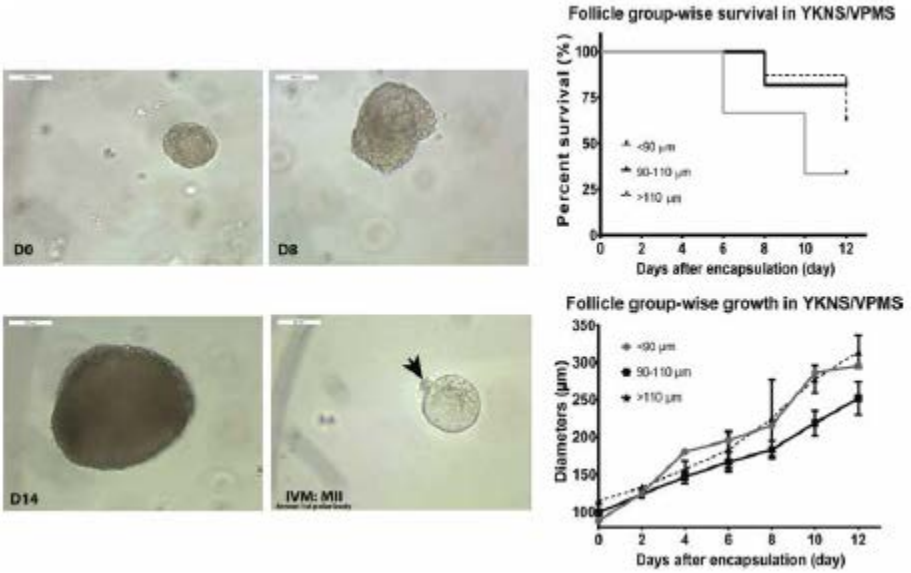

Sample sizes: for survival curves: n = 3 (<90 μm), 11 (90 – 110 μm), and 8 (> 110 μm); for growth curves: n = 1 (<90 μm), 9 (90 – 110 μm), and 2 (> 110 μm). Scale bar: 100 μm.

Fig. 17 Illustration of lentiviral transduction of enzymatically isolated ovarian follicles.

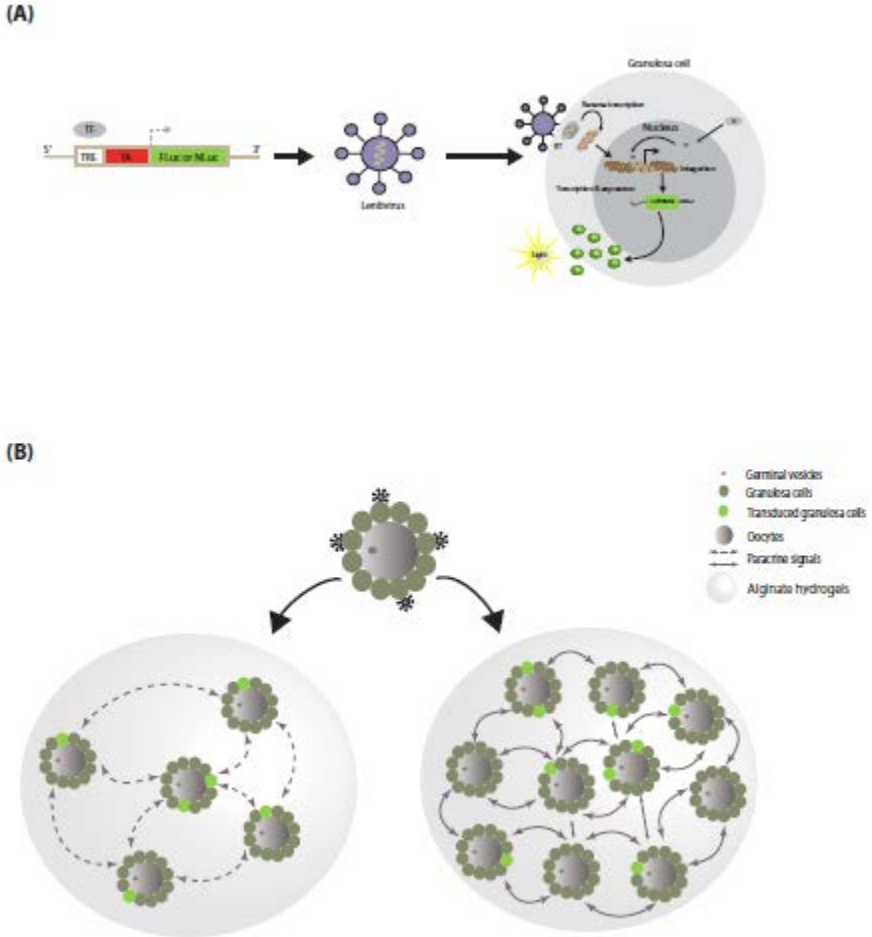

Fig. 18 The number-dependent manner of folliculogenesis in follicles cultured in either groups of five (5X) or ten (10X).

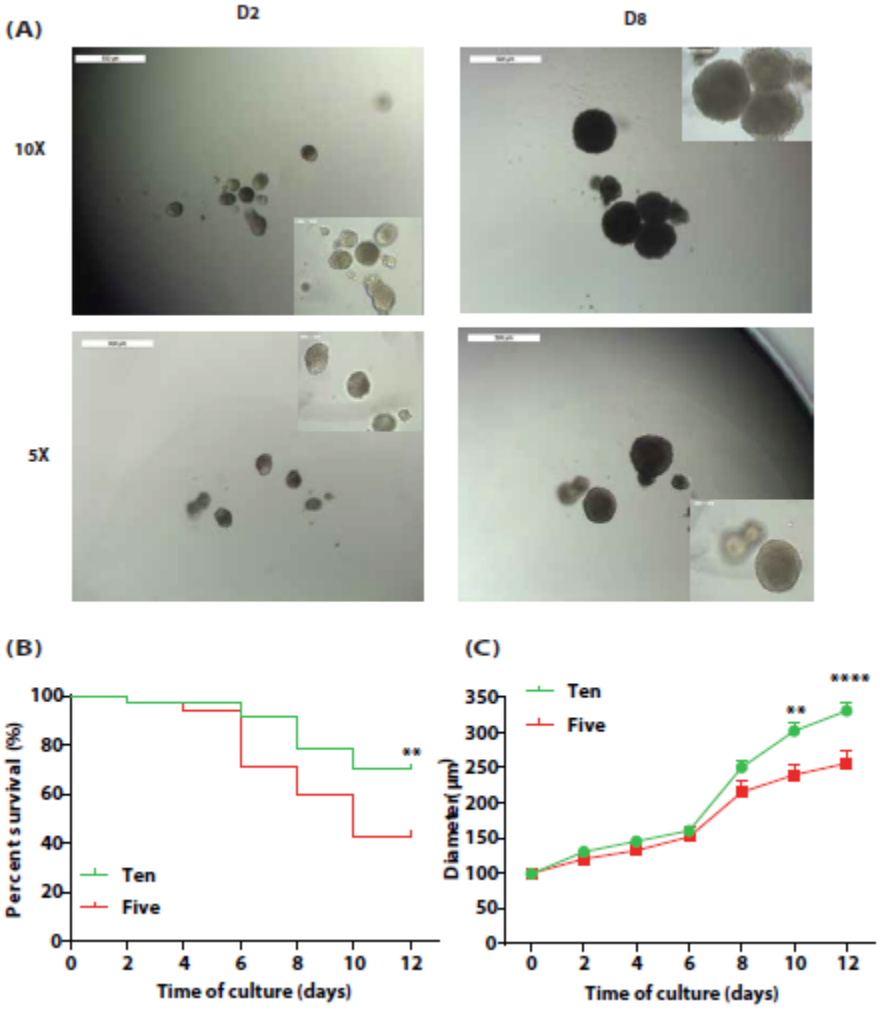

A. Representative images of eIVFG in 5X and 10X follicles. Scale bar = 500 µm (100 µm for inserts). B. Follicle survival in 5X and 10X. Sample size: n = 35 (5X) and 80 (10X). C. Follicle growth in 5X and 10X. Sample size: n = 15 (5X) and 56 (10X).

Fig. 19 Profiles of androstenedione (A4) (A), estradiol (E2) (B), and progesterone (P4) (C) in 5X and 10X follicles during eIVFG.

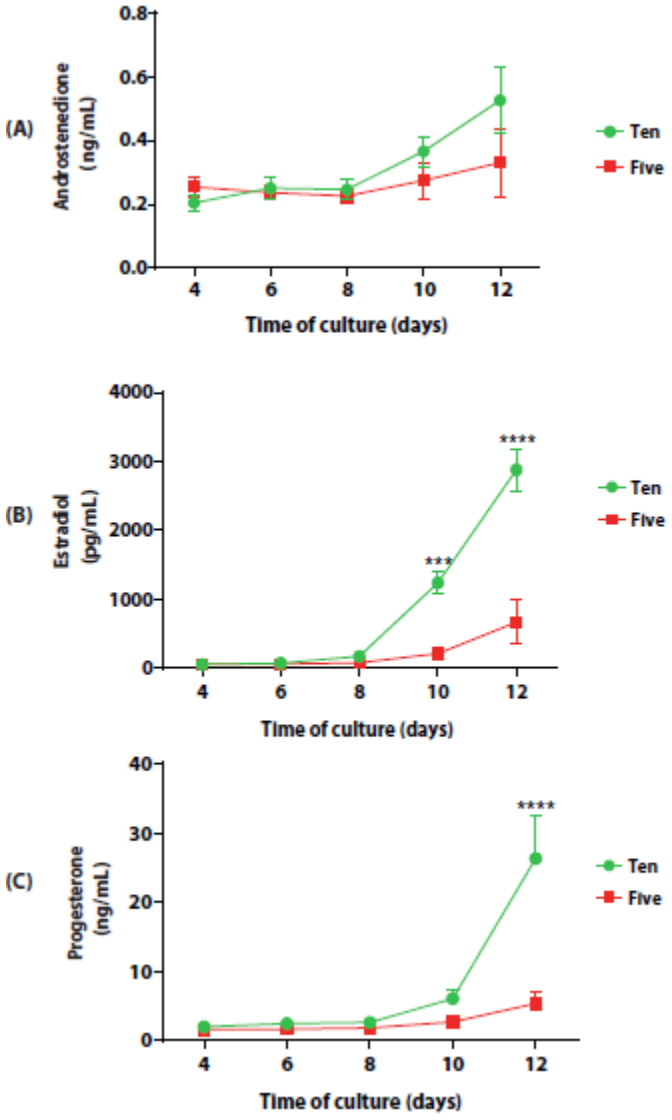

Sample size: n = 4 per time point.

Fig. 20 Bioluminescence and luciferase production from normalization vectors in transduced follicles.

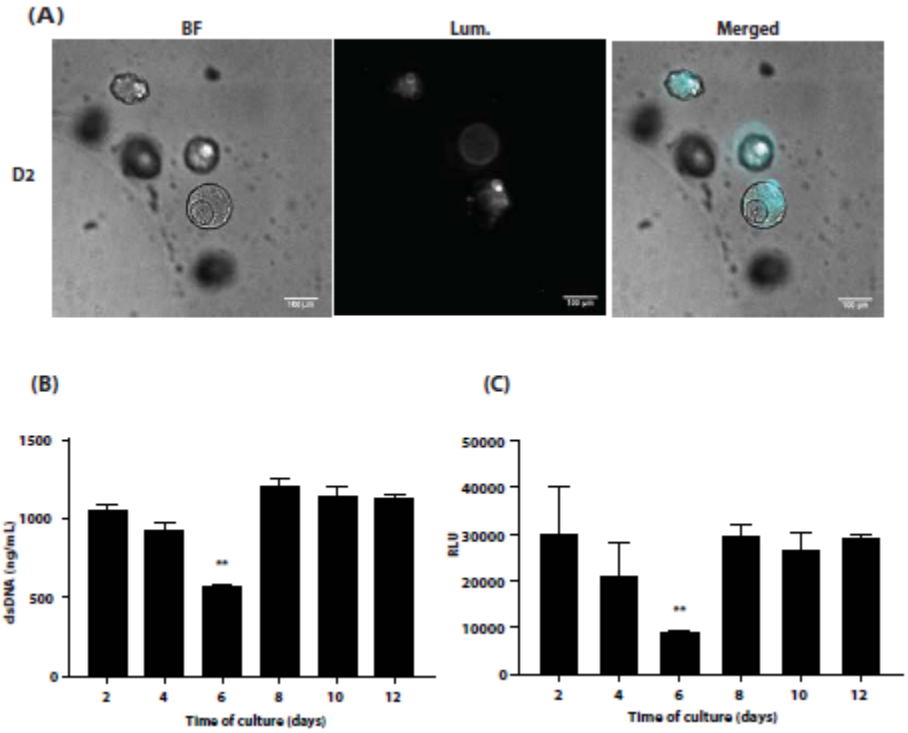

A. Representative bioluminescence images of transduced follicles to confirm luciferase expression. Scale bar : 100 µm. B. Quantification of the amount of total DNA during eIVFG. Sample size: n = 3 per time point. C. Quantification of luciferase production during eIVFG. Sample size: n = 3 per time point.

Fig. 21 Dynamic activities of selected TFs (p53 = A, NF-κB = B, Gli = C, and HIF1 = D) during folliculogenesis.

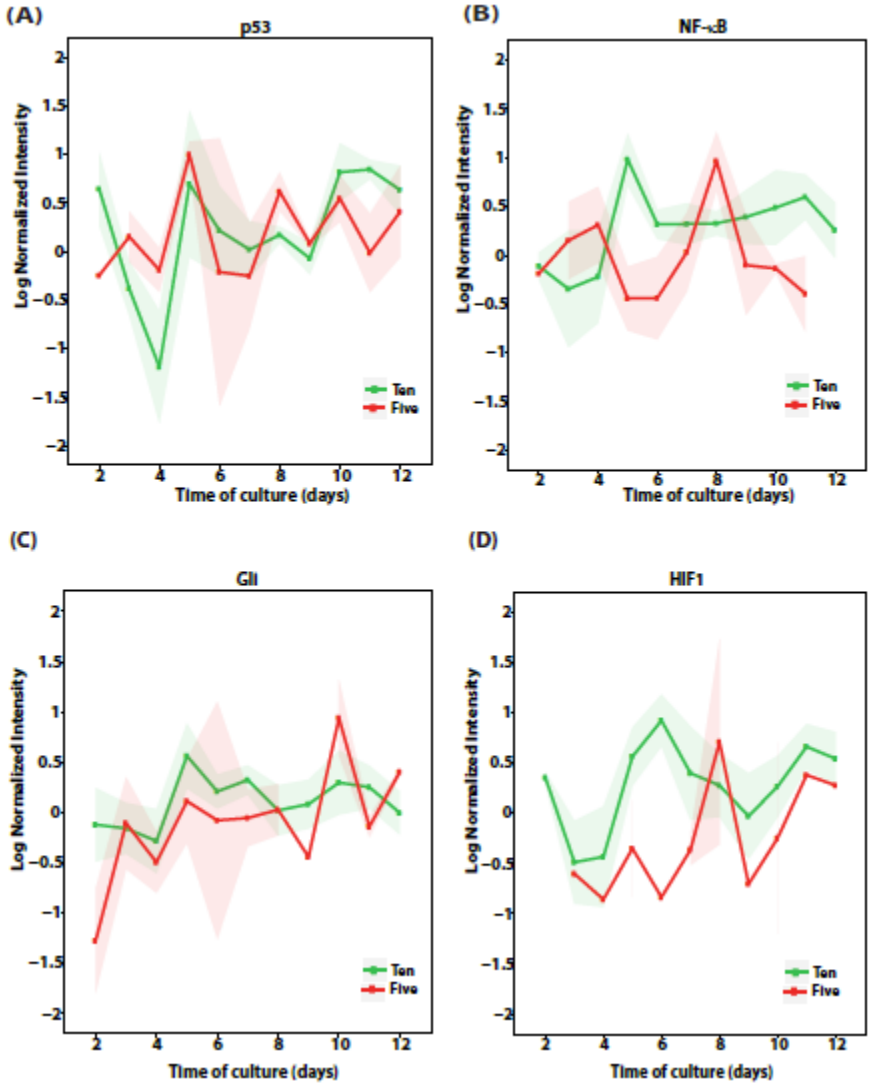

Fig. 22 Isolating ovaries from surrounding tissues.

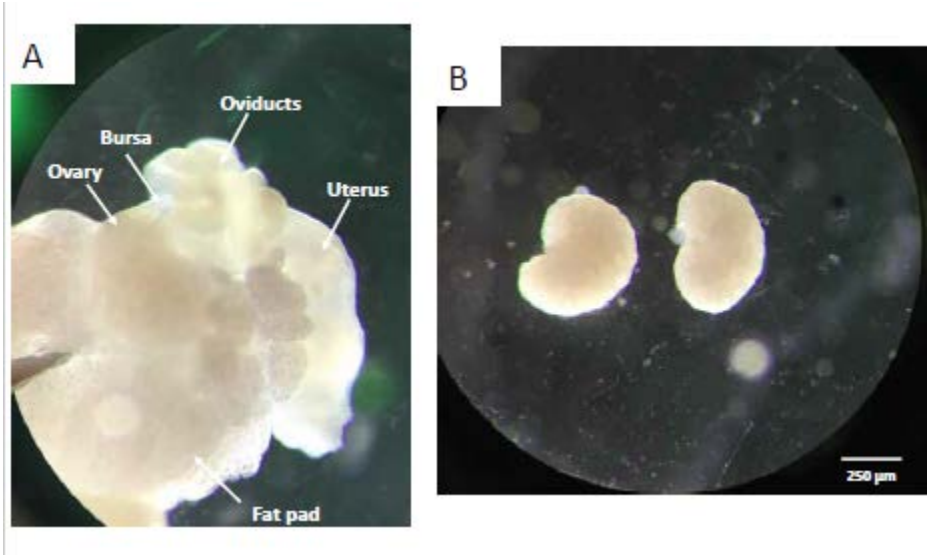

A. Resected tissues with one ovary embedded. B. Isolated ovaries clean from tissues.

Fig. 23 Follicle isolation.

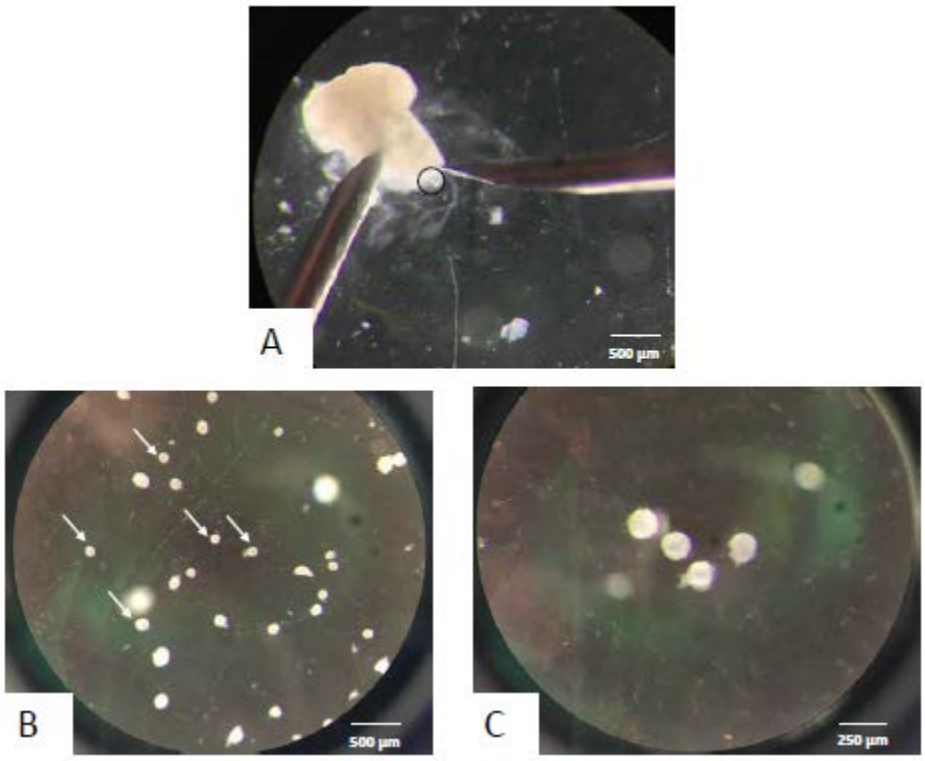

A: Needle positions relative to an identified follicle. Dashed circle: an identified follicle. The left needle is used to anchor the tissue to the bottom of the plate while the right needle is used to tease and “flick” the follicle away from the ovary. B: Isolated follicles under 50X. Try to keep isolated follicles apart to prevent them sticking back together. White arrows: example follicles; C: Suitable follicles examined under 100X for proper diameters and intact morphology.

Fig. 24 Follicle encapsulation setup for FA-IPN.

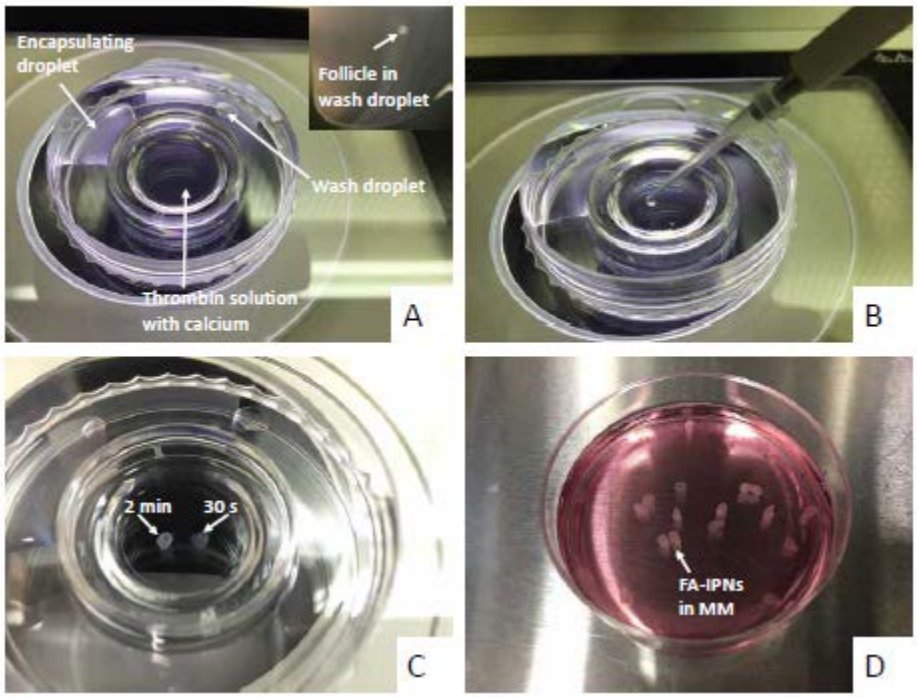

A: FA-IPN encapsulation setup with the washing droplet on the right and the encapsulating drop on the left. B. Dropping the FA-IPN with a follicle into the TBS solution with calcium. C. FA-IPN beads in the crosslinking solution the crosslinking progresses. D. FA-IPN beads in MM.

Fig. 25 Follicles encapsulated in FA-IPNs.

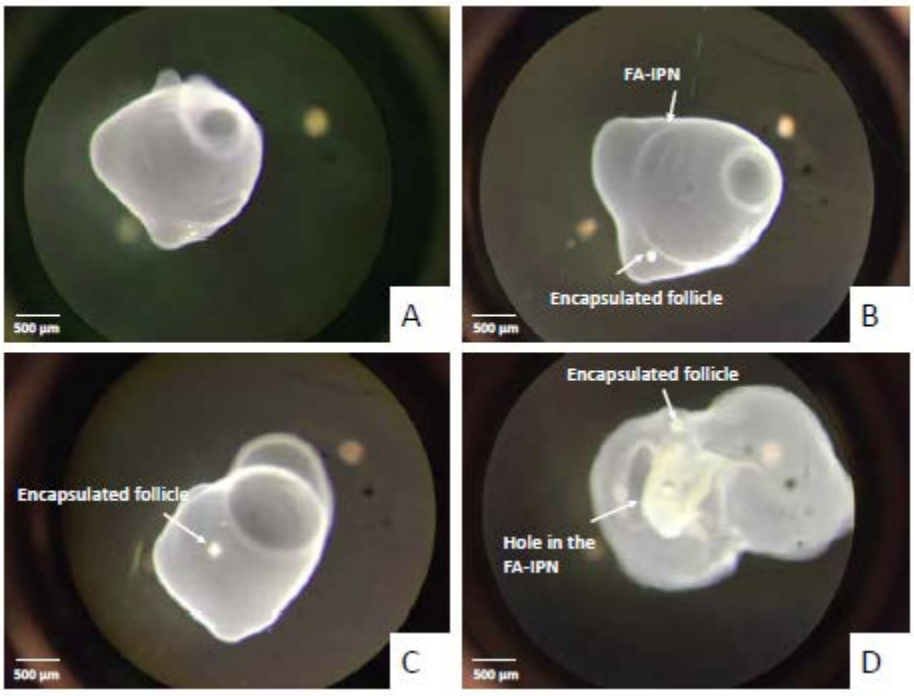

A. Empty bead; B. Follicle encapsulated at the edge of the bead; C. Follicle encapsulated towards the center of the bead; D. Bead with a hole.

Fig. 26 96-well plate setup with DPBS (blue) on the outer side as humidity control and GM (green) in the middle.

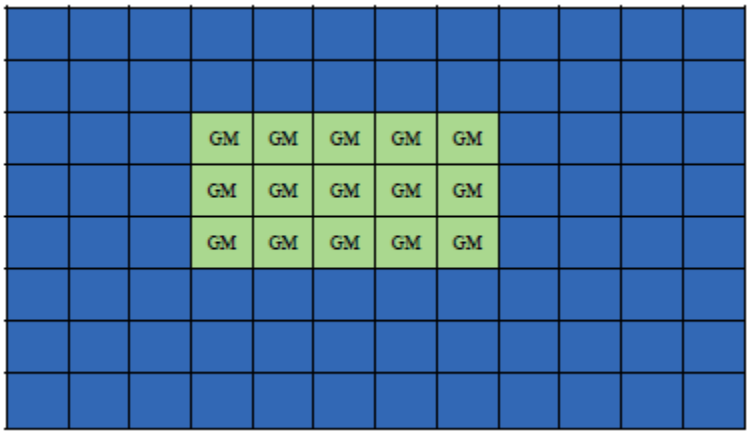

Fig. 27 Follicles in FA-IPN with aprotinin-controlled degradation are used to screen for toxicants in vitro.

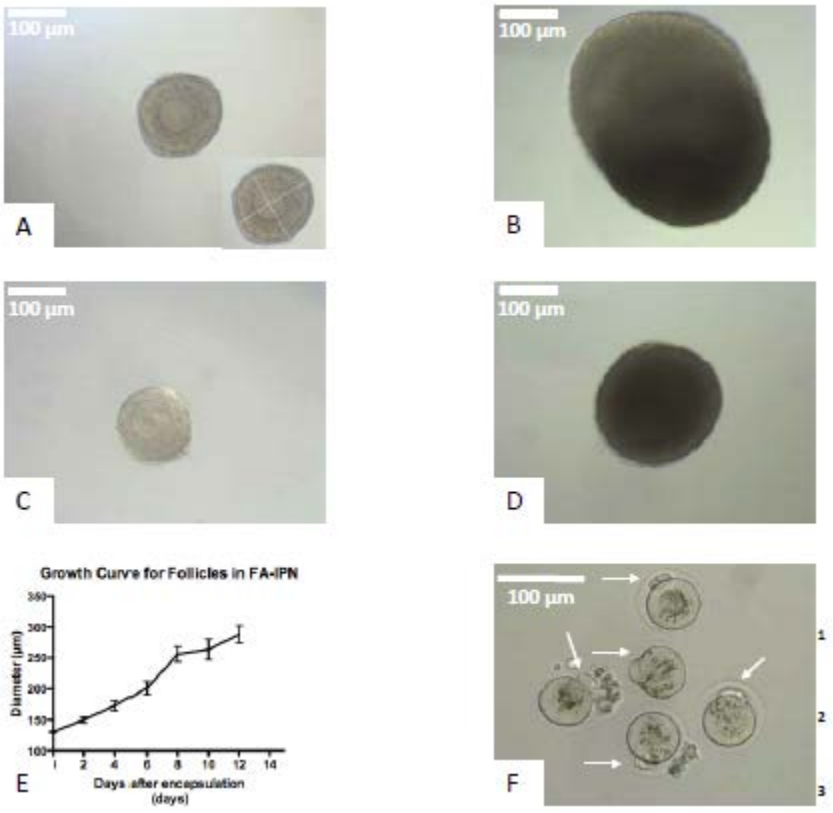

A & C: Representative images of follicles in FA-IPN on D2. Insert of A shows the measurements of follicle diameter: 2 orthogonal lines across the oocyte, excluding the ECM. B & D: Representative D10 images of live (B) and dead (D) follicles. E: Follicle growth curve in FA-IPN. Data are presented as mean ± SEM, with n = 30. F: Representative image of in vitro follicle maturation (IVFM). Arrows: MII oocytes. Arrow head: germinal vesicle.

Fig. 28 Representative D6 images of FA-IPN application for toxicology test (12.5 nM DMBA).

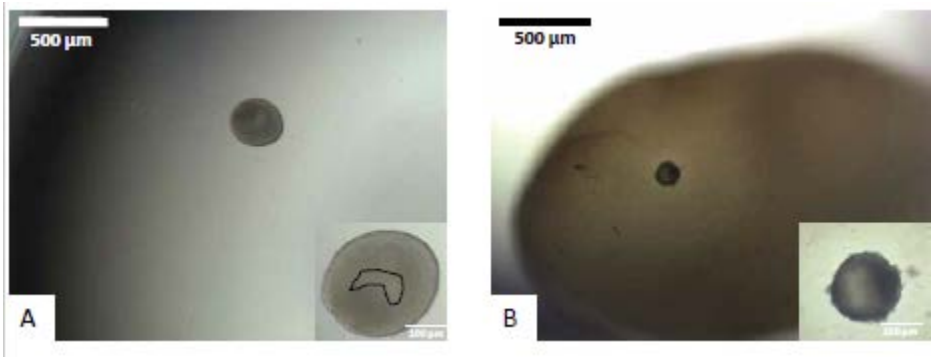

A: untreated growing follicle in the control condition, antrum outlined. B: treated and dead follicle with minimal fibrin degradation.

Fig. 29 General experimental outline for follicle and cell co-encapsulation, see text for detailed description.

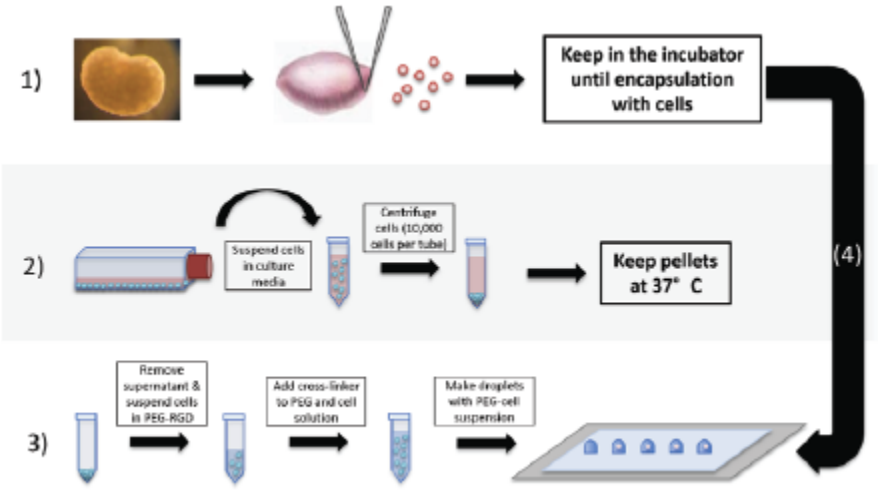

1) The experiment should start by extracting the ovary and isolating individual follicles which are then stored in an incubator for future use up to 12 hours, see “Ovarian Dissection” and “Follicle Isolation” steps. 2) Cells are then trypsinized from incubation flask, counted and centrifuged into pellets containing 100,000 cells. Cell pellets should be maintained in DMEM at 37°C during encapsulation for no longer than one hour, see “Cell and Follicle Encapsulation”. 3) Resuspend cell pellet in PEG-RGD solution and add crosslinker solution only when you are ready to begin encapsulation, see “Cell and Follicle Encapsulation”. Using the PEG-RGD-crosslinker cell suspension, form droplets on parafilm which will be used for 4) follicle encapsulation, as “Cell and Follicle Encapsulation”.

Fig. 30 Evaluation of follicle survival after the encapsulation.

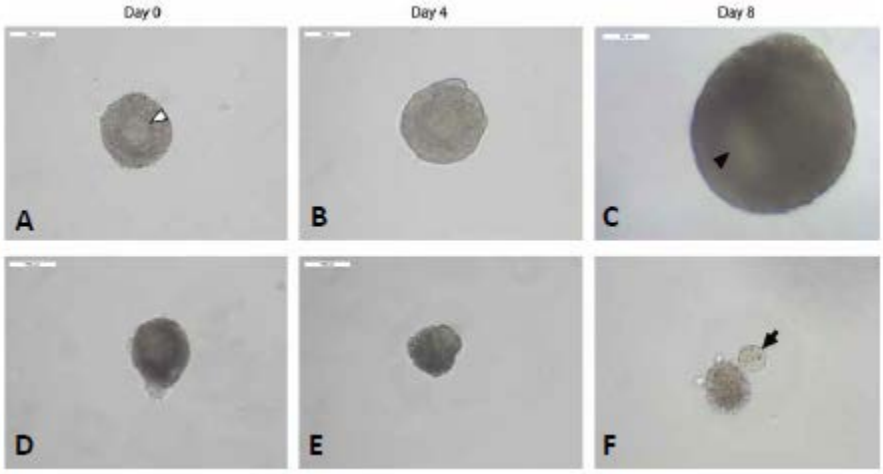

Top row: (A) a healthy follicle on Day 0 has a diameter between 100-120 µm with centrally located round intact oocyte (white arrow head) surrounded by granulosa cells. (B) A healthy follicle grows and expands and on day 8 antrum formation(C, black arrow head) promotes further development. The healthy follicle will reach a diameter of 300 µm or more on Day 8 or 10.Bottom row: (D) a non-healthy follicle has a dark complexion and the oocyte does not have a round shape with homogeneous color. Follicles with dark regions do not grow or expand and eventually extrude the oocyte (E,F black arrow points to extruded oocyte on dead follicle).

Fig. 31 Schematic of the gel preparation.

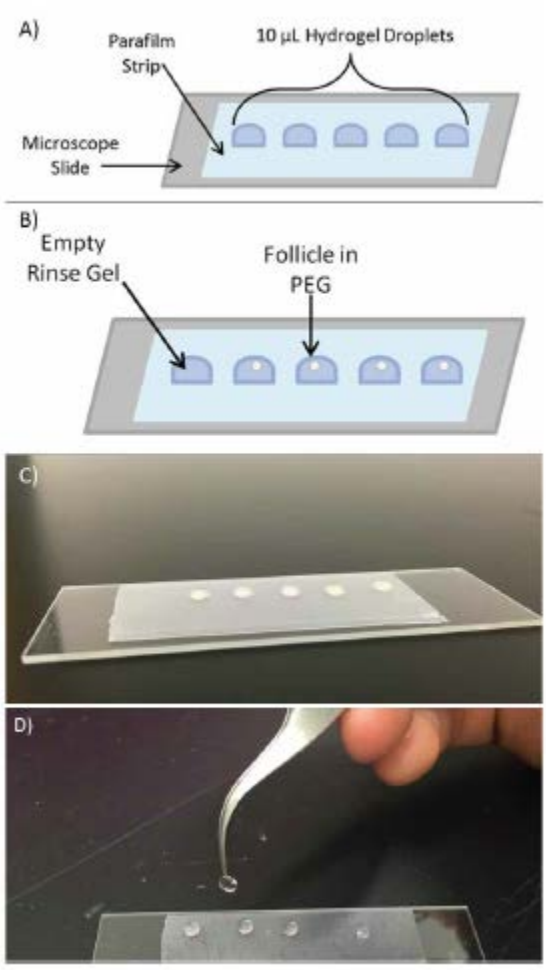

A) Glass slide coated with a hydrophobic layer of parafilm. B) Hydrogel droplets (10 µl each) on the hydrophobic surface for follicle rinse and follicle encapsulation. C) Image of a slide with hydrogel droplets. D) Image of formed hydrogel held with forceps.

Bibliography

Agarwal SK, Chang RJ. 2007. Fertility management for women with cancer. Oncofertility Fertility Preservation for Cancer Survivors:15-27.

Andersen ME, Krewski D. 2009. Toxicity testing in the 21st century: Bringing the vision to life. Toxicological Sciences 107:324-330.

Andersen ME, Krewski D. 2009. Toxicity testing in the 21st century: Bringing the vision to life. Toxicological sciences : an official journal of the Society of Toxicology 107:324-330.

Anderson LD, Hirshfield AN. 1992. An overview of follicular development in the ovary: From embryo to the fertilized ovum in vitro. Maryland medical journal (Baltimore, Md : 1985) 41:614-620.

Argyle CE, Harper JC, Davies MC. 2016. Oocyte cryopreservation: Where are we now? Human reproduction update 22:440-449.

Ataya K, Moghissi K. 1989. Chemotherapy-induced premature ovarian failure: Mechanisms and prevention. Steroids 54:607-626.

Baillet A, Mandon-Pepin B. 2012. Mammalian ovary differentiation - a focus on female meiosis. Molecular and cellular endocrinology 356:13-23.

Barpe DR, Rosa DD, Froehlich PE. 2010. Pharmacokinetic evaluation of doxorubicin plasma levels in normal and overweight patients with breast cancer and simulation of dose adjustment by different indexes of body mass. European journal of pharmaceutical sciences : official journal of the European Federation for Pharmaceutical Sciences 41:458-463.

Basavarajappa M, Peretz J, Paulose T, Gupta R, Ziv-Gal A, Flaws JA. 2016. 16 toxicity of the pregnant female reproductive system. Reproductive Toxicology:291.

Beers WH. 1975. Follicular plasminogen and plasminogen activator and the effect of plasmin on ovarian follicle wall. Cell 6:379-386.

Ben-Aharon I, Bar-Joseph H, Tzarfaty G, Kuchinsky L, Rizel S, Stemmer SM, et al. 2010. Doxorubicin-induced ovarian toxicity. Reproductive biology and endocrinology : RB&E 8:20.

Benjamini Y, Hochberg Y. 1995. Controlling the false discovery rate: A practical and powerful approach to multiple testing. Journal of the royal statistical society Series B (Methodological):289-300.

Bhattacharya P, Keating AF. 2011. Ovarian metabolism of xenobiotics. Experimental biology and medicine (Maywood, NJ) 236:765-771.

Bhattacharya P, Keating AF. 2012. Impact of environmental exposures on ovarian function and role of xenobiotic metabolism during ovotoxicity. Toxicology and applied pharmacology 261:227-235.

Boontheekul T, Kong H-J, Mooney DJ. 2005. Controlling alginate gel degradation utilizing partial oxidation and bimodal molecular weight distribution. Biomaterials 26:2455-2465.

Braw-Tal R. 2002. The initiation of follicle growth: The oocyte or the somatic cells? Molecular and cellular endocrinology 187:11-18.

Brito IR, Lima IM, Xu M, Shea LD, Woodruff TK, Figueiredo JR. 2014. Three-dimensional systems for in vitro follicular culture: Overview of alginate-based matrices. Reproduction, fertility, and development 26:915-930.

Burns KH, Owens GE, Fernandez JM, Nilson JH, Matzuk MM. 2002. Characterization of integrin expression in the mouse ovary. Biology of reproduction 67.

Chin KV, Seifer DB, Feng B, Lin Y, Shih WC. 2002. DNA microarray analysis of the expression profiles of luteinized granulosa cells as a function of ovarian reserve. Fertility and sterility 77:1214-1218.

Chu S, Nishi Y, Yanase T, Nawata H, Fuller PJ. 2004. Transrepression of estrogen receptor beta signaling by nuclear factor-kappab in ovarian granulosa cells. Mol Endocrinol 18:1919-1928.

Clarke HG, Hope SA, Byers S, Rodgers RJ. 2006. Formation of ovarian follicular fluid may be due to the osmotic potential of large glycosaminoglycans and proteoglycans. Reproduction 132:119-131.

Collins FS, Gray GM, Bucher JR. 2008. Toxicology. Transforming environmental health protection. Science 319:906-907.

Combes RD, Gaunt I, Balls M. 2004. A scientific and animal welfare assessment of the oecd health effects test guidelines for the safety testing of chemicals under the european union reach system. Alternatives to laboratory animals: ATLA 32:163-208.

Cortvrindt RG, Smitz JE. 2002. Follicle culture in reproductive toxicology: A tool for in-vitro testing of ovarian function? Hum Reprod Update 8:243-254.

Cyr DG, Devine PJ, Plante I. 2016. Immunohistochemistry and female reproductive toxicology: The ovary and mammary glands. In: Technical aspects of toxicological immunohistochemistry:Springer, 113-145.

Decker JT, Hobson EC, Zhang Y, Shin S, Thomas AL, Jeruss JS, et al. 2017. Systems analysis of dynamic transcription factor activity identifies targets for treatment in olaparib resistant cancer cells. Biotechnology and bioengineering 114:2085-2095.

Dolmans MM, Martinez-Madrid B, Gadisseux E, Guiot Y, Yuan WY, Torre A, et al. 2007. Short-term transplantation of isolated human ovarian follicles and cortical tissue into nude mice. Reproduction 134:253-262.

Donnez J, Dolmans M-M, Demylle D, Jadoul P, Pirard C, Squifflet J, et al. 2004. Livebirth after orthotopic transplantation of cryopreserved ovarian tissue. The lancet 364:1405-1410.

Donnez J, Dolmans M-M, Pellicer A, Diaz-Garcia C, Serrano MS, Schmidt KT, et al. 2013. Restoration of ovarian activity and pregnancy after transplantation of cryopreserved ovarian tissue: A review of 60 cases of reimplantation. Fertility and sterility 99:1503-1513.

Drury JL, Mooney DJ. 2003. Hydrogels for tissue engineering: Scaffold design variables and applications. Biomaterials 24:4337-4351.

Dull T, Zufferey R, Kelly M, Mandel RJ, Nguyen M, Trono D, et al. 1998. A third-generation lentivirus vector with a conditional packaging system. Journal of virology 72:8463-8471.

Edson MA, Nagaraja AK, Matzuk MM. 2009. The mammalian ovary from genesis to revelation. Endocrine reviews 30:624-712.

El-Sadi F, Nader A, Becker C. 2013. Ovulation and regulation of the menstrual cycle. Textbook of Clinical Embryology:38.

Ferrara N, Gerber H-P, LeCouter J. 2003. The biology of vegf and its receptors. Nature medicine 9:669-676.

Ganesan S, Bhattacharya P, Keating AF. 2013. 7, 12-dimethylbenz [a] anthracene exposure induces the DNA repair response in neonatal rat ovaries. Toxicology and applied pharmacology 272:690-696.

Ganesan S, Nteeba J, Keating AF. 2015. Impact of obesity on 7,12-dimethylbenz[a]anthracene-induced altered ovarian connexin gap junction proteins in female mice. Toxicology and applied pharmacology 282:1-8.

Gelboin HV. 1980. Benzo [alpha] pyrene metabolism, activation and carcinogenesis: Role and regulation of mixed-function oxidases and related enzymes. Physiological reviews 60:1107-1166.

Gimble J, Guilak F. 2003. Adipose-derived adult stem cells: Isolation, characterization, and differentiation potential. Cytotherapy 5:362-369.

Gimble JM, Katz AJ, Bunnell BA. 2007. Adipose-derived stem cells for regenerative medicine. Circulation research 100:1249-1260.

Hajializadeh N, Babaei H, Nematollahi-Mahani S, Azizollahi S. 2008. The development of mouse early embryos in vitro in fibroblasts and cumulus cells co-cultures supplemented with retinoic acid. Iranian Journal of Veterinary Research 9:1-8.

Hareng L, Pellizzer C, Bremer S, Schwarz M, Hartung T. 2005. The integrated project reprotect: A novel approach in reproductive toxicity hazard assessment. Reproductive Toxicology 20:441-452.

Hasegawa A, Kumamoto K, Mochida N, Komori S, Koyama K. 2009. Gene expression profile during ovarian folliculogenesis. Journal of reproductive immunology 83:40-44.

Hernandez-Gonzalez I, Gonzalez-Robayna I, Shimada M, Wayne CM, Ochsner SA, White L, et al. 2006. Gene expression profiles of cumulus cell oocyte complexes during ovulation reveal cumulus cells express neuronal and immune-related genes: Does this expand their role in the ovulation process? Mol Endocrinol 20:1300-1321.

Hirao Y, Nagai T, Kubo M, Miyano T, Miyake M, Kato S. 1994. In vitro growth and maturation of pig oocytes. Journal of Reproduction and Fertility 100:333-339.

Hirshfield AN. 1991. Development of follicles in the mammalian ovary. International review of cytology 124:43-101.

Hornick J, Duncan FE, Shea L, Woodruff TK. 2013. Multiple follicle culture supports primary follicle growth through paracrine-acting signals. Reproduction 145:19-32.

Hoyer PB, Keating AF. 2014. Xenobiotic effects in the ovary: Temporary versus permanent infertility. Expert opinion on drug metabolism & toxicology 10:511-523.

Hu W, Zheng T, Wang J. 2011. Regulation of fertility by the p53 family members. Genes & cancer 2:420-430.

Huang YC, Dennis RG, Larkin L, Baar K. 2005. Rapid formation of functional muscle in vitro using fibrin gels. Journal of applied physiology (Bethesda, Md : 1985) 98:706-713.

Igawa Y, Keating AF, Rajapaksa KS, Sipes IG, Hoyer PB. 2009. Evaluation of ovotoxicity induced by 7, 12-dimethylbenz[a]anthracene and its 3,4-diol metabolite utilizing a rat in vitro ovarian culture system. Toxicology and applied pharmacology 234:361-369.

Jeruss JS, Woodruff TK. 2009. Preservation of fertility in patients with cancer. New England Journal of Medicine 360:902-911.

Jick H, Porter J, Morrison A. 1977. Relation between smoking and age of natural menopause: Report from the boston collaborative drug surveillance program, boston university medical center. The Lancet 309:1354-1355.

Jin SY, Lei L, Shikanov A, Shea LD, Woodruff TK. 2010. A novel two-step strategy for in vitro culture of early-stage ovarian follicles in the mouse. Fertility and sterility 93:2633-2639.

Jurisicova A, Lee HJ, D'Estaing SG, Tilly J, Perez GI. 2006. Molecular requirements for doxorubicin-mediated death in murine oocytes. Cell death and differentiation 13:1466-1474.

Karin M, Lin A. 2002. Nf-[kappa]b at the crossroads of life and death. Nat Immunol 3:221-227.

Kastan MB, Zhan Q, El-Deiry WS, Carrier F, Jacks T, Walsh WV, et al. 1992. A mammalian cell cycle checkpoint pathway utilizing p53 and gadd45 is defective in ataxia-telangiectasia. Cell 71:587-597.

Ke FC, Fang SH, Lee MT, Sheu SY, Lai SY, Chen YJ, et al. 2005. Lindane, a gap junction blocker, suppresses fsh and transforming growth factor beta1-induced connexin43 gap junction formation and steroidogenesis in rat granulosa cells. J Endocrinol 184:555-566.

Kim SJ, Park KM, Kim N, Yeom YI. 2006. Doxorubicin prevents endoplasmic reticulum stress-induced apoptosis. Biochemical and biophysical research communications 339:463-468.

Knight PG, Glister C. 2006. Tgf-beta superfamily members and ovarian follicle development. Reproduction 132:191-206.

Kreeger PK, Fernandes NN, Woodruff TK, Shea LD. 2005. Regulation of mouse follicle development by follicle-stimulating hormone in a three-dimensional in vitro culture system is dependent on follicle stage and dose. Biology of reproduction 73:942-950.

Kuo CK, Ma PX. 2001. Ionically crosslinked alginate hydrogels as scaffolds for tissue engineering: Part 1. Structure, gelation rate and mechanical properties. Biomaterials 22:511-521.

Kutz FW, Wood PH, Bottimore DP. 1991. Organochlorine pesticides and polychlorinated biphenyls in human adipose tissue. In: Reviews of environmental contamination and toxicology:Springer, 1-82.

Laronda MM, Duncan FE, Hornick JE, Xu M, Pahnke JE, Whelan KA, et al. 2014. Alginate encapsulation supports the growth and differentiation of human primordial follicles within ovarian cortical tissue. Journal of assisted reproduction and genetics 31:1013-1028.

Lebbe M, Taylor AE, Visser JA, Kirkman-Brown J, Woodruff TK, Arlt W. 2017. The steroid metabolome in the isolated ovarian follicle and its response to androgen exposure and antagonism. Endocrinology.

Lee KY, Mooney DJ. 2001. Hydrogels for tissue engineering. Chemical reviews 101:1869-1880.

Lee SJ, Schover LR, Partridge AH, Patrizio P, Wallace WH, Hagerty K, et al. 2006. American society of clinical oncology recommendations on fertility preservation in cancer patients. Journal of clinical oncology : official journal of the American Society of Clinical Oncology 24:2917-2931.

Lenie S, Smitz J. 2009. Steroidogenesis-disrupting compounds can be effectively studied for major fertility-related endpoints using in vitro cultured mouse follicles. Toxicol Lett 185:143-152.

Li R, Mather JP. 1997. Lindane, an inhibitor of gap junction formation, abolishes oocyte directed follicle organizing activity in vitro. Endocrinology 138:4477-4480.

Liang M, Yao G, Yin M, Lu M, Tian H, Liu L, et al. 2013. Transcriptional cooperation between p53 and nf-kappab p65 regulates microrna-224 transcription in mouse ovarian granulosa cells. Molecular and cellular endocrinology 370:119-129.

Loch-Caruso R, Galvez MM, Brant K, Chung D. 2004. Cell and toxicant specific phosphorylation of conexin43: Effects of lindane and tpa on rat myometrial and wb-f344 liver cell gap junctions. Cell biology and toxicology 20:147-169.

Loch-Caruso R, Upham BL, Harris C, Trosko JE. 2005. Divergent roles for glutathione in lindane-induced acute and delayed-onset inhibition of rat myometrial gap junctions. Toxicological sciences : an official journal of the Society of Toxicology 85:694-702.

Makanji Y, Tagler D, Pahnke J, Shea LD, Woodruff TK. 2014. Hypoxia-mediated carbohydrate metabolism and transport promote early-stage murine follicle growth and survival. American Journal of Physiology - Endocrinology and Metabolism 306:E893-E903.

Makrigiannakis A, Amin K, Coukos G, Tilly JL, Coutifaris C. 2000. Regulated expression and potential roles of p53 and wilms' tumor suppressor gene (wt1) during follicular development in the human ovary. The Journal of clinical endocrinology and metabolism 85:449-459.

Markstrom E, Svensson E, Shao R, Svanberg B, Billig H. 2002. Survival factors regulating ovarian apoptosis--dependence on follicle differentiation. Reproduction 123:23-30.

Martin MT, Mendez E, Corum DG, Judson RS, Kavlock RJ, Rotroff DM, et al. 2009. Profiling the reproductive toxicity of chemicals from multigeneration studies in the toxicity reference database. Toxicological sciences : an official journal of the Society of Toxicology 110:181-190.

Matti N, Irving-Rodgers HF, Hatzirodos N, Sullivan TR, Rodgers RJ. 2010. Differential expression of focimatrix and steroidogenic enzymes before size deviation during waves of follicular development in bovine ovarian follicles. Molecular and cellular endocrinology 321.

Mattison DR. 1993. Sites of female reproductive vulnerability: Implications for testing and risk assessment. Reproductive toxicology (Elmsford, NY) 7 Suppl 1:53-62.

McGee EA, Hsueh AJ. 2000. Initial and cyclic recruitment of ovarian follicles. Endocrine reviews 21:200-214.

McLaughlin M, Telfer EE. 2010. Oocyte development in bovine primordial follicles is promoted by activin and fsh within a two-step serum-free culture system. Reproduction 139:971-978.

Memili E, Peddinti D, Shack LA, Nanduri B, McCarthy F, Sagirkaya H, et al. 2007. Bovine germinal vesicle oocyte and cumulus cell proteomics. Reproduction 133:1107-1120.

Miller KP, Gupta RK, Greenfeld CR, Babus JK, Flaws JA. 2005. Methoxychlor directly affects ovarian antral follicle growth and atresia through bcl-2- and bax-mediated pathways. Toxicological sciences : an official journal of the Society of Toxicology 88:213-221.

Miller KP, Gupta RK, Flaws JA. 2006. Methoxychlor metabolites may cause ovarian toxicity through estrogen-regulated pathways. Toxicological sciences : an official journal of the Society of Toxicology 93:180-188.

Miyata M, Furukawa M, Takahashi K, Gonzalez FJ, Yamazoe Y. 2001. Mechanism of 7, 12-dimethylbenz [a] anthracene-induced immunotoxicity: Role of metabolic activation at the target organ. The Japanese Journal of Pharmacology 86:302-309.

Moore KL, Persaud TVN, Torchia MG. 2015. The developing human: Clinically oriented embryology:Elsevier Health Sciences.

Morgan S, Lopes F, Gourley C, Anderson RA, Spears N. 2013. Cisplatin and doxorubicin induce distinct mechanisms of ovarian follicle loss; imatinib provides selective protection only against cisplatin. PLoS One 8:e70117.

Nejaty H, Lacey M, Whitehead SA. 2001. Differing effects of endocrine-disrupting chemicals on basal and fsh-stimulated progesterone production in rat granulosa-luteal cells. Experimental biology and medicine (Maywood, NJ) 226:570-576.

Noyes N, Porcu E, Borini A. 2009. Over 900 oocyte cryopreservation babies born with no apparent increase in congenital anomalies. Reproductive biomedicine online 18:769-776.

Nteeba J, Ganesan S, Keating AF. 2014. Impact of obesity on ovotoxicity induced by 7,12-dimethylbenz[a]anthracene in mice. Biology of reproduction 90:68, 61-10.

O'Brien MJ, Pendola JK, Eppig JJ. 2003. A revised protocol for in vitro development of mouse oocytes from primordial follicles dramatically improves their developmental competence. Biology of reproduction 68:1682-1686.

Oktem O, Urman B. 2010. Understanding follicle growth in vivo. Human reproduction 25:2944-2954.

Organization WH. 1991. Lindane.

Pan H, O'Brien M J, Wigglesworth K, Eppig JJ, Schultz RM. 2005. Transcript profiling during mouse oocyte development and the effect of gonadotropin priming and development in vitro. Dev Biol 286:493-506.

Pangas SA, Saudye H, Shea LD, Woodruff TK. 2003. Novel approach for the three-dimensional culture of granulosa cell-oocyte complexes. Tissue engineering 9:1013-1021.

Peddinti D, Memili E, Burgess SC. 2010. Proteomics-based systems biology modeling of bovine germinal vesicle stage oocyte and cumulus cell interaction. PLoS One 5:e11240.

Peng J, Eppig JJ, Matzuk MM. 2013. Bidirectional communication between the oocyte and surrounding somatic cells is required for successful follicular development and oocyte maturation. Ten Critical Topics in Reproductive Medicine:12.

Peretz J, Flaws JA. 2013. Bisphenol a down-regulates rate-limiting cyp11a1 to acutely inhibit steroidogenesis in cultured mouse antral follicles. Toxicology and applied pharmacology 271:249-256.

Perez GI, Knudson CM, Leykin L, Korsmeyer SJ, Tilly JL. 1997. Apoptosis-associated signaling pathways are required for chemotherapy-mediated female germ cell destruction. Nature medicine 3:1228-1232.

Peters H, Byskov AG, Himelstein-braw R, Faber M. 1975. Follicular growth: The basic event in the mouse and human ovary. Journal of Reproduction and Fertility 45:559-566.

Qu T, Jing J, Ren Y, Ma C, Feng JQ, Yu Q, et al. 2015. Complete pulpodentin complex regeneration by modulating the stiffness of biomimetic matrix. Acta biomaterialia 16:60-70.

Rebbaa A, Chou PM, Emran M, Mirkin BL. 2001. Doxorubicin-induced apoptosis in caspase-8-deficient neuroblastoma cells is mediated through direct action on mitochondria. Cancer chemotherapy and pharmacology 48:423-428.

Rebbaa A, Zheng X, Chou PM, Mirkin BL. 2003. Caspase inhibition switches doxorubicin-induced apoptosis to senescence. Oncogene 22:2805-2811.

Revelli A, Delle Piane L, Casano S, Molinari E, Massobrio M, Rinaudo P. 2009. Follicular fluid content and oocyte quality: From single biochemical markers to metabolomics. Reproductive biology and endocrinology : RB&E 7:40.

Rotroff DM, Dix DJ, Houck KA, Knudsen TB, Martin MT, McLaurin KW, et al. 2013. Using in vitro high throughput screening assays to identify potential endocrine-disrupting chemicals. Environmental health perspectives 121:7-14.

Sasson R, Dantes A, Tajima K, Amsterdam A. 2003. Novel genes modulated by fsh in normal and immortalized fsh-responsive cells: New insights into the mechanism of fsh action. FASEB journal : official publication of the Federation of American Societies for Experimental Biology 17:1256-1266.

Schneider CA, Rasband WS, Eliceiri KW. 2012. Nih image to imagej: 25 years of image analysis. Nat Meth 9:671-675.

Semenza GL. 2002. Signal transduction to hypoxia-inducible factor 1. Biochemical pharmacology 64:993-998.

Sharma A, Gill J, Banga H. 2017. Effect of low dose chronic exposure to deltamethrin and lindane on reproductive system of male mice. Theriogenology Insight: An International Journal of Reproduction in all Animals 7:25.

Shea LD, Woodruff TK, Shikanov A. 2014. Bioengineering the ovarian follicle microenvironment. Annual review of biomedical engineering 16:29-52.

Shikanov A, Xu M, Woodruff TK, Shea LD. 2009. Interpenetrating fibrin-alginate matrices for in vitro ovarian follicle development. Biomaterials 30:5476-5485.

Shikanov A, Smith RM, Xu M, Woodruff TK, Shea LD. 2011a. Hydrogel network design using multifunctional macromers to coordinate tissue maturation in ovarian follicle culture. Biomaterials 32:2524-2531.

Shikanov A, Xu M, Woodruff TK, Shea LD. 2011b. A method for ovarian follicle encapsulation and culture in a proteolytically degradable 3 dimensional system. Journal of visualized experiments : JoVE.

Shimada T, Sugie A, Shindo M, Nakajima T, Azuma E, Hashimoto M, et al. 2003. Tissue-specific induction of cytochromes p450 1a1 and 1b1 by polycyclic aromatic hydrocarbons and polychlorinated biphenyls in engineered c57bl/6j mice of arylhydrocarbon receptor gene. Toxicology and applied pharmacology 187:1-10.

Shiverick KT. 2017. Cigarette smoking and reproductive and developmental toxicity. Reproductive and Developmental Toxicology:447.

Silva GM, Rossetto R, Chaves RN, Duarte AB, Araujo VR, Feltrin C, et al. 2015. In vitro development of secondary follicles from pre-pubertal and adult goats cultured in two-dimensional or three-dimensional systems. Zygote (Cambridge, England) 23:475-484.

Skinner MK, Schmidt M, Savenkova MI, Sadler-Riggleman I, Nilsson EE. 2008. Regulation of granulosa and theca cell transcriptomes during ovarian antral follicle development. Mol Reprod Dev 75:1457-1472.

Smyth GK, Ritchie M, Thorne N, Wettenhall J. 2005. Limma: Linear models for microarray data. In bioinformatics and computational biology solutions using r and bioconductor. Statistics for biology and health.

Spears N, Boland NI, Murray AA, Gosden RG. 1994. Mouse oocytes derived from in vitro grown primary ovarian follicles are fertile. Human reproduction 9:527-532.

Spicer LJ, Sudo S, Aad PY, Wang LS, Chun S-Y, Ben-Shlomo I, et al. 2009. The hedgehog-patched signaling pathway and function in the mammalian ovary: A novel role for hedgehog proteins in stimulating proliferation and steroidogenesis of theca cells. Reproduction 138:329-339.

Sriraman V, Rudd MD, Lohmann SM, Mulders SM, Richards JS. 2006. Cyclic guanosine 5'-monophosphate-dependent protein kinase ii is induced by luteinizing hormone and progesterone receptor-dependent mechanisms in granulosa cells and cumulus oocyte complexes of ovulating follicles. Mol Endocrinol 20:348-361.

Stefansdottir A, Fowler PA, Powles-Glover N, Anderson RA, Spears N. 2014. Use of ovary culture techniques in reproductive toxicology. Reproductive toxicology (Elmsford, NY) 49:117-135.

Symonds DA, Miller KP, Tomic D, Flaws JA. 2006. Effect of methoxychlor and estradiol on cytochrome p450 enzymes in the mouse ovarian surface epithelium. Toxicological sciences : an official journal of the Society of Toxicology 89:510-514.

Tagler D, Tu T, Smith RM, Anderson NR, Tingen CM, Woodruff TK, et al. 2012. Embryonic fibroblasts enable the culture of primary ovarian follicles within alginate hydrogels. Tissue engineering Part A 18:1229-1238.

Tagler D, Makanji Y, Anderson NR, Woodruff TK, Shea LD. 2013. Supplemented alphamem/f12-based medium enables the survival and growth of primary ovarian follicles encapsulated in alginate hydrogels. Biotechnology and bioengineering 110:3258-3268.

Telfer EE, Zelinski MB. 2013. Ovarian follicle culture: Advances and challenges for human and nonhuman primates. Fertility and sterility 99:1523-1533.

Tiemann U. 2008. In vivo and in vitro effects of the organochlorine pesticides ddt, tcpm, methoxychlor, and lindane on the female reproductive tract of mammals: A review. Reproductive toxicology (Elmsford, NY) 25:316-326.

Tingen CM, Kiesewetter SE, Jozefik J, Thomas C, Tagler D, Shea L, et al. 2011. A macrophage and theca cell-enriched stromal cell population influences growth and survival of immature murine follicles in vitro. Reproduction 141:809-820.

Tomic D, Frech MS, Babus JK, Gupta RK, Furth PA, Koos RD, et al. 2006. Methoxychlor induces atresia of antral follicles in eralpha-overexpressing mice. Toxicological sciences : an official journal of the Society of Toxicology 93:196-204.

Vanden Bilcke C. 2002. The stockholm convention on persistent organic pollutants. Review of European Community & International Environmental Law 11:328-342.

Vandenberg LN, Colborn T, Hayes TB, Heindel JJ, Jacobs DR, Jr., Lee DH, et al. 2012. Hormones and endocrine-disrupting chemicals: Low-dose effects and nonmonotonic dose responses. Endocrine reviews 33:378-455.

Vanselow J, Spitschak M, Nimz M, Furbass R. 2010. DNA methylation is not involved in preovulatory down-regulation of cyp11a1, hsd3b1, and cyp19a1 in bovine follicles but may have a role in permanent silencing of cyp19a1 in large granulosa lutein cells. Biology of reproduction 82:289-298.

Walmsley SR, Print C, Farahi N, Peyssonnaux C, Johnson RS, Cramer T, et al. 2005. Hypoxia-induced neutrophil survival is mediated by hif-1α–dependent nf-κb activity. The Journal of Experimental Medicine 201:105-115.

Wang Y, Chan S, Tsang BK. 2002. Involvement of inhibitory nuclear factor-kappab (nfkappab)-independent nfkappab activation in the gonadotropic regulation of x-linked inhibitor of apoptosis expression during ovarian follicular development in vitro. Endocrinology 143:2732-2740.

West-Farrell ER, Xu M, Gomberg MA, Chow YH, Woodruff TK, Shea LD. 2009. The mouse follicle microenvironment regulates antrum formation and steroid production: Alterations in gene expression profiles. Biology of reproduction 80:432-439.

West ER, Shea LD, Woodruff TK. Engineering the follicle microenvironment. In: Proceedings of the Seminars in reproductive medicine, 2007, Vol. 25Copyright© 2007 by Thieme Medical Publishers, Inc., 333 Seventh Avenue, New York, NY 10001, USA., 287-299.

West ER, Xu M, Woodruff TK, Shea LD. 2007. Physical properties of alginate hydrogels and their effects on in vitro follicle development. Biomaterials 28:4439-4448.

Wigglesworth K, Lee K-B, O'Brien MJ, Peng J, Matzuk MM, Eppig JJ. 2013. Bidirectional communication between oocytes and ovarian follicular somatic cells is required for meiotic arrest of mammalian oocytes. Proceedings of the National Academy of Sciences 110:E3723-E3729.

Wijgerde M, Ooms M, Hoogerbrugge JW, Grootegoed JA. 2005. Hedgehog signaling in mouse ovary: Indian hedgehog and desert hedgehog from granulosa cells induce target gene expression in developing theca cells. Endocrinology 146:3558-3566.

Wilkinson PM, Mawer GE. 1974. The persistence of adriamycin in man and rat. British journal of clinical pharmacology 1:241-247.

Wood JR, Nelson VL, Ho C, Jansen E, Wang CY, Urbanek M, et al. 2003. The molecular phenotype of polycystic ovary syndrome (pcos) theca cells and new candidate pcos genes defined by microarray analysis. J Biol Chem 278:26380-26390.

Woodruff T. 2007. The emergence of a new interdiscipline: Oncofertility. Oncofertility Fertility Preservation for Cancer Survivors:3-11.

Woodruff TK, Shea LD. 2011. A new hypothesis regarding ovarian follicle development: Ovarian rigidity as a regulator of selection and health. Journal of assisted reproduction and genetics 28:3-6.

Xiao S, Zhang J, Romero MM, Smith KN, Shea LD, Woodruff TK. 2015. In vitro follicle growth supports human oocyte meiotic maturation. Scientific reports 5:17323.

Xiao S, Coppeta JR, Rogers HB, Isenberg BC, Zhu J, Olalekan SA, et al. 2017a. A microfluidic culture model of the human reproductive tract and 28-day menstrual cycle. Nature communications 8:14584.

Xiao S, Zhang J, Liu M, Iwahata H, Rogers HB, Woodruff TK. 2017b. Doxorubicin has dose-dependent toxicity on mouse ovarian follicle development, hormone secretion, and oocyte maturation. Toxicological sciences : an official journal of the Society of Toxicology.

Xu J, Bernuci MP, Lawson MS, Yeoman RR, Fisher TE, Zelinski MB, et al. 2010. Survival, growth, and maturation of secondary follicles from prepubertal, young, and older adult rhesus monkeys during encapsulated three-dimensional culture: Effects of gonadotropins and insulin. Reproduction 140:685-697.

Xu J, Lawson MS, Yeoman RR, Pau KY, Barrett SL, Zelinski MB, et al. 2011. Secondary follicle growth and oocyte maturation during encapsulated three-dimensional culture in rhesus monkeys: Effects of gonadotrophins, oxygen and fetuin. Human reproduction 26:1061-1072.

Xu J, Lawson MS, Yeoman RR, Molskness TA, Ting AY, Stouffer RL, et al. 2013a. Fibrin promotes development and function of macaque primary follicles during encapsulated three-dimensional culture. Human reproduction 28:2187-2200.

Xu J, Xu M, Bernuci MP, Fisher TE, Shea LD, Woodruff TK, et al. 2013b. Primate follicular development and oocyte maturation in vitro. Advances in experimental medicine and biology 761:43-67.

Xu M, Kreeger PK, Shea LD, Woodruff TK. 2006. Tissue-engineered follicles produce live, fertile offspring. Tissue engineering 12:2739-2746.

Xu M, Banc A, Woodruff TK, Shea LD. 2009a. Secondary follicle growth and oocyte maturation by culture in alginate hydrogel following cryopreservation of the ovary or individual follicles. Biotechnology and bioengineering 103:378-386.

Xu M, West-Farrell ER, Stouffer RL, Shea LD, Woodruff TK, Zelinski MB. 2009b. Encapsulated three-dimensional culture supports development of nonhuman primate secondary follicles. Biology of reproduction 81:587-594.

Xu M, Fazleabas AT, Shikanov A, Jackson E, Barrett SL, Hirshfeld-Cytron J, et al. 2011. In vitro oocyte maturation and preantral follicle culture from the luteal-phase baboon ovary produce mature oocytes. Biology of reproduction 84:689-697.

Xu Y, Duncan FE, Xu M, Woodruff TK. 2015. Use of an organotypic mammalian in vitro follicle growth assay to facilitate female reproductive toxicity screening. Reproduction, fertility, and development.

Yeung F, Hoberg JE, Ramsey CS, Keller MD, Jones DR, Frye RA, et al. 2004. Modulation of nf-κb-dependent transcription and cell survival by the sirt1 deacetylase. The EMBO Journal 23:2369-2380.

Yoon SJ, Kim KH, Chung HM, Choi DH, Lee WS, Cha KY, et al. 2006. Gene expression profiling of early follicular development in primordial, primary, and secondary follicles. Fertility and sterility 85:193-203.

Young JM, McNeilly AS. 2010. Theca: The forgotten cell of the ovarian follicle. Reproduction 140:489-504.

Yuksel H, Ispir Ü, Ulucan A, Turk C, Taysı MR. 2016. Effects of hexachlorocyclohexane (hch-γ-isomer, lindane) on the reproductive system of zebrafish (danio rerio). Turkish Journal of Fisheries and Aquatic Sciences 16:917-921.

Zhou H, Malik MA, Arab A, Hill MT, Shikanov A. 2015. Hydrogel based 3-dimensional (3d) system for toxicity and high-throughput (htp) analysis for cultured murine ovarian follicles. PLoS One 10:e0140205.

Zhu J. 2010. Bioactive modification of poly(ethylene glycol) hydrogels for tissue engineering. Biomaterials 31:4639-4656.

Ziv-Gal A, Craig ZR, Wang W, Flaws JA. 2013. Bisphenol a inhibits cultured mouse ovarian follicle growth partially via the aryl hydrocarbon receptor signaling pathway. Reproductive toxicology (Elmsford, NY) 42:58-67.